UNCLASSIFIED

FINAL REPORT - Part I

FOR

LAKE HEFNER MODEL STUDIES

OF WIND STRUCTURE AND

EVAPORATION

This report covers the period October 1951 to November 1953

COLORADO
AGRICULTURAL AND MECHANICAL COLLEGE

Department of Civil Engineering

Fort Collins, Colorado

NAVY DEPARTMENT BUREAU OF SHIPS ELECTRONICS DIVISIONS

Contract No. NObsr-57053
Index No. NE 120202
November 1953

UNCLASSIFIED

ACKNOWLEDGMENTS

TABLE OF CONTENTS

LIST OF FIGURES

Chapter I

INTRODUCTION

Civilization finds it necessary because of the lack of an inexhaustible supply of natural resources to recognize the importance of conservation to its growth, development, and advancement. Because of this, mankind is taking steps to store and use the available resources in such a fashion that the greatest utility will be derived from them. Although this report does not explicitly represent a conservation study of any resources, it describes a study of two natural phenomena by means of a model which when better understood may lead to conservation. These phenomena are evaporation from Lake Hefner and the wind structure near the terrain surrounding Lake Hefner.

A large amount of work has been performed by such investigators as Carl Rohwer $(14)^{1}$, N. W. Cummings (4), O. G. Sutton (16), and H. U. Sverdrup (17) in an endeavor to correlate the numerous factors influencing evaporation. A considerable amount of effort has been directed toward correlating the evaporation of water from a pan with that from a large body of water with a qualified degree of success. As the understanding of the laws governing the behavior of the factors influencing evaporation increased, several physical concepts of the evaporation phenomena were formulated. The result has been an evolution of the "mass transfer" and "energy budget" approach to evaporation.

Experiments including measurement of evaporation from areas of limited extent have supported to varying degrees the concepts concerning mass transfer, energy budget, and evaporation pans. However, when these concepts were applied to areas of large extent, their applicability has been questionable because of the lack of supporting experimental data. It was this latter fact which prompted the U. S. Navy, U. S. Bureau of Reclamation, U. S. Weather

---

1 The first number in parenthesis is the bibliographical entry number and a number following a colon is the page number.

Bureau, and U. S. Geological Survey to consider undertaking the study of evaporation from a large body of water. The ground work for a study of this nature was laid in 1947 and the actual study was conducted at Lake Hefner, Oklahoma in 1950-1951 (2 and 18). The results of the Lake Hefner undertaking were gratifying and very enlightening and will be of considerable value to scientists and engineers in many fields.

The Lake Hefner study presented an opportunity to investigate the possibilities of duplicating by means of a model the prototype evaporation and wind structure. Prior to the Lake Hefner undertaking, a model study of this nature would have had very limited application because of the scarcity of accurate substantiating prototype data. If it were possible to evaluate the evaporation and wind structure by means of model studies, models may be used to determine the evaporation and wind structure for situations which as yet are too complex for theoretical analysis.

With the idea of ascertaining the feasibility of model studies for the determination of wind structure and lake and reservoir evaporation, the U. S. Bureau of Ships awarded Colorado A & M College a contract to undertake a study of this nature in cooperation with the U. S. Geological Survey.

Specifically, the object of the Lake Hefner model study is to determine:

1. Correlations of wind structure between model and prototype.

2. Correlations of evaporation between model and prototype.

The Colorado Agricultural and Mechanical Research Foundation of Colorado A & M College entered into a contract to undertake this model study in October 1951. It is now anticipated that this work will require approximately three years to complete.

The model of Lake Hefner and the surrounding terrain was constructed during the spring and summer of 1952. Initial model tests were conducted in the wind tunnel during the autumn of 1952. This report covers the work and results up to December 1952 wherein little is said concerning the significance and application of the results. The two latter phases of the study will be discussed in Part II of the Final Report after the results of the Summer-1953

testing program have been evaluated. In this report reference is made to the prototype study only insofar as is necessary to compare the prototype and model data.

The model of Lake Hefner was subjected to additional tests during the summer of 1953. This testing program will supplement the data on hand and will allow investigation of certain aspects of modeling techniques in more detail. The results of this latter program, together with conclusions regarding data analyzed in this report, will be published as Part II of the Final Report of the Lake Hefner Model Studies.

List of Symbols

The following symbols are used in this report. An endeavor was made to have these agree as closely as possible to those appearing in the Lake Hefner studies technical report (18). The English system of units -- pounds, feet, and seconds -- has been used wherever convenient. Any other system would be equally applicable when proper cognizance was taken of the conversion factors.

Symbol	Definition	Dimensions
a	denotes a thermocouple junction made up of a single copper and a single constantan wire	--
b	denotes a thermocouple junction made up of two copper and two constantan wires (made from multistrand wire only)	--
e	water vapor pressure of the air -- a subscript refers to the elevation at which it was measured	millibars
e_o	water vapor pressure of saturated air at the evaporation surface temperature	millibars
Δe	difference between the vapor pressure of the air in contact with the evaporation surface and the vapor pressure of the air	millibars
f	denotes a thermocouple junction made up of all the copper and all the constantan wires contained in the multistrand wires	--
g	denotes either single strand copper or single strand constantan wire	--
h	denotes either multistrand copper or multistrand constantan wire	--
log	denotes logarithm to base 10 (Logarithms to any other base were not used in this report.)	--
m	subscript referring to the model	--
p	subscript referring to the prototype	--
p_a	total atmospheric pressure	millibars
q_h	specific humidity	pound/pound
r	roughness ratio -- by definition $r = \dfrac{\epsilon_w}{\epsilon_\ell}$	dimensionless
r'	relative roughness -- by definition $r' = \dfrac{\sqrt{A}}{\epsilon_w}$	dimensionless
u'	the instantaneous velocity fluctuation from U	feet/second
$\overline{u'w'}$	temporal mean value of velocity fluctuation product	feet^2/second^2

Symbol	Definition	Dimensions
w'	the instantaneous velocity fluctuation in the z direction	feet/second
x	the distance in the model from the leading edge of the modeled terrain to the point at which the velocity profile is measured	feet
z	vertical height above surface	feet
z_o	roughness parameter	feet
z_{ol}	roughness parameter of the land surface	feet
z_{ow}	roughness parameter of the water surface	feet
A	area of surface from which evaporation takes place	feet^2
C_A	absolute humidity of the ambient air	pound/feet^3
C_o	absolute humidity of the air in contact with the surface from which evaporation takes place	pound/feet^3
ΔC	difference between the absolute humidity of the air in contact with the evaporation surface and the absolute humidity of the ambient air	pound/feet^3
$\Delta C'$	difference between the mixing ratio of the air in contact with the evaporation surface and the mixing ratio of the ambient air	pound/pound
C_e	by definition $C_e = \dfrac{E}{\gamma \Delta C' U_o}$	dimensionless
C_f	drag coefficient	dimensionless
D	wind direction	dimensionless
E	average rate of evaporation per unit area	pound/feet^2-second
E'	average rate of evaporation per unit area	inch/feet^2-day
L	length of evaporation surface	feet
N	form of Nusselt number -- by definition $N = \dfrac{E\sqrt{A}}{\Delta C\, \nu_e}$	dimensionless
R	Reynolds number -- by definition $R = \dfrac{U_o \sqrt{A}}{\nu}$	dimensionless
R_*	form of Reynolds number -- by definition $R_* = \dfrac{U_* \sqrt{A}}{\nu_e}$	dimensionless
S	shape factor of the surface from which evaporation takes place	dimensionless
T_o	temperature of the evaporation surface	^oF

6

Symbol	Definition	Dimensions
T_{AD}	temperature (model only) of the air as measured by the dry bulb of the forward tunnel psychrometer	$^\circ F$
T_{AW}	temperature (model only) as indicated by the wet bulb of the forward tunnel psychrometer	$^\circ F$
U	temporal mean wind velocity in horizontal plane -- a single subscript other than zero indicates the height above the surface in feet; a binary subscript indicates both the height above the surface in feet and the station at which the velocity was measured	feet/second
U_0	ambient wind velocity at height equal to or greater than δ	feet/second
U_*	shear velocity -- by definition $U_* = \sqrt{\tau_0/\rho}$	feet/second
γ	specific weight of dry air	pound/feet^3
δ	thickness of the boundary layer	feet
δ'	thickness of the laminar sub-layer	feet
ϵ	equivalent sand roughness	feet
ϵ_l	equivalent sand roughness of the land surface	feet
ϵ_w	equivalent sand roughness of the water surface	feet
ν	kinematic viscosity of the air	feet^2/second
ν_e	coefficient of molecular diffusion for water vapor	feet^2/second
ρ	density of dry air -- subscript refers to elevation at which temperature was measured. Subscript zero denotes that the density is based on the temperature of the surface from which evaporation takes place	pound-second^2/feet^4
σ	Prandtl number -- by definition $\sigma = \dfrac{\nu}{\nu_e}$	dimensionless
τ_0	shear at surface	pound/feet^2

Chapter II

DIMENSIONAL AND THEORETICAL ANALYSIS

The purpose of this chapter is to develop a basis for the comparison of model and prototype wind structure and evaporation for Lake Hefner and other artificial or natural bodies of water. The two objects of interest in this project -- wind structure and evaporation -- will be treated separately.

Wind Structure

The phase of the wind structure which was to be investigated under this contract was that portion which dealt with the variation of the mean horizontal velocity with height. The term wind structure as used in this report shall always connote just this one aspect of the wind structure. In connection with the wind structure aspect of the Lake Hefner model study, it will be profitable to review briefly some aspects of turbulent boundary layer theory. The wind structure for the model and prototype might then be interpreted more effectively.

When a turbulent fluid flows near a stationary boundary, the mean velocity of the fluid near the boundary is different from that of the free stream because of the shear stress exerted on the fluid by the boundary. As a result of this shear stress, a fluid layer of reduced and varying velocity, called the boundary layer, is created. The velocity distribution of the fluid within this layer which varies from zero at the stationary boundary to approximately 99% of the free stream velocity, is governed by laws of molecular transfer of momentum and laws of molar transfer of momentum (turbulence). As a consequence, two general types of boundary layers may be formed for turbulent flow depending on the interrelationship of the boundary and flow characteristics. Both of these boundary layers have one property in common and that is -- the velocity distribution within the turbulent portion of the boundary layer may be assumed to vary as the logarithm of height for adiabatic

7

8

lapse rates. The work of Prandtl and von Kármán (12 and 5) led to a development of the following equation which describes the velocity distribution within this turbulent portion of the boundary layer:

$$\frac{U_z}{U_*} = 5.75 \log\left(\frac{z}{z_o}\right) \tag{1}$$

where

> U_z - mean velocity of the air at height z -- feet/second,
>
> U_* - shear velocity -- feet/second,
>
> z - vertical distance above the surface -- feet,
>
> z_o - "roughness parameter" -- feet.

If the boundary is "smooth", the boundary layer is composed of two layers. The flow in contact with and adjacent to the wall is laminar and is called the laminar sub-layer. The remainder of the boundary layer is turbulent. The velocity distribution within this laminar sub-layer may be described by

$$\frac{U_z}{U_*} = \frac{U_* z}{\nu} \tag{2}$$

where

> ν - kinematic viscosity of air -- feet^2/second.

The work of Nikuradse (10) enabled formulation of an empirical equation for the thickness of this layer

$$\delta' = \frac{11.6\nu}{U_*} \tag{3}$$

where

> δ'- thickness of the laminar sub-layer -- feet.

The portion of the boundary layer above the laminar sub-layer is turbulent. Thus through the work of Nikuradse (on flow in smooth pipes), Eq. 1 may be written as

$$\frac{U_z}{U_*} = 5.75 \log\left(\frac{9.06\ U_* z}{\nu}\right) \tag{4}$$

when z_o is considered to be equal to

$$z_o = \frac{\delta'}{107} = \frac{0.108\ \nu}{U_*}. \tag{5}$$

A boundary is considered smooth if the height of the roughness along the

boundary is less than about one-fourth the thickness of the laminar sub-layer.

If the boundary is "rough", the boundary layer is composed of a single turbulent layer. In this case, the height of the roughness is usually greater than six times that of the laminar sub-layer as given by Eq. 3 so that the roughness projects through the laminar sub-layer and destroys it. Eq. 1 may be used to evaluate the velocity distribution within the turbulent boundary layer or on the basis of further work by Nikuradse (11) Eq. 1 may be rewritten in terms of an equivalent sand roughness as follows:

$$\frac{U}{U_*} = 5.75 \log \left(\frac{30z}{\epsilon}\right) \tag{6}$$

where

$$\epsilon = 30z_0 , \tag{7}$$

ϵ - equivalent sand roughness -- feet.

The wind structures for both the prototype and the model will be discussed in Chapter IV, Presentation and Discussion of Results, in light of this brief review of the boundary layer theory.

Evaporation

A solution to the problem of correlating evaporation with the important parameters will be approached by means of a dimensional analysis. The dimensionless parameters obtained through this dimensional analysis will then be expressed in functional form by making use of the von Kármán (6) extension of the Reynolds (13) analogy and the appropriate drag coefficient formulae for flat surfaces.

Dimensional Analysis

The variables of major importance which affect the rate of evaporation E from a water surface may be formed into an equation as follows:

$$E = \phi_1 \left(\sqrt{\tau_0/\rho}, \Delta C, \nu_e, \nu, \epsilon_\ell, \epsilon_w, S, D, A\right) \tag{8}$$

where

E - average rate of evaporation per unit area --

pound/feet^2-second,

A — area of the surface from which evaporation takes place -- feet^2,

ΔC — difference between the absolute humidity of the air in contact with the evaporation surface and the absolute humidity of the ambient air -- pound/feet^3,

D — wind direction -- dimensionless,

S — shape factor of the surface from which evaporation takes place -- dimensionless,

ϵ_ℓ — ͏ralent sand roughness of the land surface -- feet,

ϵ_w — equivalent sand roughness of the water surface -- feet,

ν — kinematic viscosity of the air -- feet^2/second,

ν_e — coefficient of molecular diffusion for water vapor into air -- feet^2/second,

ρ — density of dry air -- pound-second^2/feet^4,

τ_o — shear at the ground surface -- pound/feet^2.

By the principles of Buckingham's π theorem, the variables of Eq. 8 may be grouped into dimensionless parameters to form the following equation:

$$\frac{E\sqrt{A}}{\nu_e\,\Delta C} = \phi_2\left(\frac{U_*\sqrt{A}}{\nu_e}, \frac{\nu}{\nu_e}, \frac{\epsilon_w}{\epsilon_\ell}, \frac{\sqrt{A}}{\epsilon_w}, D\right).\qquad(9)$$

The shape parameter S has been omitted from Eq. 9 since the shape for a particular lake will be practically constant for small changes of stage and will, of course, be the same for a model and the prototype. For convenience, the terms in Eq. 9 may be renamed such that

$$N = \phi_2\ (R_*,\ \sigma,\ r,\ r',\ D)\qquad(10)$$

in which

$N = \dfrac{E\sqrt{A}}{\nu_e\,\Delta C}$ and is similar to the Nusselt number used in heat transfer analyses -- dimensionless,

$R_* = \dfrac{U_*\sqrt{A}}{\nu_e}$ and characterizes the product of a type of Reynolds number and Prandtl number -- dimensionless,

$\sigma = \dfrac{\nu}{\nu_e}$ - the Prandtl number -- dimensionless,

$$r = \frac{\epsilon_w}{\epsilon_\ell}$$ - the roughness ratio -- dimensionless,

$$r' = \frac{\sqrt{A}}{\epsilon_w}$$ - the relative roughness of the water surface -- dimensionless.

U_* was chosen to define a Reynolds number because the shear velocity is an indirect measurement of the turbulent properties and hence the diffusive power of the atmosphere. Based upon the mixing length approach to the analysis of diffusion in a turbulent fluid field as shown by Sutton (16:73), the mean rate of transfer of a quantity such as water vapor may in fact be expressed in terms of U_* as follows:

$$E = U_*^2 \left(\frac{dU_z}{dz}\right)^{-1} \frac{dC}{dz} = \overline{u'w'} \left(\frac{dU_z}{dz}\right)^{-1} \frac{dC}{dz} \tag{11}$$

where

C   - absolute humidity of the air -- pound/feet^3,

$\overline{u'w'}$ - temporal mean value of the product of fluctuations in the direction of the mean flow and the vertical, respectively -- feet^2/second^2.

Also, Reynolds number based on U_* rather than U_o , yields a parameter which is indicative of the actual wind structure and one which may be measured in the prototype.

In order to obtain complete geometrical and dynamical similarity between a model and the prototype -- in other words, the same function ϕ_2 for the model as for the prototype -- a model should be designed and tested such that the five parameters in the right hand part of Eq. 10 have values comparable in magnitude to those for the prototype. Unfortunately, with modeling techniques now known, the value of $(R_*)_m$[1] and $(R_*)_p$ as defined in this report (where the scale ratio is 1:2000 as in this study) cannot be made equal. In fact, the ratio of $(R_*)_m$ to $(R_*)_p$ is approximately equal to the scale ratio since the two variables of R_* , $(U_*)_m$ and $(\nu_e)_m$, are approximately equal

---

[1] The subscripts m and p refer to the model and prototype respectively.

to $(U_*)_p$ and $(\nu_e)_p$ respectively. The values of $(\sigma)_m$ and $(\sigma)_p$ are equal since the same fluids are used in both the model and the prototype. By proper design and by using average roughness values, the values of $(r)_m$ and $(r')_m$ can be made equal to the respective prototype parameters. Finally, the direction $(D)_m$ can be chosen at will to correspond to significant directions for the prototype.

The immediate problem then is to find a sound basis for extrapolation of model data where the value of $(R_*)_m$ is approximately $1/2000$ of $(R_*)_p$. A possible method of attack is to obtain a theoretical relationship between the parameters of Eq. 10 and then proceed to verify the results by making laboratory and field measurements. In the following section, use is made of the von Kármán extension of Reynolds analogy to form a basis for extrapolation. The effect of r and D upon N is not predicted theoretically and must be determined by experiment. Also the effect upon evaporation rates of any mountainous or hilly terrain near the flat water surface must be determined by experiment.

Momentum and Mass Transfer Analogy

In the case of zero longitudinal pressure gradient and turbulent flow with the presence of a laminar sub-layer, von Kármán expresses the Reynolds analogy between momentum transfer and mass transfer by

$$\frac{1}{C_e} = \frac{2}{C_f} + 5\left(\frac{2}{C_f}\right)^{\frac{1}{2}}\left\{\sigma - 1 + 2.303 \log\left[1 + \frac{5}{6}(\sigma - 1)\right]\right\} \tag{12}$$

where

$C_e = \dfrac{E}{\Upsilon \Delta C' U_o}$ -- dimensionless,

C_f - drag coefficient -- dimensionless,

$\Delta C'$ - difference between the mixing ratio of the air in contact with the evaporating surface and the mixing ratio of the ambient air -- pound/pound,

Υ - specific weight of dry air -- pound/feet^3,

U_o - ambient wind velocity -- feet/second,

$$\sigma = \frac{\nu}{\nu_e}$$ - the Prandtl number, $\sigma = 0.6$ for the evaporation of water into air -- dimensionless.

In the case of zero longitudinal pressure gradient and completely turbulent flow, the analogy between momentum transfer and mass transfer may be expressed as

$$C_e = \frac{C_f}{2} . \tag{13}$$

Eq. 13 is based on either one or the other of the following two premises:

1. The value of the Prandtl number σ is approximately one.

2. When the flow field is turbulent throughout, the eddy diffusivity is much greater than ν_e and for this reason ν_e may be omitted.

For hydrodynamically smooth plates, the drag coefficient C_f in turbulent flow is expressed as a function of the Reynolds number R ; and for rough surfaces, C_f is expressed as a function of R and $\frac{L}{\epsilon_w}$. In the usual equations for the evaluation of C_f , R is defined as $\frac{U_o L}{\nu}$ where L is the plate length. In this report, the following analysis will be based on taking the value of $\sqrt{A}$ as the plate length L . Only if the evaporation surface were a square would the similarity between $\sqrt{A}$ and L be exact and any effect resulting from variation of the surface from a square area must be determined by experiments.

The next step in the development of a functional relationship for Reynolds analogy between momentum and mass transfer is to express C_e in terms of N and to express R in terms of R_* . The relationship between N and C_e , which may be easily verified, is

$$N = \sigma C_e R \tag{14}$$

where both C_e and R are expressed as functions of the ambient velocity U_o . To obtain R in terms of R_* and consequently N in terms of both C_e and R_* , reference must be made to the vertical velocity distribution at a selected station on or near the water surface. Since R is based on the ambient velocity U_o , the relationships between R and R_* should be derived on this basis. Methods of correlating R and R_* based on U_o for

various ranges of R_* are presented in the following paragraphs.

For <u>values</u> <u>of</u> R_* <u>in</u> <u>the</u> <u>range</u> $\underline{10^3 \lessgtr R_* \lessgtr 10^5}$ (<u>corresponding</u> <u>to</u> $\underline{5 \times 10^5 \lessgtr R \lessgtr 10^7}$), the 1/7-power relationship (7:12) is a close approximation for calculation of the velocity distribution and gives

$$\frac{U_z}{U_*} = 8.16 \left(\frac{zU_*}{\nu}\right)^{1/7} . \tag{15}$$

The value of U_z becomes U_0 when z is equal to the boundary layer thickness δ . The boundary layer thickness may be evaluated through use of the expression (15:33):

$$\delta = \frac{0.377x}{\left(\frac{U_0 x}{\nu}\right)^{1/5}} \tag{16}$$

where

δ - thickness of the boundary layer -- feet,

x - distance in the model from the leading edge of the modeled

terrain to the point at which the velocity profile is

measured -- feet.

When z of Eq. 15 is considered to be equal to δ expressed by Eq. 16, the relationship between R_* and R becomes

$$R = 11.85 \, (R_*)^{10/9} \left(\frac{x}{\sqrt{A}}\right)^{1/9} . \tag{17}$$

Eq. 14 may now be changed through use of Eq. 17 to

$$N = 7.11 \, C_e \, (R_*)^{10/9} \left(\frac{x}{\sqrt{A}}\right)^{1/9} \tag{18}$$

with validity in the range $10^3 \lessgtr R_* \lessgtr 10^5$.

For <u>values</u> <u>of</u> R_* <u>greater</u> <u>than</u> $\underline{10^5}$, the logarithmic velocity distribution should be used to correlate R and R_* . Considering only the case in which the terrain approaching the upwind station is hydrodynamically rough, the logarithmic velocity distribution given by Eq. 1 may be used:

$$\frac{U_z}{U_*} = 5.75 \log\left(\frac{z}{z_{0\ell}}\right) \tag{1a}$$

in which

$z_{o\ell}$ - equivalent sand roughness parameter for a land surface -- feet.

A land station is used as a reference since the "equivalent sand roughness" for a stationary solid boundary is better understood than that for a movable liquid boundary. In the case of the prototype, Lake Hefner, the liquid boundary is the free water surface from which evaporation takes place. According to Sutton (16:15), the planetary boundary layer extends to a height of about 1000 meters (3280 ft). For the present development, U_z will be taken as U_o when z is equal to 3280 ft. The relationship between R and R_* based on Eq. 1a then becomes

$$R = 9.58 \ R_* \ \log \left(\frac{3280}{z_{o\ell}} \right) \tag{19}$$

Combining Eqs. 14 and 19 results in the following expression for N in terms of R_* and $z_{o\ell}$:

$$N = 5.75 \ C_e R_* \ \log \left(\frac{3280}{z_{o\ell}} \right) \tag{20}$$

which will be valid for R_* greater than 10^5.

Evaporation equation for $10^3 \lesseqgtr R_* \lesseqgtr 10^5$. For a smooth surface and for the range $10^3 \lesseqgtr R_* \lesseqgtr 10^5$ (model range), Schlichting (15:33) gives the drag coefficient

$$C_f = \frac{0.074}{R^{1/5}} \ . \tag{21}$$

Upon substitution of Eq. 21 into Eq. 12 and making use of Eqs. 17 and 18, the equation

$$\frac{1}{N} = \frac{6.23}{(R_*)^{8/9} \left(\frac{x}{\sqrt{A}} \right)^{4/45}} - \frac{3.77}{R_* \left(\frac{x}{\sqrt{A}} \right)^{1/10}} \tag{22}$$

results. Eq. 22 should yield the proper evaporation coefficient N for the indicated range of R_* under the conditions of a hydrodynamically smooth evaporation surface.

Evaporation equation for $R_* \leqq 10^5$. For a _smooth surface_ and large values of R_*, the Schultz-Grunow drag coefficient equation given by Schlichting (15:39) is

$$C_f = \frac{0.427}{(-0.407 + \log R)^{2.64}} .$$ (23)

Eq. 23 may be substituted into Eq. 12 together with Eqs. 19 and 20 to obtain

$$\frac{1}{N} = \frac{0.174}{R_* \log \left(\frac{3280}{z_{o\ell}}\right)} \left\{ 4.68 \left\{ 0.574 + \log \left[\log \left(\frac{3280}{z_{o\ell}}\right)\right] + \log R_* \right\}^{2.64} \right.$$

$$\left. - 8.70 \left\{ 0.574 + \log \left[\log \left(\frac{3280}{z_{o\ell}}\right)\right] + \log R_* \right\}^{1.32} \right\} .$$ (24)

For a _rough surface_ Schlichting (15:41) gives the drag coefficient (where $\frac{U_* \epsilon_w}{\nu} > 70$) as

$$C_f = \frac{1}{\left(1.89 + 1.62 \log \frac{L}{\epsilon_w}\right)^{2.5}}$$ (25)

where $\frac{L}{\epsilon_w}$ will be considered equivalent to r' ; i.e., $r' = \sqrt{A}/\epsilon_w$. Since Schlichting (15:41) gives the drag coefficient C_f of Eq. 25 in terms of the surface roughness, the use of ϵ_w is unavoidable. In the case of the rough surface, the flow is considered to be turbulent throughout. Therefore Eq. 13 is used to express Reynolds analogy between momentum transfer and mass transfer. Substituting Eqs. 25 and 13 into Eq. 20, N may be expressed as follows:

$$N = \frac{2.875 R_*}{\left[1.89 + 1.62 \log \left(\frac{\sqrt{A}}{\epsilon_w}\right)\right]^{2.5}} \log \left(\frac{3280}{z_{o\ell}}\right) .$$ (26)

Chapter III

EQUIPMENT AND PROCEDURE

This chapter is devoted to a brief description and explanation of the equipment used and procedures followed in the Lake Hefner Model Study. In the process of condensing the material presented in this section, certain of the minor points were omitted. A detailed description and explanation of the equipment and procedures followed can be found in Appendixes A and C.

Equipment

The model of Lake Hefner was tested in the wind tunnel located on the campus of Colorado A & M College. This tunnel has a test section 9 feet square and 26 ft long. The wind tunnel was operated as a non-recirculating tunnel because of the change in the moisture content of the air due to the evaporation taking place from the model.

The terrain surrounding the lake was modeled to a scale of 1/2000 both horizontally and vertically. Nails driven into 1/2-in. plywood to the proper height along the contour lines served as a means of vertical and horizontal control for modeling purposes. A Persolite-cement mixture was used satisfactorily as a modeling material and filled the voids between the nails. The Persolite-cement surface was sanded smooth and painted. The model was placed in the tunnel so that the air passing over it simulated a south wind. This was the only wind direction under which the model was tested during the Fall-1952 testing program.

Lake Hefner itself was modeled to a scale of 1/2000 in the horizontal direction. No attempt was made to scale the actual depth of the lake. The area of the modeled lake was 25.01 sq ft which corresponded to a prototype area of 2296.8 acres at a lake stage of 1193.6 ft. A free water surface was not used in the model because of the large quantity of water which might have been lost through waves and splashing. Instead, a plaster of Paris

evaporation surface, 1/2-in. thick, was utilized. The surface was made very smooth in an endeavor to scale the prototype roughness. The smooth terrain and lake surface in effect made the values of r equal for model and proto-type. This was also true for r'. A small amount of difficulty was experienced with dry spots developing on this evaporating surface. Cognizance was taken of this fact when treating the data. The evaporation surface was placed in a metal pan which contained supporting gravel for the surface.

Two hot wire anemometers were used to measure the mean air velocity in the tunnel. The sensing element of one hot wire anemometer was located so as to measure the ambient air velocity in the tunnel. The other was mounted on a traversing mechanism which permitted measurement of velocity profiles above the modeled terrain and lake. Tungsten wire was used for the sensing elements of the hot wire anemometer and they were calibrated by a revolving arm method.

Copper-constantan thermocouples were used for the most part to measure the temperature at the various locations. Thirteen thermocouples were placed at the surface of the evaporating surface. Five thermocouples rested on the bottom of the pan containing the evaporation surface. Four were spaced at equal distances between the top of the evaporation surface and the bottom of the pan so that any temperature gradient present might be measured. Ten thermocouples were located at various points on the tunnel walls and terrain. One thermocouple was used to measure the temperature of the water being fed the lake. Four thermocouples were used to form two psychrometers. One psychrometer was so situated as to indicate the temperature and humidity of the ambient air in the tunnel. The other was mounted on the same traverse mechanism as the hot wire anemometer. This latter psychrometer was used to measure temperature and humidity profiles above the modeled terrain and lake.

Two water supply systems were incorporated in the model. One was of an automatic type which fed water automatically to the lake when the level of the water in the lake dropped below some predetermined level. The other was of the manual type, and consisted of a valve controlled burette. When the water dropped below a specified level as indicated by means of an electrical hook

gage, water was fed to the lake by opening the burette valve. The manual system was used during the course of a test to measure accurately the amount of water which had been evaporated from the model. Distilled water was used at all times.

Testing Procedure

Before the data of a test were collected, certain phases of the instrumentation were set in order and procedures deemed in accord with good research techniques were followed. The hot wire anemometers were calibrated and air was forced to move over the model for approximately one hour before the data of a test were taken. This latter step was followed to insure the establishment of thermal equilibrium.

All the thermocouples installed in and around the model were read just before and just after the taking of the main test data. The temperature data gathered in this fashion formed a part of the test data and have been included in summary form in Appendix B.

The traverse mechanism was situated so that the sensing elements were above the location at which the velocity profile was to be measured. Part of the main test data derived from the sensing elements on the traverse mechanism consisted of the velocity and psychrometer readings for different heights above the terrain. Also included in the main test data was the amount of water evaporated and ambient air psychrometer readings. These data in summary form have also been included in Appendix B.

Four meteorological stations were located on and around Lake Hefner during the prototype study. In the course of the model study, meteorological data were collected over four points occupying positions similar in location to the stations in the prototype. A brief description of each station follows.

Sta. 1. This station was located approximately at the center of Lake Hefner.

Sta. 2. This station was located on land along the south shore of the

20

lake. It was the upwind station for the prevailing southerly winds.

Sta. 3. This station was located on land along the northeast shore of the lake.

Sta. 4. This station was located on a tower approximately 100 ft from the dam which forms the north edge of the lake.

Transformation of Data

This section of Chapter III is devoted to a brief description of the methods used to transform the various forms of data into parameters which were consistent with the theoretical analysis. A detailed description of these methods has been included in Appendix C. Broadly speaking, there are four sources from which comparable data could be drawn. Each will be treated separately in the paragraphs that follow.

Evaluation of the von Kármán Extension of Reynolds Analogy Based on the Lake Hefner Model and Prototype Data.

Case I -- Smooth Boundary -- $10^3 \leqq R_* \leqq 10^5$. Since R_* for the model data fell in this range, the quantity x was considered to be the distance from the upstream edge of the modeled terrain to Sta. 2 and measured approximately 7.8 ft. When x and $\sqrt{A}$ were considered equal to 7.8 ft and 5.00 ft respectively, Eq. 22 reduced to

$$\frac{1}{N} = \frac{5.99}{(R_*)^{8/9}} - \frac{3.61}{R_*} . \tag{22a}$$

Case II -- Smooth Boundary -- $R_* \gtrless 10^5$. The prototype data indicated that the 16-month average wind speed at Sta. 1 was 19.4 ft/sec (18:7). A correlation between the wind speed at Stas. 1 and 2 was evolved using the 1/2-hour southerly wind data, Fig. 1. Based on Fig. 1, a velocity of 16.2 ft/sec for Sta. 2 corresponded to the 16-month average velocity for Sta. 1. The 1/2-hour data used in the derivation of the relationship for Fig. 1 were also used to ascertain the relationship between the velocity at Sta. 2 and
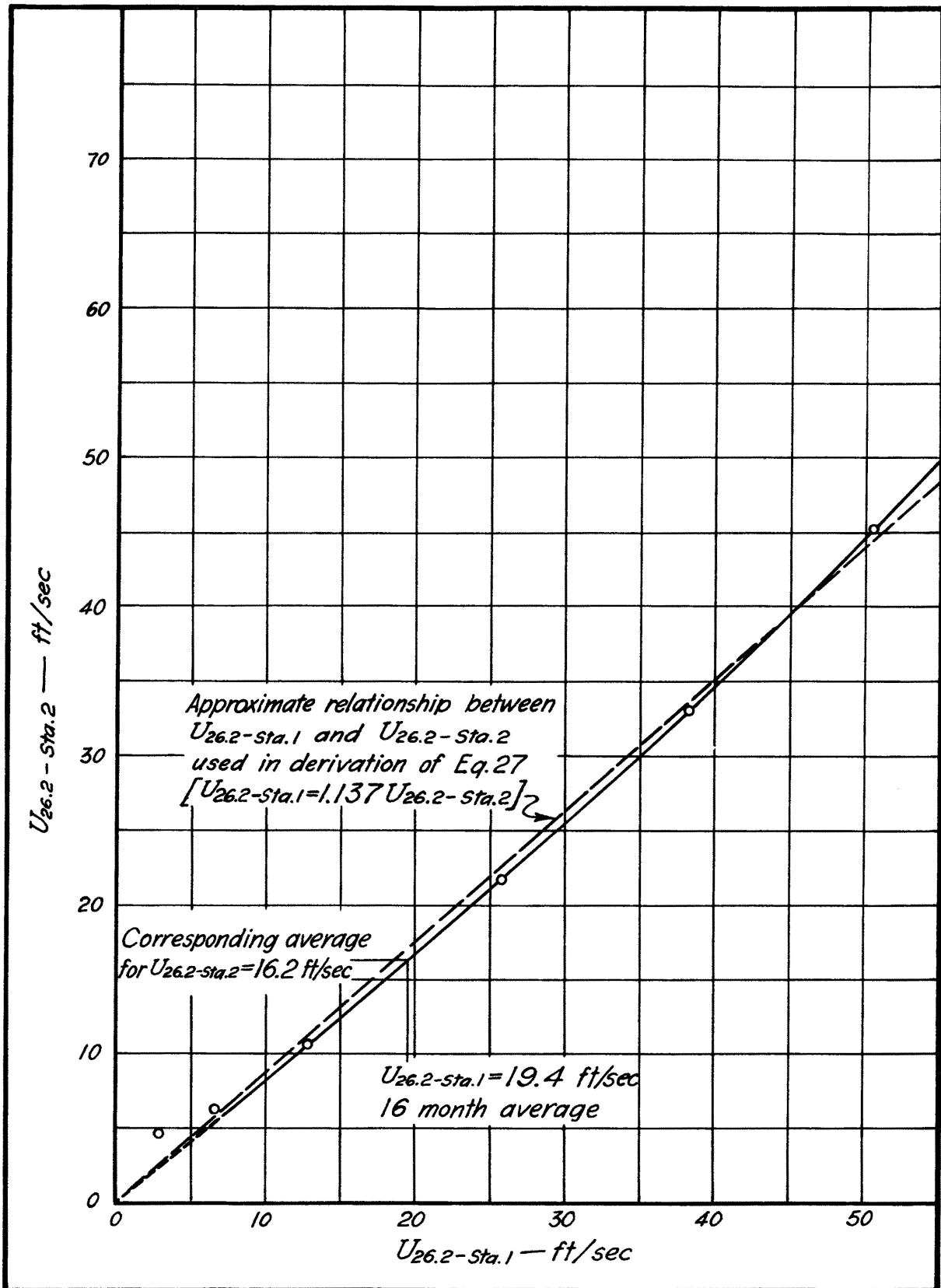
Fig. 1.   Relationship between $U_{26.2-Sta.1}$ and $U_{26.2-Sta.2}$ based on $\frac{1}{2}$-hour prototype data.

the roughness parameter $z_{o\ell}$ for Sta. 2, Fig. 2. On the basis of Fig. 2, the value of the roughness parameter $z_{o\ell}$ corresponding to a velocity of 16.2 ft/sec was found to be 0.22 ft. When a value of $z_{o\ell}$ equal to 0.22 ft was substituted into Eq. 24, the result was

$$\frac{1}{N} = \frac{0.0417}{R_*}\left[4.68\,(1.194 + \log R_*)^{2.64}\right.$$
$$\left. - 8.70\,(1.194 + \log R_*)^{1.32}\right]. \tag{24a}$$

Case III -- Rough Boundary -- $R_* \gtrsim 10^5$. Upon the insertion of definite values for the parameters r' and $z_{o\ell}$ into Eq. 26, the result was

$$N = 0.0546\,R_* . \tag{26a}$$

As in Case II, $z_{o\ell}$ was given the value of 0.22 ft. The value of $\sqrt{A}$ was considered to remain constant at 10,000 ft. The effective roughness of the actual water surface ϵ_w was also considered to be constant at 0.754 ft. This value of ϵ_w was based on the velocity profile data in Table I - Appendix B, and the 16-month average wind velocity at Sta. 1 (18:7 and 49). Lake Hefner Prototype Data.

3-Hour Average Data -- Individual Values of N Versus R_* . Only part of the original Lake Hefner data were analyzed. Sufficient data were available so that the variables E , $\sqrt{A}$, ΔC , ν_e , U , and U_* could be evaluated and placed into the necessary forms for comparison purposes (Table II - Appendix B).

U. S. Geological Survey Cir. 229. An empirical equation was presented in U. S. Geological Survey Cir. 229 (18) which correlated the significant parameters concerning evaporation. Only a few minor approximations were required to transform this equation into a form consistent with the dimensional analysis; namely

$$N = 0.0203\,R_* . \tag{27}$$

Lake Hefner Model Data.

Individual Values of N Versus R_*. The significant parameters disclosed by the dimensional analysis were kept in mind when the data were
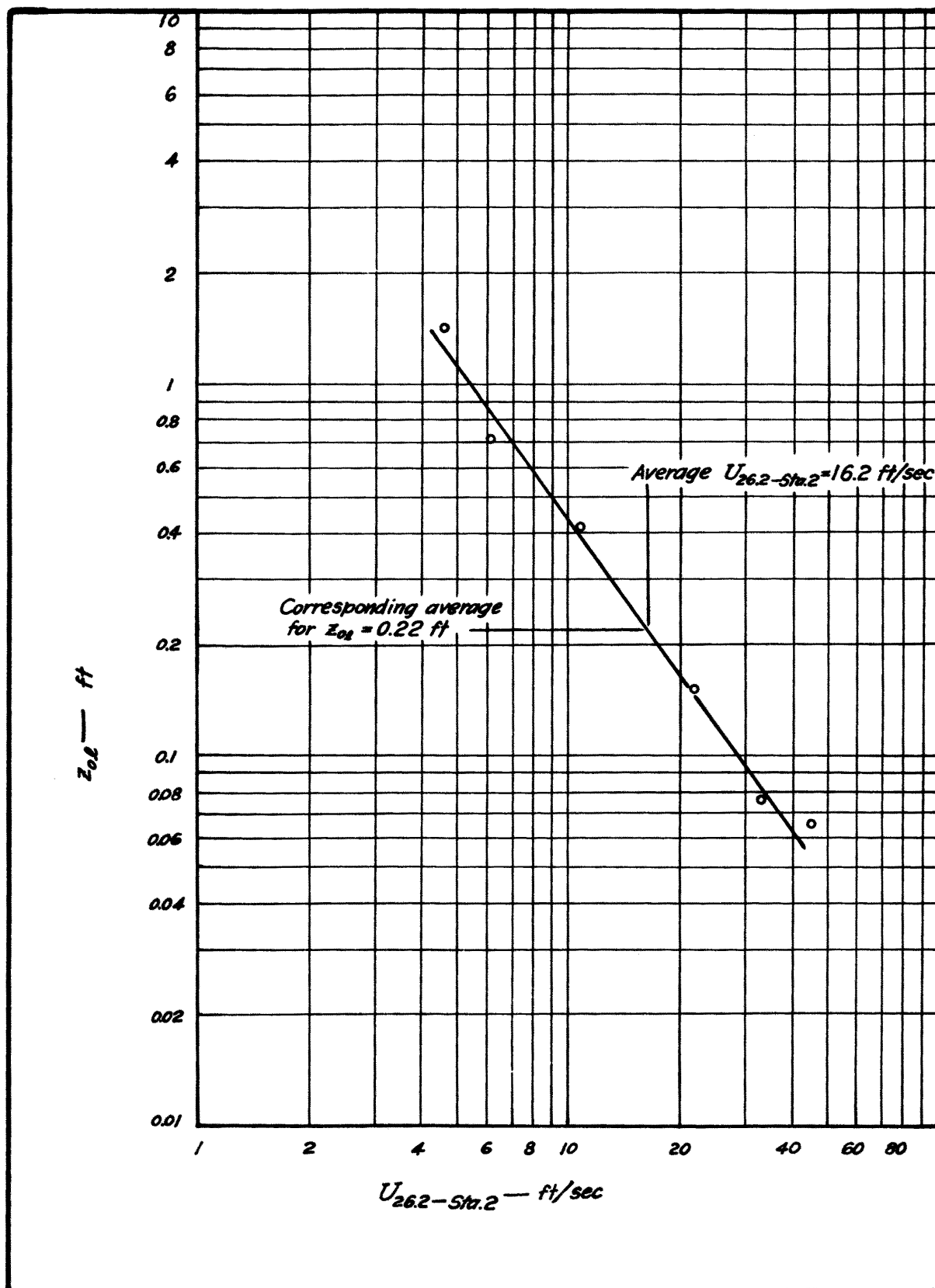
Fig. 2. Relationship between $U_{26.2-Sta.2}$ and $z_{0\ell}$ based on ½-hour prototype data.

collected from the Lake Hefner model. As a result, the data were easily placed into the forms necessary for comparison purposes (Table III - Appendix B).

Evaporation Data of Albertson.

Albertson [1] reported on evaporation from a plane boundary for a range of R_* of $3 \times 10^1 < R_* < 3 \times 10^3$. The form of these data was in agreement with that dictated by the dimensional analysis.

Chapter IV

PRESENTATION AND DISCUSSION OF RESULTS

The two main objectives of the Lake Hefner model study were to determine:

1. Correlations of wind structure between model and prototype.

2. Correlations of evaporation between model and prototype.

In this Chapter, each objective will be treated separately. It must be remembered that the results presented in this Chapter will not be evaluated in terms of their practical application until the data of the Summer 1953 testing program have been analyzed. The significance and application of all the results of the study will then be presented in Part II of the Final Report.

Wind Structure

The similarities and differences between the wind structure of the model and prototype will be brought out by means of two graphs. The first graph, Fig. 5, is a plot of $\log \left(\frac{z}{z_o}\right)$ versus $\frac{U_z}{U_*}$ and shows the correlations between actual data for model and prototype and the Prandtl-von Kármán relationship for wind structure; namely,

$$\frac{U_z}{U_*} = 5.75 \log \left(\frac{z}{z_o}\right). \tag{1}$$

The second graph, Fig. 6, illustrates the relationship between $U_{52.5}$ and U_* for both the model and the prototype. The prototype data for Figs. 5 and 6 were taken from the 1/2-hour wind profile data.

Model Data

Velocity profiles. A review of the variation of velocity with height found during the testing of the model may be in order as a prelude to the evaluation of the model data for Figs. 5 and 6. In the course of the model testing during the Summer of 1952, a total of 29 sets of data were collected. These data consisted of velocity profiles above the 4 stations in the model whose location corresponded to the position of the stations in the prototype.

The velocity profiles from each of the 29 tests were plotted with U_z as abscissa and log z as the ordinate. Two of the 29 profiles are presented in Fig. 3.

Based on the velocity profiles from the 29 tests, the general statement can be made that the velocity variation with height above a certain elevation may be considered logarithmic. In most cases this elevation was less than 0.1 in. although Velocity Profile No. 1 of Fig. 3 discloses that it was as great as 0.185 in. The Prandtl-von Kármán relationships indicate that for turbulent flow near a boundary U_z is a linear function of log z . Since in the course of the model study U_z was found to vary as log z above a certain elevation, usually 0.1 in., the conclusion was reached that above this elevation the boundary layer was turbulent and the velocity distribution agreed with Eq. 1. In light of this, the relationships for turbulent flow concerning z_o , ϵ , and δ' based on the work of Nikuradse were also considered applicable; that is,

$$z_o = \frac{\delta'}{107} = \frac{0.108\nu}{U_*} \text{ (smooth boundary)} \tag{5}$$

and

$$z_o = \frac{\epsilon}{30} \text{ (rough boundary)} . \tag{7}$$

The profiles of Figs. 3 and 4 along with others of the 29 tests indicate that the velocity distribution below the turbulent region of the boundary layer, that is below this approximate elevation of 0.1 in., does not follow the same type of relationship between U_z and z in all cases. Velocity Profile No. 1 of Fig. 4 indicates that in this case U_z varies directly as z . Whereas Velocity Profile No. 2 of Fig. 4 tends to show that the relationship between U_z and z is non-linear. In fact, based on Fig. 3, U_z appears to vary as the logarithm of z . Besides, this logarithmic relationship between U_z and z is not the same throughout the thickness of the boundary layer.

An investigation of the values of δ' and ϵ based on actual wind tunnel conditions and the Prandtl-von Kármán equations for turbulent flow discloses when compared with estimated actual model roughness that variations
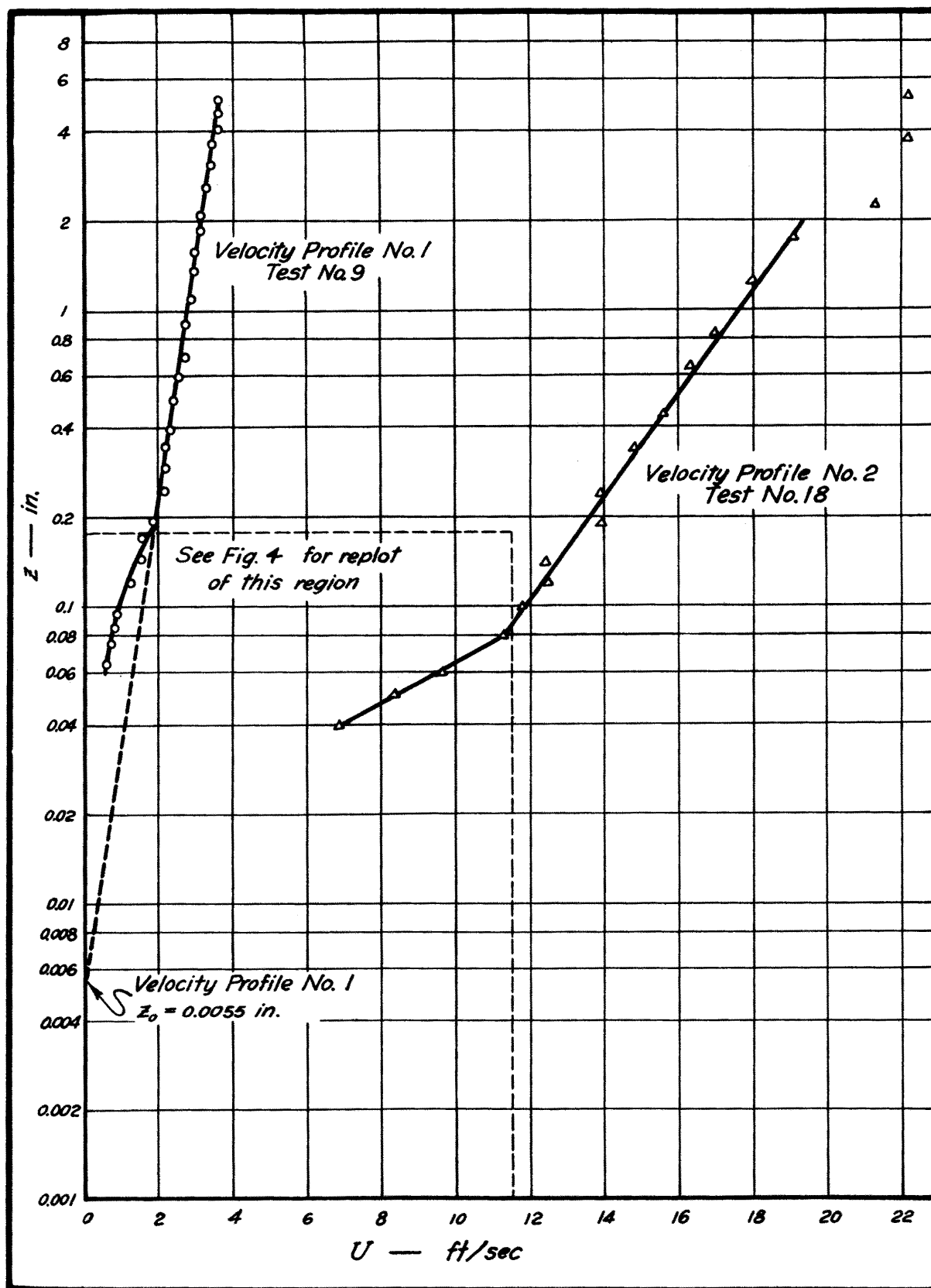
Fig. 3. Examples of entire velocity profiles for model.
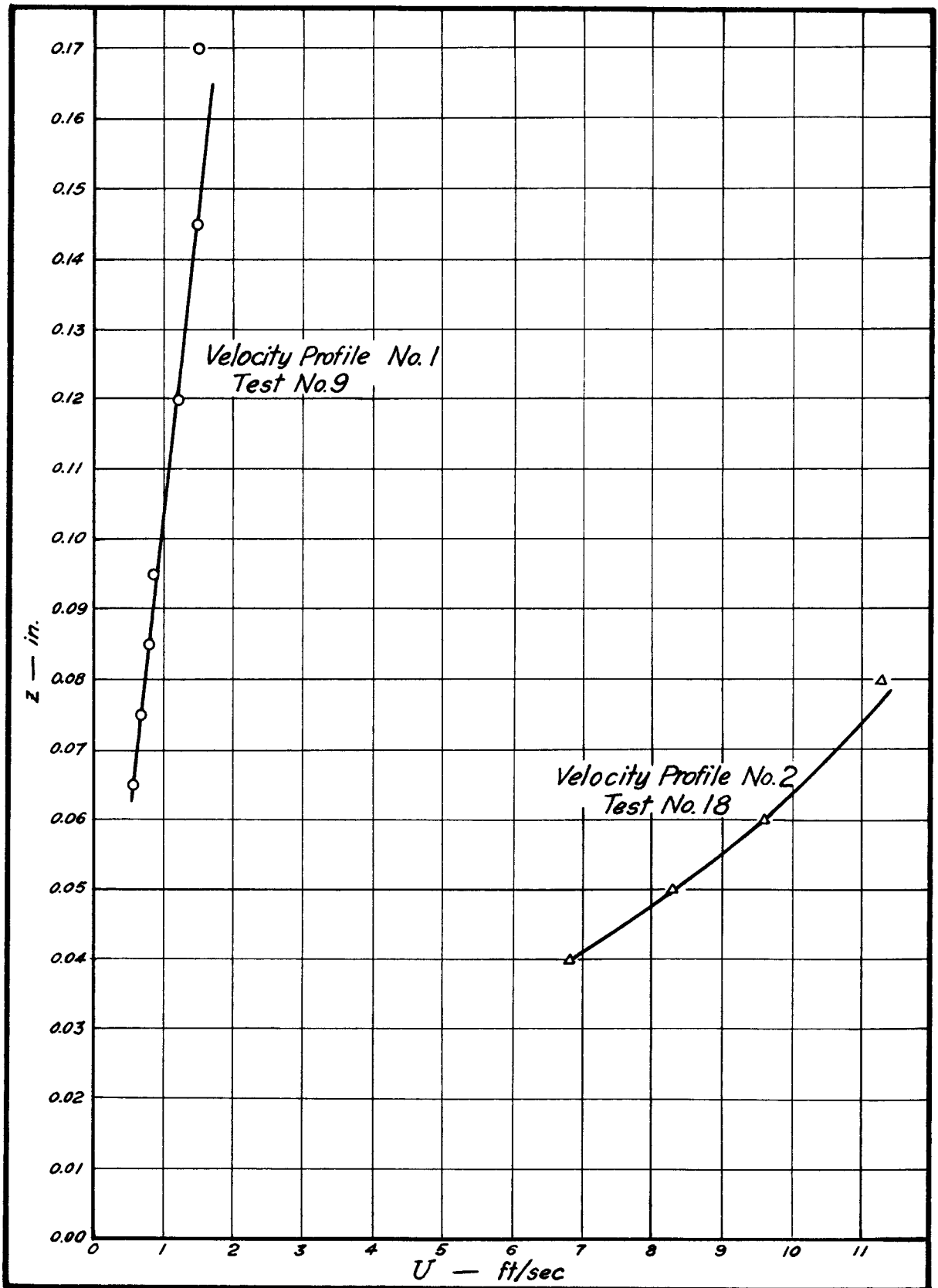
Fig. 4. Examples of lower portion of velocity profiles for model.

in the relationship between U_z and z might be expected for different ambient velocities. This point will be brought out by a review of δ', ϵ, and the estimated model roughness for the two velocity profiles plotted in Fig. 4.

The computation of U_* was based on the applicability of Eq. 1 to the upper turbulent region of the boundary layer. U_* was found by the simultaneous solution of the two equations which were obtained when particular values for U_z and z from the upper region of the boundary layer were substituted into Eq. 1. The evaluation of a roughness ϵ was predicated on the assumption of the existence of a completely turbulent boundary layer and the application of Eqs. 1 and 7. The evaluation of the thickness of the laminar sub-layer δ' was based on the assumption that a laminar sub-layer existed and that Eq. 5 was applicable.

The computation of δ' and ϵ for Velocity Profile No. 1 reveals that

$$\delta' = 0.126 \text{ in.}$$

$$\epsilon = 0.180 \text{ in.}$$

when $\nu = 1.955 \text{ ft}^2/\text{sec.}$

The general roughness of the model was estimated to be 0.02 in. which is approximately 1/9 the roughness necessary to maintain a completely turbulent boundary layer whose upper portion was identical to the turbulent region of Velocity Profile No. 1. The thickness of the computed laminar sub-layer is approximately 6 times greater than the actual surface roughness of 0.02 in. In Chapter II mention was made of the fact that the surface roughness does not affect the laminar sub-layer when the height of the roughness is less than 1/4 the thickness of the laminar sub-layer. Therefore, based on these computations and comparisons, the presence of a laminar sub-layer may be anticipated for Velocity Profile No. 1. A review of Fig. 4 reveals that the lower region of the boundary layer is made up of a laminar sub-layer where U_z varies directly as z.

The computation of δ' and ϵ for Velocity Profile No. 2 indicates that

$$\delta' = 0.025 \text{ in.}$$

$$\epsilon = 0.027 \text{ in.}$$

when $\qquad \nu = 1.832 \text{ ft}^2/\text{sec.}$

In the case of this profile, δ', ϵ, and the estimated model roughness all
have the same approximate value of 0.02 in. As mentioned in Chapter II, a
boundary is considered rough when the surface roughness is greater than 6
times the thickness of the laminar sub-layer. Based on the criteria for
smooth and rough boundaries, the boundary for the case of Velocity Profile
No. 2 cannot be considered to be either smooth or rough; therefore, Velocity
Profile No. 2 might be expected to differ from that produced by a smooth
surface and from that produced by a rough surface. Fig. 3 illustrates the
fact that in the lower portion of the boundary layer for Velocity Profile
No. 2 U_z is a logarithmic function of z and this function is not the same
throughout the height of the boundary layer. This type of relationship is not
typical of flow caused by either a smooth or a rough boundary. Therefore, the
flow may be considered to be of the type in the transitional zone which exists
when a boundary cannot be classified as either smooth or rough according to
the aforementioned criteria.

Recapitulating, the velocity profile above the model was in general
found to be composed of two regions. In the region next to the boundary, the
flow was indicative of either laminar flow or flow produced by a boundary
which could not be classified as either smooth or rough. The outer portion of
the boundary layer was found to be turbulent wherein U_z varied as log z .
U_* could be determined by the application of Eq. 1 to the upper portion of
the boundary layer.

Transformation of model wind structure data for presentation in Figs. 5
and 6. For purposes of comparison with the prototype, the model data were
placed in forms compatible with Figs. 5 and 6 and the prototype data. This
was accomplished in the following manner:

   a. U_z -- velocity at an elevation z used in Fig. 5 only --
ft/sec. The velocities represented in this figure are the actual
velocities measured during the tests at the elevations z .

b. $U_{52.5}$ -- velocity at an elevation of 52.5 ft used in Fig. 6 only -- ft/sec. The velocity in the model which corresponded to an elevation of 52.5 ft in the prototype was measured at an elevation of 1/2000 of that of the prototype elevation which equaled an elevation of 0.315 in. in the model. The velocity distribution in the turbulent region of the boundary layer in the model was considered to be represented by a linear relationship between U_z and the log z . $U_{52.5}$ which corresponded to an elevation of 0.315 in. in the model was taken from the linear relationship between U_z and log z .

c. U_* -- shear velocity -- ft/sec. U_* was based on the applicability of Eq. 1 to the upper turbulent region of the boundary layer where U_z was considered to be a linear function of log z .

d. z_o -- roughness parameter -- ft. In the case of a smooth boundary the nomenclature of z_o as a roughness parameter is a misnomer. However, be that as it may, z_o was assumed to have that value of z for which U_z was equal to zero. This value of z was found by the extrapolation of the line representing the linear relationship between U_z and log z to the point where U_z equals zero. This procedure is illustrated for Velocity Profile No. 1 of Fig. 3 in which case z_o = 0.0055 in.

The model data presented in Fig. 5 was for Sta. 2 only and was obtained by treating the raw data in the fashion outlined in Steps a, c, and d. Each of the velocity profiles from the model for Sta. 2 was made up of many points and the data represented by each point is presented in Fig. 5. It may be well to emphasize the fact that the velocity for each point of the model data presented in Fig. 5 was the actual velocity at that point in the velocity profile and not that velocity indicated by the linear relationship between U_z and the log z .

In Fig. 6, the results of the 29 tests for all four model stations are presented. The model data $U_{52.5}$ and U_* were obtained according to Steps b and c.

Prototype Data

Selection of data for Figs. 5 and 6. The 1/2-hour raw data for the
prototype were reviewed in an endeavor to select significant data in light of
the work done at Colorado A & M College. Only the data which satisfied all
of the following restrictions were selected for analysis:

1. The prevailing wind for a particular 1/2-hour period at each of the
   four meteorological stations was from the south.

2. The average velocity for a 1/2-hour period at Sta. 1 at an elevation
   of 52.5 ft was 3.38, 6.75, 13.52, 27.0, 40.5, or 54.1 ft/sec.

3. The difference between the temperatures recorded at the 6.56 ft and
   52.5 ft levels at Sta. 2 was not greater than + 0.2^{o}C and not less
   than + 0.1^{o}C. This criterion was adopted as being representative of
   adiabatic conditions. In only one instance was the reference temper-
   ature difference taken as + 0.3^{o}C in order to secure data represent-
   ing a velocity of 6.56 ft/sec.

Only 14 profiles were found for Sta. 2 which met these stringent
requirements. The one non-adiabatic case was included in this group.

Transformation of prototype wind structure data for presentation in
Figs. 5 and 6. The data for these 14 profiles were treated in the following
manner to determine the various parameters for Figs. 5 and 6:

a. U_z -- velocity at an elevation z used in Fig. 5 only --
ft/sec. Each of the 14 wind profiles for Sta. 2 was made up of the
velocity at four different elevations. The velocity used in Fig. 5 for
each point of each profile was the actual velocity for that point as
given in the 1/2-hour data. This velocity was used in preference to that
given by the straight line describing the relationship between U_z and
log z because the linear correlation masks the scatter of the actual
data. The value z used in Fig. 5 corresponded to the heights at
which the actual velocities were measured.

b. $U_{52.5}$ -- velocity for Sta. 2 at the 52.5 ft level -- ft/sec.
The velocities at the four elevations of 6.56, 13.12, 26.25, and 52.5 ft

which represented each velocity profile were plotted with log z as
ordinate and U_z as abscissa. The data representing each profile were
found to follow a linear relationship on this type of plot. $U_{52.5}$ as
used in Fig. 6 was taken from the line describing this linear relation-
ship and in general is not the actual value of $U_{52.5}$ as given in the
basic data. Even though the difference between $U_{52.5}$ taken from the
line and $U_{52.5}$ as given in the basic data was small, the value of $U_{52.5}$
as given by the line was considered to be more representative of the
entire profile than that given by the actual data.

c. z_o -- roughness parameter -- ft. z_o was taken as the ordinate
intercept when the straight line representing the relationship between
U_z and log z was extended to cross the ordinate axis at U_z equal to
zero. This method of determining z_o is the same as that used for the
model data.

d. U_* -- shear velocity -- ft/sec. As in the case of the model
data, U_* for a particular wind profile was based on the simultaneous
solution of the equations resulting from insertion of velocities for two
different elevations in Eq. 1. The value of the velocities inserted in
Eq. 1 were taken from the straight line depicting the relationship
between U_z and log z .

The data for Fig. 5 were obtained by treating the raw prototype data in
the fashion outlined in Steps a, c, and d. The data for Fig. 6 were derived
from the raw prototype data according to the procedures outlined in Steps
b and d.

Prototype and Model Wind Structure Comparisons

The prototype and model wind structures will be compared on the basis of
Figs. 5 and 6.

Fig. 5 -- Prototype data. A review of Fig. 5 indicates that the
prototype data for the 14 profiles are dispersed along the Prandtl-von Kármán
relationship (Eq. 1) in four groups. The data plot in four general groups
because the velocities for each profile were measured at four different
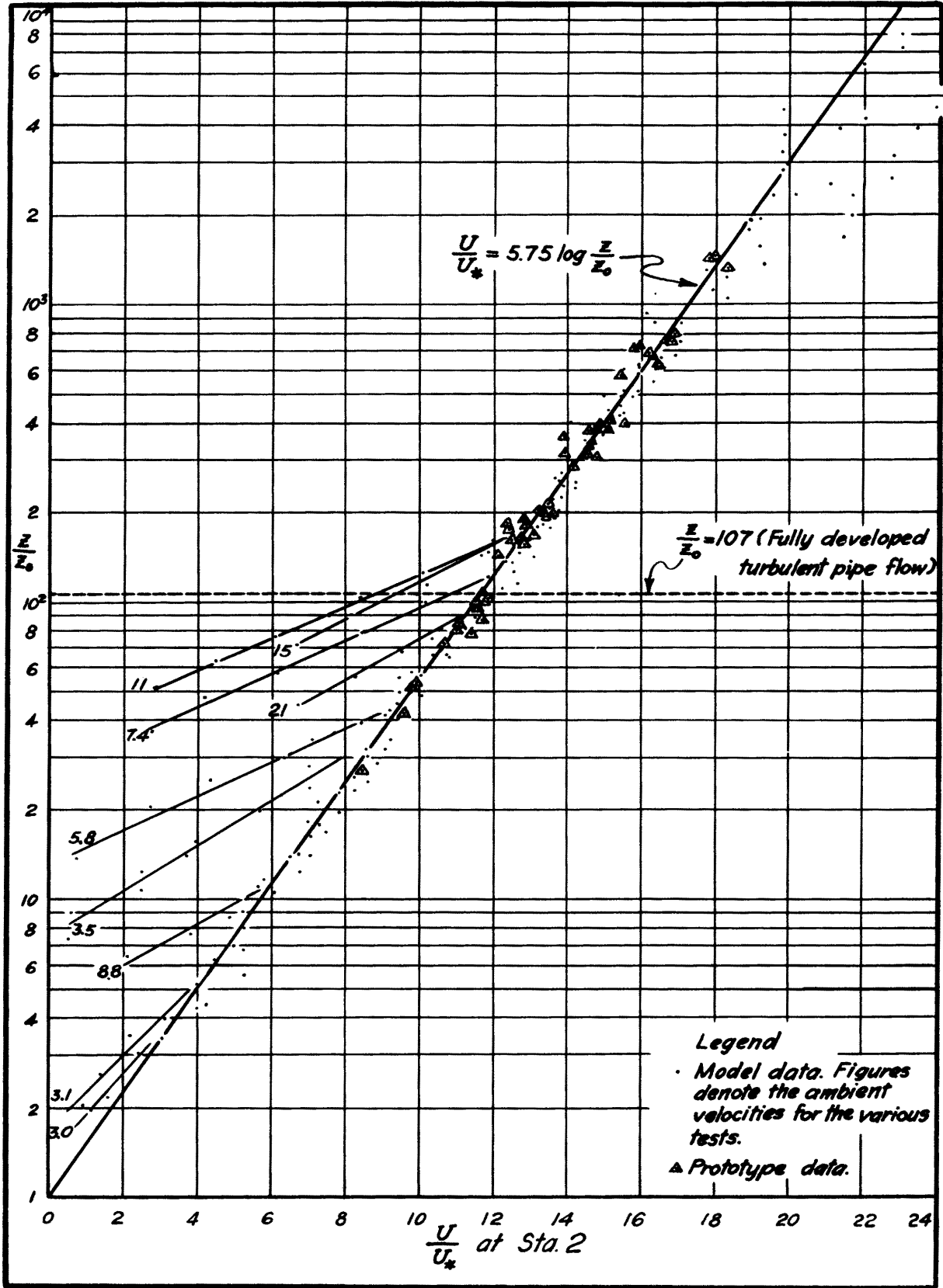
Fig. 5. $\frac{Z}{Z_0}$ vs. $\frac{U}{U_*}$ at Sta.2 for model and prototype.

elevations and these elevations were the same for each profile. Since the relationship between U_z , U_* , z , and z_0 as expressed by Eq. 1 was used in ascertaining z_0 and U_* , the data should fall near the line representing Eq. 1 in Fig. 5.

Fig. 5 -- Model data. Fig. 5 indicates that the model data fall into three ranges:

$$\text{Range 1.} \quad 1 \leqq \frac{z}{z_0} \leqq 10^2$$

$$\text{Range 2.} \quad 10^2 \leqq \frac{z}{z_0} \leqq 10^3$$

$$\text{Range 3.} \quad 10^3 \leqq \frac{z}{z_0}$$

The data comprising the first range may be considered to be those data concerning the lower portion of the boundary layer; that is, the portion usually below 0.1 in. In this region, the points from the various profiles have been joined by lines which become tangent to the line representing Eq. 1. For cases of relatively large ambient velocity, these lines become tangent to the Eq. 1 line at a value of z/z_0 of approximately 107. This fact is significant because it agrees with the empirical relationship between z_0 and δ' which has been derived by other investigators. In other cases, these lines become tangent to the Eq. 1 line at values of z/z_0 less than 107. This deviation from the anticipated pattern may be due to inaccurate measurements or to the incomplete development of the boundary layer.

The data within the second range represent the turbulent portion of the boundary layer. The model data of Fig. 5 for the turbulent region group well around the line representing Eq. 1. There exists a certain amount of scatter but it is not excessive. Such a small degree of dispersion justifies representation of the data by an equation having the form of Eq. 1; however, the von Kármán constant of 0.4 still remains open to question.

The data comprising the third range is scattered. This scatter may be due to instrumentation and/or the presence of a transition zone between the turbulent boundary layer and the ambient air of lower turbulence intensity.

Fig. 5 -- Model and prototype data. The prototype data are in good
agreement with the relationship expressed by Eq. 1. The model data for the
turbulent zone of the boundary layer are also in accord with Eq. 1. The
deviations of the model data in the lower range, $1 \lessapprox z/z_0 \lessapprox 10^2$, are due in
part if not altogether to the presence of the lower portion of the boundary
layer where the flow may be laminar or turbulent. The deviations of the
model data in the upper range $z/z_0 > 10^3$ may be due to instrumentation or a
transition zone between the turbulent boundary layer and the ambient air.

Fig. 6 -- Prototype data. The significant parameters for this plot were
taken from the 14 profiles of the prototype data for Sta. 2. All but one of
the profiles were for adiabatic conditions. The points representing the 14
profiles do not fall on one line as might be hoped for. Though, the points
taken as a whole tend to scatter about a curved line as is to be expected from
the Prandtl-von Kármán relationship, Eq. 1, when z_0 is a function of wind
speed.

Fig. 6 -- Model data. The data of the 29 tests, irrespective of the
station at which the velocity profile was measured, are represented in this
figure. The data for each of the 4 stations have been given a separate
symbol. A review of the data for each station indicates that there is no
marked difference between the relationships of $U_{52.5}$ and U_* for each of the
stations and therefore these model data may be treated as a group. When these
data are treated as a group, a single curved line may be used to approximate
the data.

Fig. 6 -- Model and prototype data. A single curved line may be drawn
through the points representing both model and prototype data. The indicated
correlation between U_* and U at homologous points in the model and
prototype which differ in absolute elevation by the scale factor of 2000,
shows that an approximate modeling of the prototype wind structure has been
effected.

The feasibility of modeling wind structure may be brought out by the
following analysis. When the Reynolds number is used as the criteria for wind
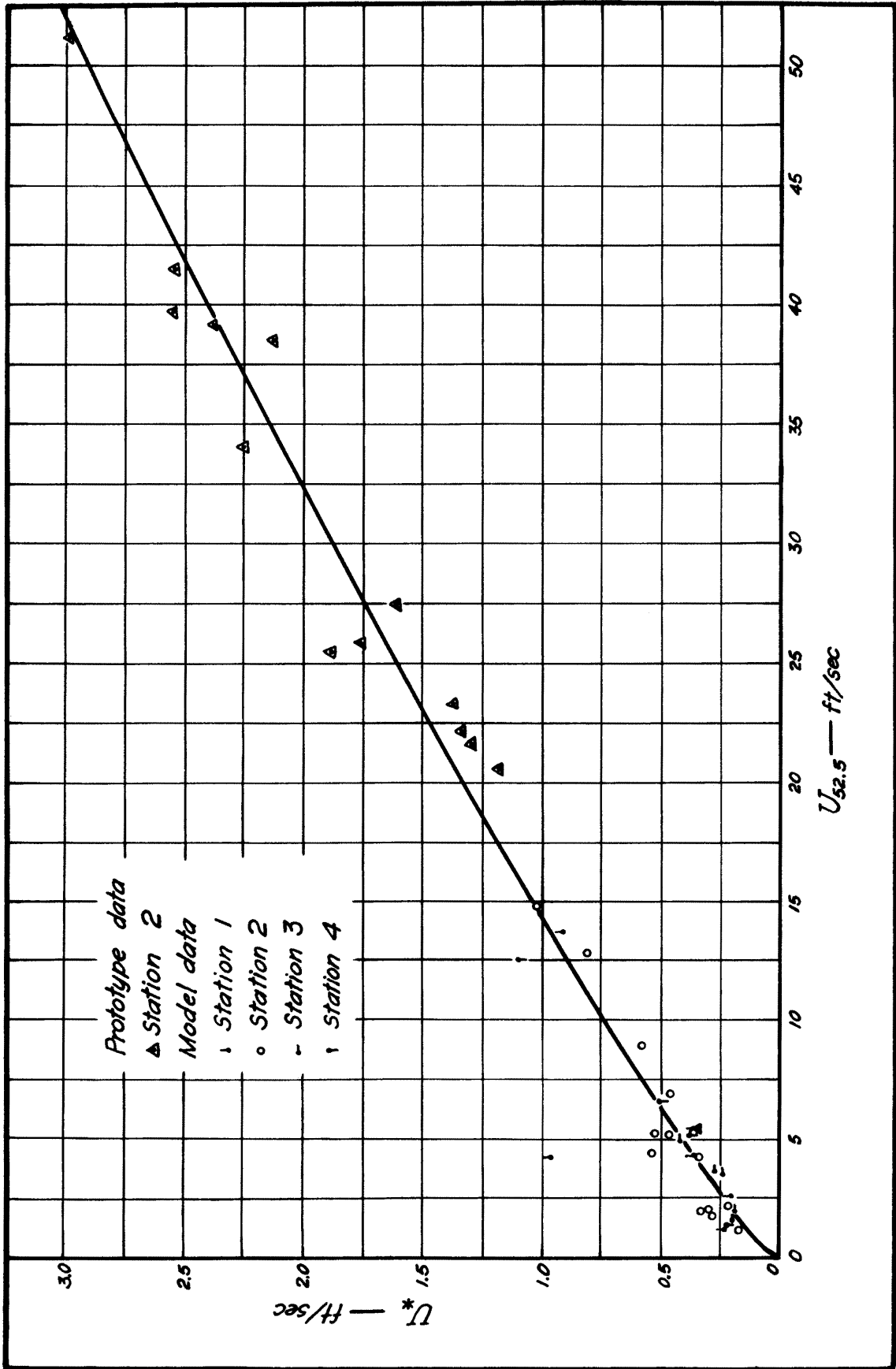
Fig. 6. U_* versus $U_{52.5}$ for model and prototype.

structure similarity between model and prototype, the following relationships
can be evolved:

$$R = \frac{\text{Inertia Forces}}{\text{Viscous Forces}}$$

$$= \rho \frac{U^2}{L} \left(\frac{\tau}{L}\right)^{-1}$$

$$= \frac{U^2}{U_*^2} \, , \tag{28}$$

$$R_m = \left(\frac{U_m}{U_{*m}}\right)^2 , \tag{29}$$

$$R_p = \left(\frac{U_p}{U_{*p}}\right)^2 . \tag{30}$$

R_m should equal R_p for dynamical similarity between model and prototype;
therefore,

$$\frac{U_m}{U_{*m}} = \frac{U_p}{U_{*p}} . \tag{31}$$

The single curved line representing model and prototype data in Fig. 6
indicates that the relationship in Eq. 31 has been approximately satisfied.

In accepting the results of Fig. 6, one should bear in mind the
restricted nature of the data presented. The similarity of results for model
and prototype is applicable in the model only in the turbulent portion of the
boundary layer above the laminar sub-layer -- above about 17 ft in the
prototype. Also, the prototype wind structure was modeled for the condition
of a rather flat terrain and adiabatic lapse rates.

An unsuccessful attempt was made to corroborate the "apparent" agreement
between actual data and Eq. 31 as depicted in Fig. 6. This endeavor was
based on the application of boundary layer equations to the conditions
existing at the model and prototype. Several sources of uncertainty were
encountered which may account in part or in whole for this lack of success.
First, the relationship between ϵ_ℓ and U for the prototype was uncertain.
Second, the applicability of a constant relationship between z_o and ϵ
over a wide range of velocities was a source of concern. Justification of

Fig. 6 based on the relationship governing velocity profiles and shear stress will be given additional consideration in the future.

Evaporation

As indicated in the theoretical analysis a direct comparison of evaporation between the model and the prototype was not forthcoming because of the difference in values of R_* for the model and the prototype due to the scale ratio. Elimination of the reference length, $\sqrt{A}$, from the model and prototype parameters did not afford significant correlations because of the scale effect upon the average vapor transfer rate.

A considerable amount of data concerning momentum transfer has been gathered for a wide range of Reynolds number. Based on Reynolds analogy, it seemed reasonable therefore, that if the proper interpretation were given to these data, it could be extended to vapor transfer (evaporation). If this were possible, then the model data might be expected to follow this extension within its range of Reynolds number and the prototype data might also be expected to agree with this extension within its range of Reynolds number. If such agreement were verified, then the Reynolds analogy based on momentum transfer, could be used to predict evaporation rates. This is the approach which was adopted in an attempt to correlate model and prototype evaporation. The discussion of the data which follows is governed by this goal.

The correlations between N and R_* were drawn from several sources. These sources were grouped as follows:

1. Evaluation of N and R_* through Reynolds analogy.

   a. Case I -- Smooth boundary -- $10^3 \lesssim R_* \lesssim 10^5$.

$$\frac{1}{N} = \frac{5.99}{R_*^{8/9}} - \frac{3.61}{R_*} \tag{22a}$$

   b. Case II -- Smooth boundary -- $R_* \gtrsim 10^5$.

$$\frac{1}{N} = \frac{0.0417}{R_*} \left[4.68 \ (1.194 + \log R_*)^{2.64} \right.$$
$$\left. -8.70 \ (1.194 + \log R_*)^{1.32} \right] \tag{24a}$$

    c. Case III -- Rough boundary -- $R_* \gtrless 10^5$.

$$N = 0.0546 \ R_* \tag{26a}$$

2. Lake Hefner prototype data.

    a. 3-hour average data -- individual values of N versus R_*.

    b. Empirical evaporation equation based on U. S. Geological Survey Circular #229 (18:65, Eq. 58).

$$N = 0.0203 \ R_* \tag{27}$$

3. Lake Hefner model data.

    a. Individual values of N versus R_* .

4. Albertson's (1) data.

    a. Individual values of N versus R_* .

The reader is referred to Appendix C for a description of the approximations and methods used in changing the data to the aforementioned forms. All of the data comprising the four groups have been represented in Fig. 7.

In Fig. 7 the individual values of N versus R_* for Albertson's data were plotted. These data substantiate Eq. 22a when $R_* \gtreqless 6 \times 10^2$ for the values of $x/\sqrt{A}$ used in Albertson's experimental study. This result adds support to the validity of the von Karman extension.

The agreement between the Lake Hefner model data as represented by points plotted in Fig. 7 and Eq. 22a is fair. In spite of using $\sqrt{A}$ for L in the analysis and the deviation of the lake shape from a square, one may conclude that the von Kármán extension of Reynolds analogy is valid.

An inspection of the 3-hour average prototype data plotted in Fig. 7 indicates that it groups rather well about the prototype empirical equation, Eq. 27. This tends to imply that the assumptions made in the derivation of Eq. 27 from that given in U. S. Geological Survey Circular #229 were not groundless. Therefore, the prototype data will be considered to be represented by Eq. 27 in further discussions.

Fig. 7 indicates that the relationship between N and R_* given by Eq. 24a is similar to that given by Eq. 27. In the neighborhood of $R_* = 3 \times 10^7$, both equations give practically the same results although the
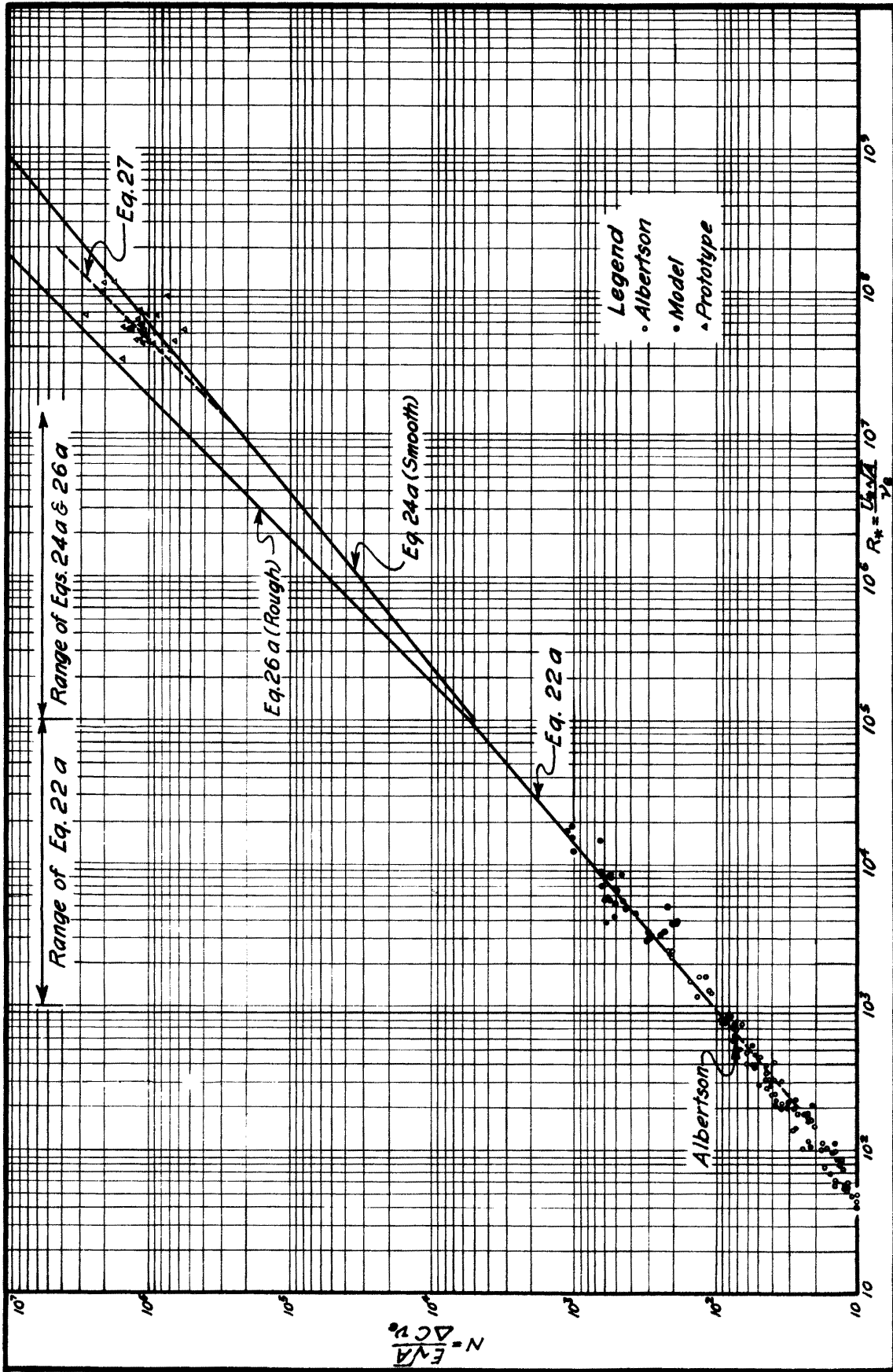
Fig. 7. Evaporation Correlations.

similarity decreases as R_* increases beyond this value. Despite this increasing divergence as R_* becomes larger, the overall agreement between actual data (Eq. 27) and that predicted by the von Kármán extension of the Reynolds analogy (Eq. 24a) is striking. This is particularly evident when consideration is given to the fact that Eq. 24a is based on a drag coefficient C_f for a smooth, non-moving, rectangular boundary which can only be applied with reservations to a moving water surface disturbed by waves.

In the range of $R_* \gtrless 10^5$, the values of N predicted by Eq. 26a are too large when co 1red to values given by Eq. 27. The value of C_f used in Eq. 26a is based on an average lake surface roughness ϵ_w of 0.754 ft which was taken __om Table I - Appendix B. The value of C_f appears to be too large which is in part due to using too large a value for ϵ_w. Values of ϵ_w were based on the data contained in U. S. Geological Survey Circular #229 (18:49) which were computed on the assumption that Eqs. 6 and 7 are valid over a free water surface. The assumption is questionable and the value of C_f may be resolved better after C_f for Lake Hefner has been determined from measured magnitudes of "set-up". The utility of Eq. 26a lies in the fact that it establishes an upper bound on N .

One must remember when evaluating these results that Eqs. 24a and 26a were derived on the basis of the planetary boundary layer being 3280 ft thick. This thickness is not constant and may at times deviate considerably. However, the error introduced by assuming δ as 3280 ft is not too serious since a variation of $\pm$ 50% from the value used causes only a change of about $\pm$ 15% in N .

In the range of $R_* \gtrless 10^5$, Fig. 7 indicates that the extension of Reynolds analogy for a smooth surface gives results which are more nearly comparable to actual data than does the extension for a rough surface. This implies that the water surface, although it may appear rough by the presence of waves, in reality behaves more nearly as though it were smooth. This statement is not meant to dismiss the water surface roughness in its entirety but rather is intended to imply that the water surface roughness is not as

great as might be imagined from the appearance of the waves. This may be accounted for, at least in part, by the fact that not only do the waves travel in the direction of the wind but the water at the surface also moves in the direction of the wind. If a means were known by which water surface roughness could be more properly evaluated, then the extension of Reynolds analogy might coincide more favorably with actual data. Additional research must be performed to correlate the relationships between wind, waves, and surface drag.

In summary it may be stated that the agreement between actual data and the extension of Reynolds analogy for $R_* < 10^5$ is good. For $R_* > 10^5$, the extension of Reynolds analogy tends to bracket actual evaporation results with the analogy for a smooth surface in much closer agreement with actual data than that for a rough surface. In order to improve the correlations between N and R_* as given by actual data and that predicted by the extension of Reynolds analogy, a better understanding must be had of the relationships between wind, waves, and surface drag.

Chapter V

SUMMARY

The Lake Hefner model study was undertaken to determine:

1. Correlations of wind structure between model and prototype.

2. Correlations of evaporation between model and prototype.

Only the results of the work to December 1952 are presented in this report. The practical significance of this work will be discussed in Part II of the Final Report.

Wind Structure

Measurements of wind structure above the 1:2000 undistorted scale model and the prototype indicated the following:

1. The boundary layer above the model was composed of two regions. The lower region was characterized by two different types of flow. In some instances the flow was laminar which was indicative of flow near a smooth boundary. In others, the flow was of a type which might be indicative of a boundary which was in the transitional zone between a rough and smooth boundary. The upper portion of the boundary layer was turbulent and followed the Prandtl-von Kármán equation

$$\frac{U}{U_*} = 5.75 \log \left(\frac{z}{z_o}\right) . \tag{1}$$

2. The wind structure data (Fig. 6) indicate that fair similarity existed between model and prototype for the relationship of $U_{52.5}$ versus U_* . This similarity based on the upper portion of the boundary layer above the model implies that the prototype wind structure was modeled for the conditions of a flat terrain and an adiabatic lapse rate.

44

<u>Evaporation</u>

A comparison of evaporation rates for model and prototype indicates the following:

1. The evaporation coefficient N may be defined in terms of R_* for both the model and the prototype.

2. The data for the model are closely represented by Eq. 22a which was derived from an extension of Reynolds analogy.

3. The data for the prototype are closely represented by Eq. 27 in terms of N and R_* .

4. The range of R_* for the model was $2 \times 10^3 < R_* < 2 \times 10^4$ while the range of R_* for the prototype was $3 \times 10^7 < R_* < 2 \times 10^8$. In the case of flat surrounding terrain, this study indicates that Reynolds analogy may offer a means of estimating evaporation when R_* for particular bodies of water fall in the range of $10^3 < R_* < 10^9$.

5. The significance of Reynolds analogy as applied to evaporation might be increased by a better understanding of the relationships between wind, waves, and surface drag.

6. No practical modeling technique was conceived which would permit direct evaluation of N_p from model measurements.

<u>Recommended Investigations</u>

Investigation along the following lines may increase the applicability of models for the determination of evaporation and wind structure. Additional research may also improve the correlation between Reynolds analogy and actual evaporation. The work to be performed under the remainder of the contract for the Lake Hefner Model Study includes plans for a study of some of these suggestions.

1. Measure the intensity of turbulence above the model. Measurements of this nature may permit duplication in other wind tunnels of the results obtained from this study.

2. Determine the effect of wind direction on the rates of evaporation from the model of Lake Hefner.

3. Determine the effect on evaporation of an upwind barrier which might be considered to simulate a range of hills. A study of this nature may indicate the feasibility of model studies for bodies of water which are surrounded by terrain which is not relatively flat.

4. Obtain data for N within the range of $10^4 \lessgtr R_* \lessgtr 10^7$ based on the work of other investigators.

5. Study the relationships between wind, waves, and surface drag. Better correlation between actual evaporation data and Reynolds analogy might be forthcoming if the relationships between wind, waves, and surface drag were better understood.

6. Study further the possibility of direct correlation between the model evaporation data and the prototype evaporation data.

BIBLIOGRAPHY

1. Albertson, M. L.   Evaporation from a plane boundary. Heat Transfer and Fluid Mechanics Institute (Preprints of papers) held at Stanford University, pp. 243-254, June 1951.

2. Anderson, E. R., Anderson, L. J., and Marciano, J. J.   A review of evaporation theory and development of instrumentation (Interim report: Lake Mead Water Loss Investigations). U. S. Navy Electronics Laboratory, San Diego, California, Report #159, February 1, 1950.

3. Berry, F. A., Bollay, E., and Beers, Norman R.   "Handbook of Meteorology." McGraw-Hill Book Company, Inc., 1945.   1068 p.

4. Cummings, N. W.   The evaporation-energy equations and their practical application. Trans. American Geophysical Union, vol. 21, part 2, pp. 512-522, 1940.

5. von Kármán, Th.   Mechanische Ähnlichkeit und Turbulenz.   Nachr. Ges. Wiss. Göttingen, Math. Phys. Klasse, p. 58, 1930.

√ 6. von Kármán, Th.   The analogy between fluid friction and heat transfer. Trans. A.S.M.E., vol. 61, pp. 705-710, 1939.

7. Klebanoff, P. S. and Diehl, Z. W.   Some features of artifically thickened fully developed turbulent boundary layers with zero pressure gradient.   NACA Technical Note No. 2475, Washington, D. C., October 1951.

8. Linsley, R. K., Kohler, Max A., and Paulhus, J. L. H.   "Applied Hydrology." McGraw-Hill Book Co., Inc. 1949.   689 p.

9. Marvin, C. F.   Psychrometric tables for obtaining the vapor pressure, relative humidity, and temperature of the dew point. W. B. No. 235, U. S. Department of Commerce, Weather Bureau, 1941.

10. Nikuradse, J.   Strömung in glätten Rohren.   VDI - Forschungsheft 356, 1932.

11. Nikuradse, J.   Strömungsgesetze in rauhen Rohren.   VDI - Forschungsheft 361, Berlin, 1933.

12. Prandtl, L.   Ueber die ausgebildete Turbulenz. ZAMM, p. 136, 1925, and Verhdl. II. Internat. Kongress f. Angew. Mech., Zürich, 1926.

√ 13. Reynolds, O.   Proc. Lit. Phil. Soc. of Manchester, vol. 14, 1875.

14. Rohwer, Carl   Evaporation from free surfaces. Technical Bulletin No. 271, U. S. Dept. of Agric. in cooperation with Colorado Agricultural Experiment Station, December 1931.

15. Schlichting, H.   Lecture Series "Boundary layer theory Part II-Turbulent flows." NACA Technical Memorandum 1218, April 1949.

48

16. Sutton, O. G. "Micrometeorology." McGraw-Hill Book Co., 1953. 333 p.

17. Sverdrup, H. U. On the evaporation from oceans. Journal Marine Research, vol. 1, No. 1, pp. 3-14, 1937-38.

18. - - - - - - - - Water-loss investigations: Volume 1 -- Lake Hefner studies technical report. Circular No. 229. U. S. Geological Survey, 1952. (This report is also issued as N.E.L. Report 327, San Diego 52, California).

APPENDIX

Table of Contents

Appendix A

DETAILS OF EQUIPMENT AND PROCEDURES

This section of the Lake Hefner Model Study report is devoted to the description of the experimental equipment and procedures. The details concerning this work and the attendant problems may serve as a guide for future work of this nature.

Description and Operation of Equipment

Tunnel

The tunnel used for the Lake Hefner model study was constructed by Colorado A & M College under a contract with the Office of Naval Research, Figs. 8, 9, and 10. This tunnel, as originally designed, was meant to be used chiefly as a recirculating tunnel, but due to the fact that evaporation of water was a part of the Lake Hefner study, the possibility of the humidity changing continually as the air was recirculated in the tunnel had to be eliminated. Therefore, the tunnel was operated as a non-recirculating tunnel. This was accomplished by the installation of a check wall which prevented recirculation of the air within the tunnel and by the opening of the intake and exhaust doors.

The design of the tunnel is such that test sections of various sizes can be installed. Prior to the Lake Hefner study, the tunnel was equipped with a test section made up of a 6 feet square section 13 ft long and a 9 feet square section 13 ft long. The plans for Lake Hefner called for a test section 9 feet square and 26 ft long. Therefore, two new 9 feet square test sections, one 8 ft long and the other 5 ft long, were built to be used with existing sections, Fig. 11.

The new 5-ft section was constructed with a movable floor. The object of the movable floor was to provide a means of raising the floor of the tunnel upstream from the model so that it was at the same elevation as that of the

50
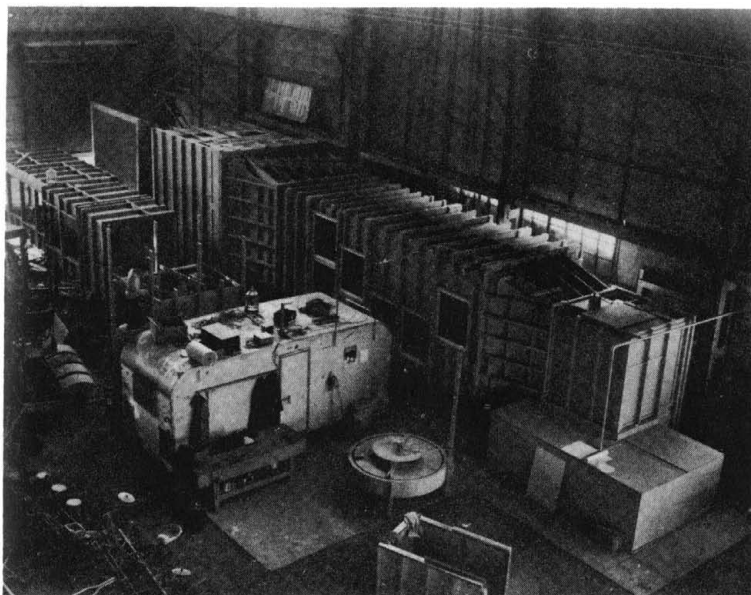
Fig. 8. Interior portion of
the wind tunnel at
Colorado A & M
College.
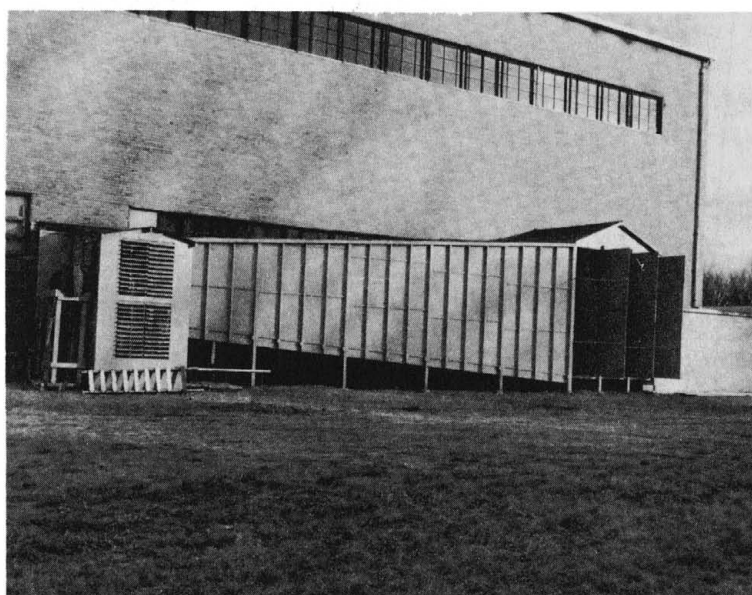
Fig. 9. Exterior portion of
the wind tunnel at
Colorado A & M
College.

terrain, Fig. 12. The movable floor was warped only along the longitudinal
axis of the tunnel and was so shaped as to be horizontal at each end. This
gradual bending allowed a change in floor elevation of 2-1/8 in. in a
distance of 5 ft.
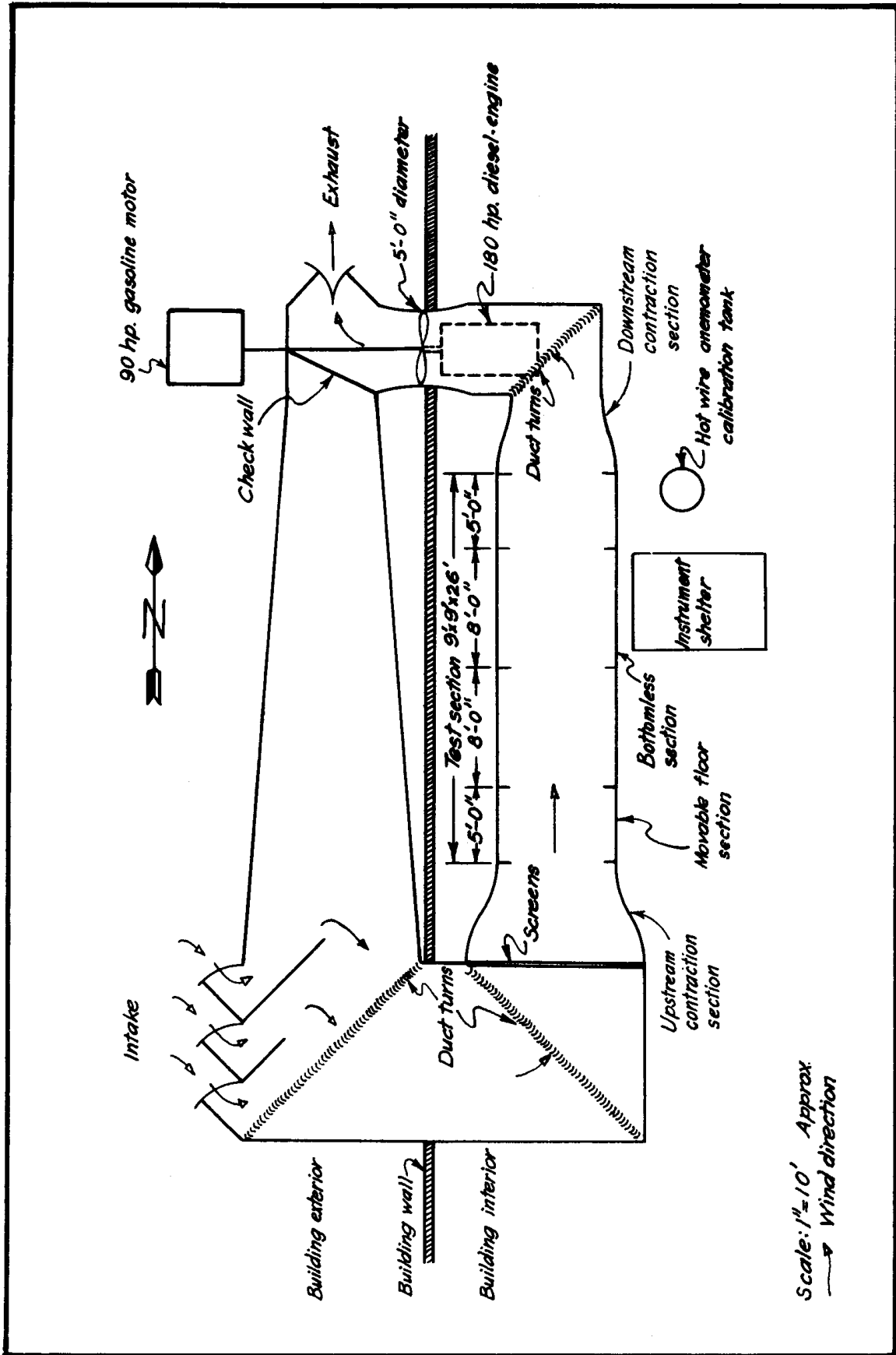
Fig. 10. Schematic diagram of wind tunnel.
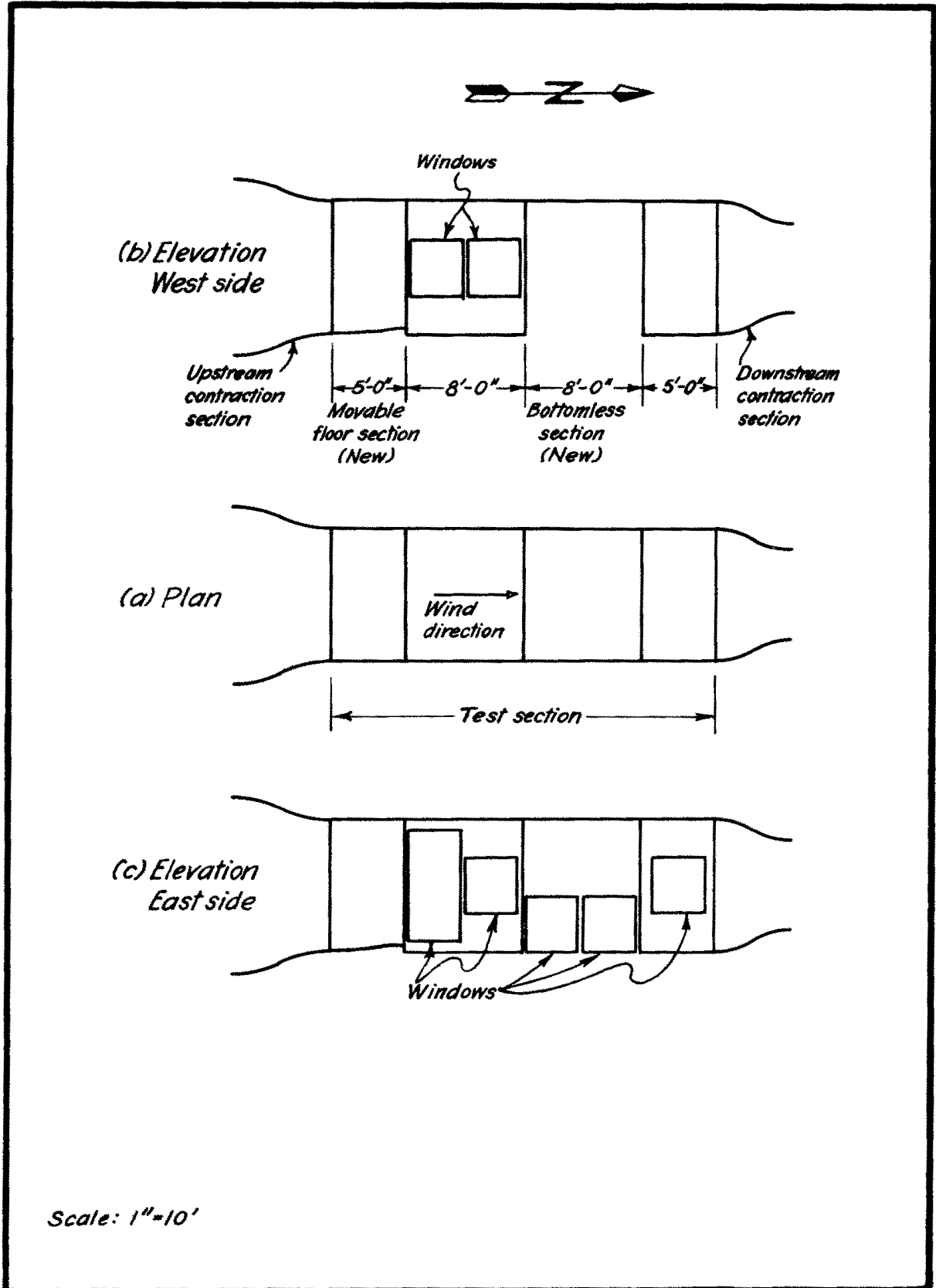
Fig. 11. Test section of the wind tunnel.
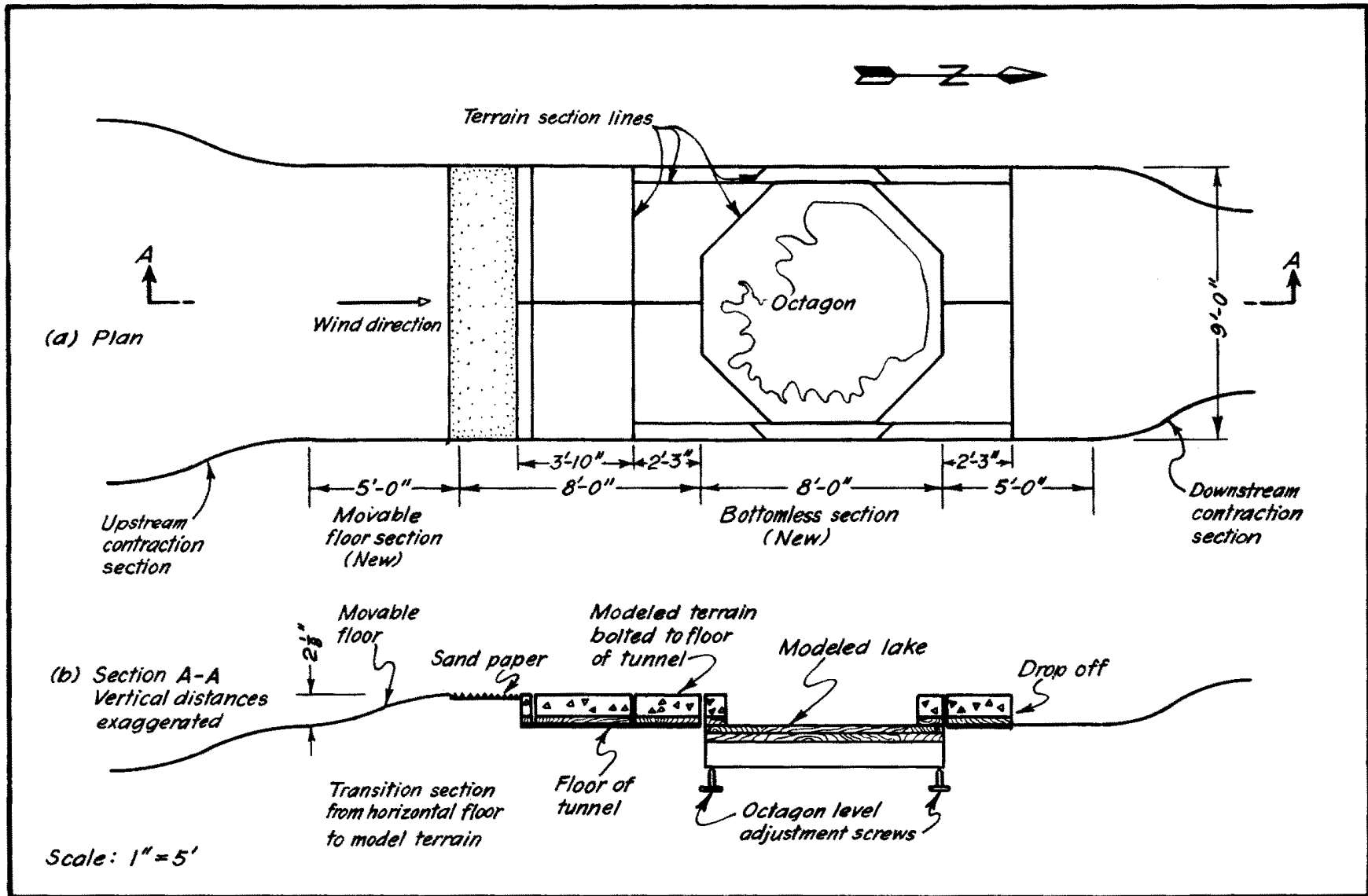
Fig. 12. Sectioning and model arrangement in the tunnel.

(a) Plan

Terrain section lines

Octagon

Wind direction

9'-0"

A

A

Upstream contraction section

5'-0"

Movable floor section (New)

3'-10"

2'-3"

8'-0"

8'-0"

Bottomless section (New)

2'-3"

5'-0"

Downstream contraction section

(b) Section A-A Vertical distances exaggerated

Movable floor

2¼"

Sand paper

Modeled terrain bolted to floor of tunnel

Modeled lake

Drop off

Transition section from horizontal floor to model terrain

Floor of tunnel

Octagon level adjustment screws

Scale: 1" = 5'

The new 8-ft section, Figs. 11 and 12, was constructed without a bottom to permit installation of that part of the model called the octagon. The octagon was the portion of the model which included the model of the lake.

Eight windows were installed in the walls of the tunnel to permit observation of the model during operation, Fig. 11.

The propeller which circulated the air within the tunnel was a 5-ft wooden four-bladed run-in propeller. It could be driven by either a 92-HP gasoline engine or by a 180-HP diesel engine as dictated by the power requirements.

Terrain

A consideration of the scale effect indicated that the similarity between the model and the prototype would improve as the size of the model is increased. As the size of the model is decreased, the effects of the following become more significant:

1. Lateral diffusion of water vapor.

2. Inaccuracies in the measurement of the various meteorological factors.

3. Difference in Reynolds number between model and prototype.

It was decided to use a tunnel test section 9 feet square and 26 ft long for the Lake Hefner model study. This size test section permitted the adoption of the convenient scale of 1:2000, both horizontally and vertically.

The model of Lake Hefner and the surrounding terrain was based on the U. S. Geological Survey advance print of Britton Quadrangle, Oklahoma. Because of the extraneous amount of detail on the advanced print of the U.S.G.S. quadrangle sheet, a tracing of it was made on which were copied only the contour lines and outline of the lake. A system of horizontal control was also laid out on the tracing. This control consisted of marks placed 3 in. on center in both a north-south and east-west direction.

The terrain surrounding the lake was divided into sections in such a manner as to increase the ease of handling and to permit placing of the model in the wind tunnel in any one of the eight cardinal directions.

The basic plan for the construction of the model was as follows:

1. Photographic negatives were made of the tracing of the U.S.G.S. map.

2. The 1/2-in. plywood, which formed the base of the model, was cut into the various shapes dictated by the sectioning plan for the model, Fig. 12 (plan).

3. By the use of a photographic enlarger and the negatives of the traced map, the topographic features were projected upon the 1/2-in. plywood base sections to the proper scale. These projected terrain features were copied onto the plywood. The horizontal control points placed on the tracing served at this point as a means of establishing the horizontal scale, 1:2000. They also provided a means of checking for distortion in the projected map. The amount of distortion present was negligible.

4. Nails were driven into the 1/2-in. plywood base along the copied contours. The nails were driven to a height which was proportional to the elevation represented by the contours.

5. The terrain between the nails was modeled with a Persolite-cement mixture.

6. A thin coat of plaster of Paris was placed on the Persolite. The model was sanded down to the heads of the nails so as to provide a smooth surface.

7. The sections were installed in the tunnel.

8. The alignment of the sections was checked.

9. The cracks between the sectioned terrain were repaired.

10. The surface was painted to improve the smoothness and appearance.

The horizontal control was maintained in the model by means of nails driven along each of the contours. These same nails also served as the vertical control since the height they protruded from the plywood was proportional to the elevation represented by the contour. The elevation of the lowest point modeled was 1080 ft. The thickness of the modeling material at this elevation was set at 1/2 in. Each 10 ft change in elevation in the

prototype, as represented by the contour lines, was modeled by a change of 0.06 in. in the height of the nails. Since elevation 1080 ft was represented by a nail height of 0.5 in., elevation 1340 ft, the highest elevation modeled, was represented by a nail height above the plywood base of 2.06 in. A separate template was made for driving the nails along each contour. These templates were made from a piece of 1 in. round steel cut to the proper length with a hole drilled along the longitudinal axis of such a size as to permit the passage of the heads of the nails.

In order to check the vertical alignment of the model after it had been installed in the tunnel, a set of brass plugs were made and placed at strategic points on each section of the terrain. These plugs were made of brass so that they could be easily distinguished from the steel nails. The brass elevation markers were installed in a manner similar to that used in placing the steel nails.

Consideration was given to several types of modeling material. It would have been desirable from the consideration of strength to model the terrain with a sand-cement concrete but this method was discarded because of the great weight. Vermiculite combined with cement was satisfactory as a modeling material so far as weight was concerned but was not used because of its "spongy" behavior during placement. A Persolite-cement mixture was found satisfactory and adopted. It was light enough in weight so that there was no problem in moving the sections of terrain. The rather "dry" mix of water, Persolite, and cement was compacted to make a dense yet light molding material when dried out. For modeling purposes, the Persolite-cement mix had adequate compressive strength. But, the bond between this molding material and the nails and the wooden base was not very strong. Therefore, a higher tensile strength for the Persolite-cement mix would have been desirable.

In the process of modeling the terrain, the Persolite mixture was placed so as to cover the nails entirely. Then after the Persolite had set, it was scraped down to the elevation indicated by the tops of the nails. As a result of this scraping, the surface of the Persolite was rough. Therefore,

a thin coat of plaster of Paris was applied to the surface. After the plaster of Paris had set and dried, it was sanded down to the elevation indicated by the nails. The terrain surface, as a result of this procedure, was rather smooth and the average local roughness of the surface was estimated to be 0.02 in. by comparison with the elements of a machinist's feeler gauge.

The center section of the model which contained the lake was made in the shape of an octagon. The size and shape of the octagon was such that it could be positioned in the tunnel in any direction which was an integral multiple of 45° from the north-south direction of the model.

During the assembly of the sections of the wind tunnel, particular attention was given to the alignment of the tunnel floor. The octagon, which set in the section without a floor, was provided with four screw jacks so that the position of the octagon could be adjusted vertically. After the sections of terrain were placed on the floor of the tunnel, they were bolted down along with those sections on the octagon. After the terrain had been placed in the wind tunnel, a set of levels was run on the brass plugs used for elevation controls. It was found that the model was in good vertical alignment. There was little question concerning the horizontal alignment since the method of modeling precluded any significant deviation in this direction.

Plaster of Paris was used as a fill material for the cracks between the sections. The modeled terrain was given several coats of gray paint to smooth out the surface and to improve its appearance. To prevent the escape of water from the lake, the cracks between the terrain and the pan were sealed by the application of a coat of rubber cement.

To help produce a fully developed turbulent boundary layer over the model, a strip of sandpaper, 23-1/2 in. long and the width of the tunnel was installed, Figs. 12 and 13. Particulars concerning this paper are:

1. Manufacturer: Minnesota Mining and Manufacturing Company, St. Paul 6, Minnesota.

2. Grade and trade name: 3M Imperial Flint Paper.
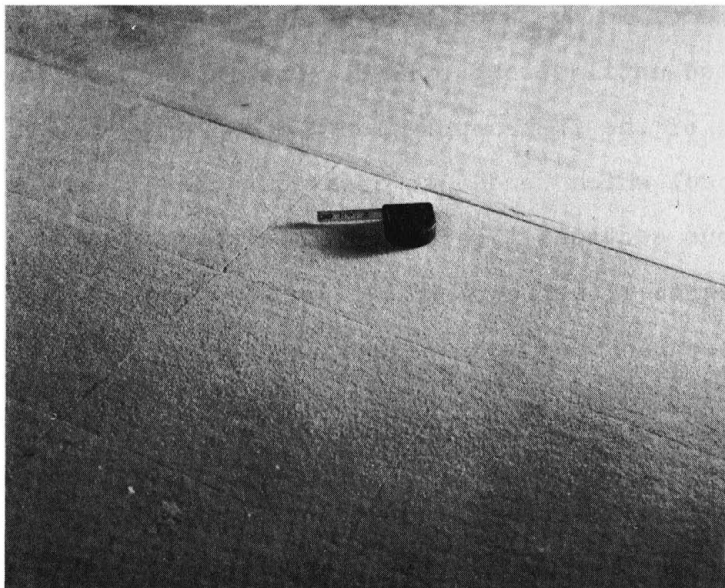
Fig. 13. Sandpaper upwind from the model.

3. The size of the sand grains on this sandpaper was estimated to be approximately 1/32 in. in diameter. The sand grains were densely placed on the paper.

The terrain downstream from the lake was permitted to end abruptly because the belief was held that this drop would not affect measurements being made at the lake, Figs. 12 and 14.
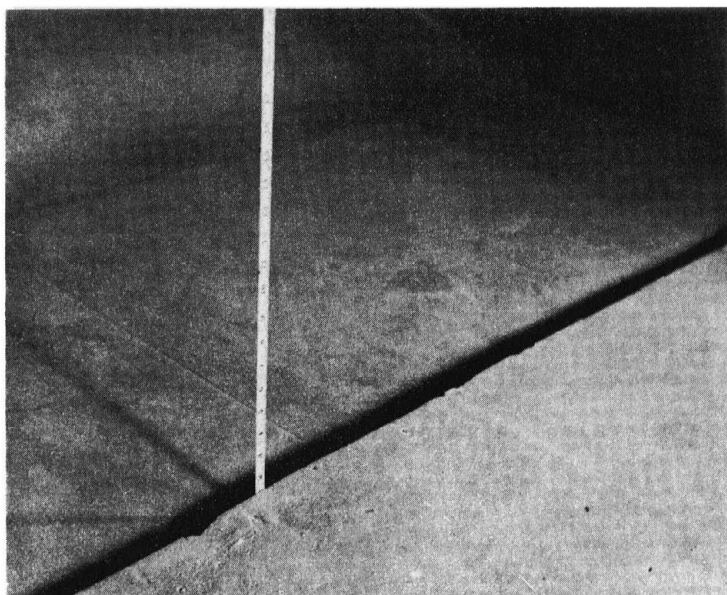
Fig. 14. Drop at downstream end of modeled terrain.

The installation of the model in the wind tunnel was completed in July, 1952 and it was not tested until October, 1952. The intervening time was absorbed in the perfection of the instrumentation. This latter work necessitated walking on the model which tended to break out the plaster of Paris filler between the various sections. These cracks were replastered and refinished but never to the degree of perfection that existed when the model was first completed. It was assumed that these slight imperfections were not serious since most of them were a foot or more from the lake.

Lake

Consideration of the outline of the lake as presented by the U. S. Geological Survey in the advance print of the Britton Quadrangle, Oklahoma (Scale 1:20,000, C.I. 10 ft) indicated that it could be duplicated in the model as drawn only with considerable difficulty, Fig. 15. Therefore, the liberty was taken while tracing the advanced print of rounding off the sharp corners of the lake, Fig. 16, while still maintaining the same approximate area.

During the data taking period for the prototype study, the lake stage varied between an elevation of 1190.8 ft and 1195.3 ft. This change of stage for the prototype was, relatively speaking, small and therefore duplication of this change in stage for the model was considered unnecessary (a 4-ft elevation change in the prototype was represented by 0.024 in. change in the model). A change of stage in the model would have been a major undertaking. The area of the model of the lake was 25.01 sq ft which corresponded to the area of the prototype at a lake stage of 1193.6 ft.

The bottom and sides of the pan for the lake were made from 20-gage galvanized sheet metal. The outline of the lake was transferred from the negative of the tracing of the advance print of the Britton Quadrangle in the same manner as that used for the terrain. After the sides of the pan were soldered to the bottom they were filed down so that the rim height corresponded to an elevation of 1193.6 ft in the assembled model, Fig. 17. Consideration of all factors involved resulted in the inside depth of the pan
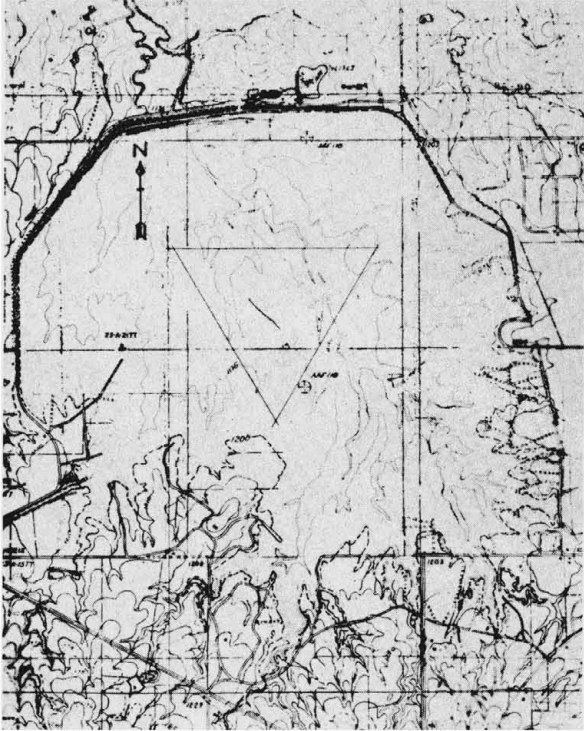
Fig. 15. Lake Hefner and vicinity -- advance print of U.S.G.S. Quadrangle sheet, Britton, SE, Oklahoma.
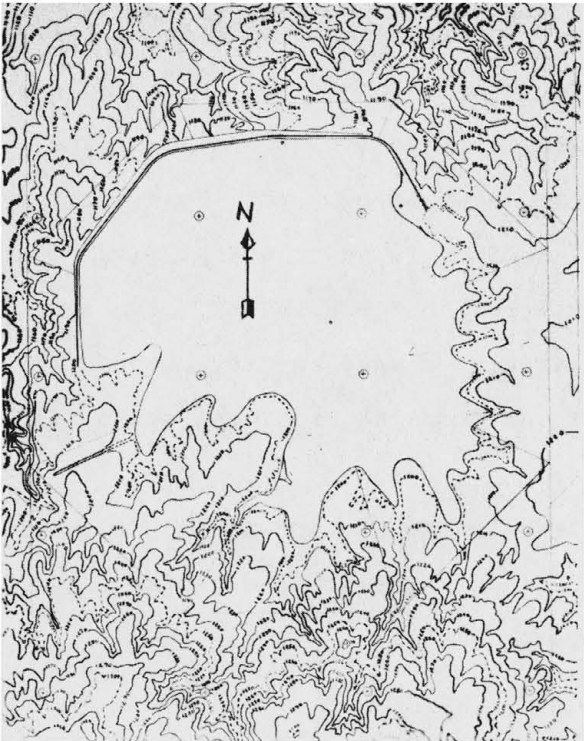
Fig. 16. Modified lake outline.
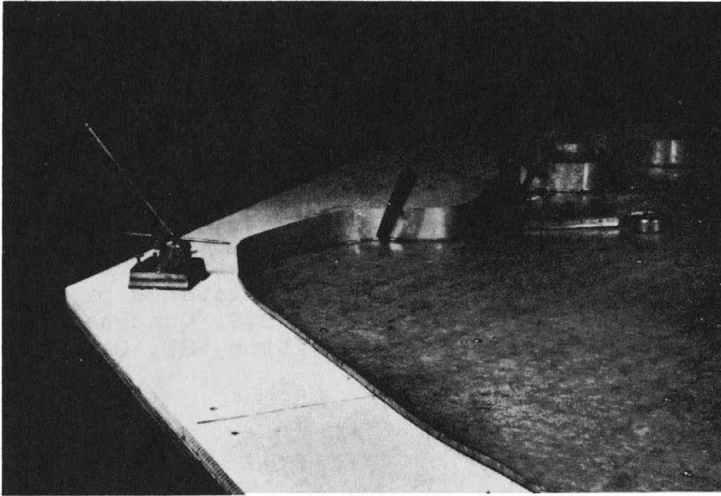
Fig. 17. Fabrication of sheet metal pan for the modeled lake.

being 1.67 in., Fig. 18.

Two appurtenances were placed in the bottom of the lake to accommodate various phases of the instrumentation. One of the appurtenances provided for the egress of wires from the lake stage indicator and the thermocouples, Fig. 19a. The other served as the water supply connection. An air trap was incorporated in the design of this water supply connection so as to trap air before it could reach the lake, Fig. 19b. Air on the underside of the evaporation surface might have been a troublesome problem. However, very little air was caught in this trap. This fact is attributable to the lack of air in the distilled water used for evaporation purposes and to an airtight water supply system. A thermocouple was also placed in the water supply connection attached to the pan so that the temperature of the water being supplied to the lake could be measured.

After all appurtenances were affixed to the pan and the pan secured to the octagon, several coats of a rubber cement were applied to the interior and exterior of the pan as an added precaution against leaking.

Evaporation Surface

One of the major problems to be overcome during the course of the Lake Hefner project was the development of a suitable evaporation surface. The use

Plaster of Paris evaporating surface

Elevation 1193.6

1/2"

1.67"

.04"

1/4" Gravel

20 Gage sheet metal

Solder

Elevation 1193.6

Nails—Vertical and horizontal control

Persolite cement molding medium

Elevation 1193.6

Elevation 1080.0

.68"

.50"

.53"

1/2" (nominal) Plywood

1/2" Plywood

1/2" Plywood

Method of bolting model to octagon

Height proportional to the elevation of the modeled terrain

Section through Model

Section through part of Octagon

Scale: Full size

Fig. 18. Details of modeled lake and surrounding terrain.
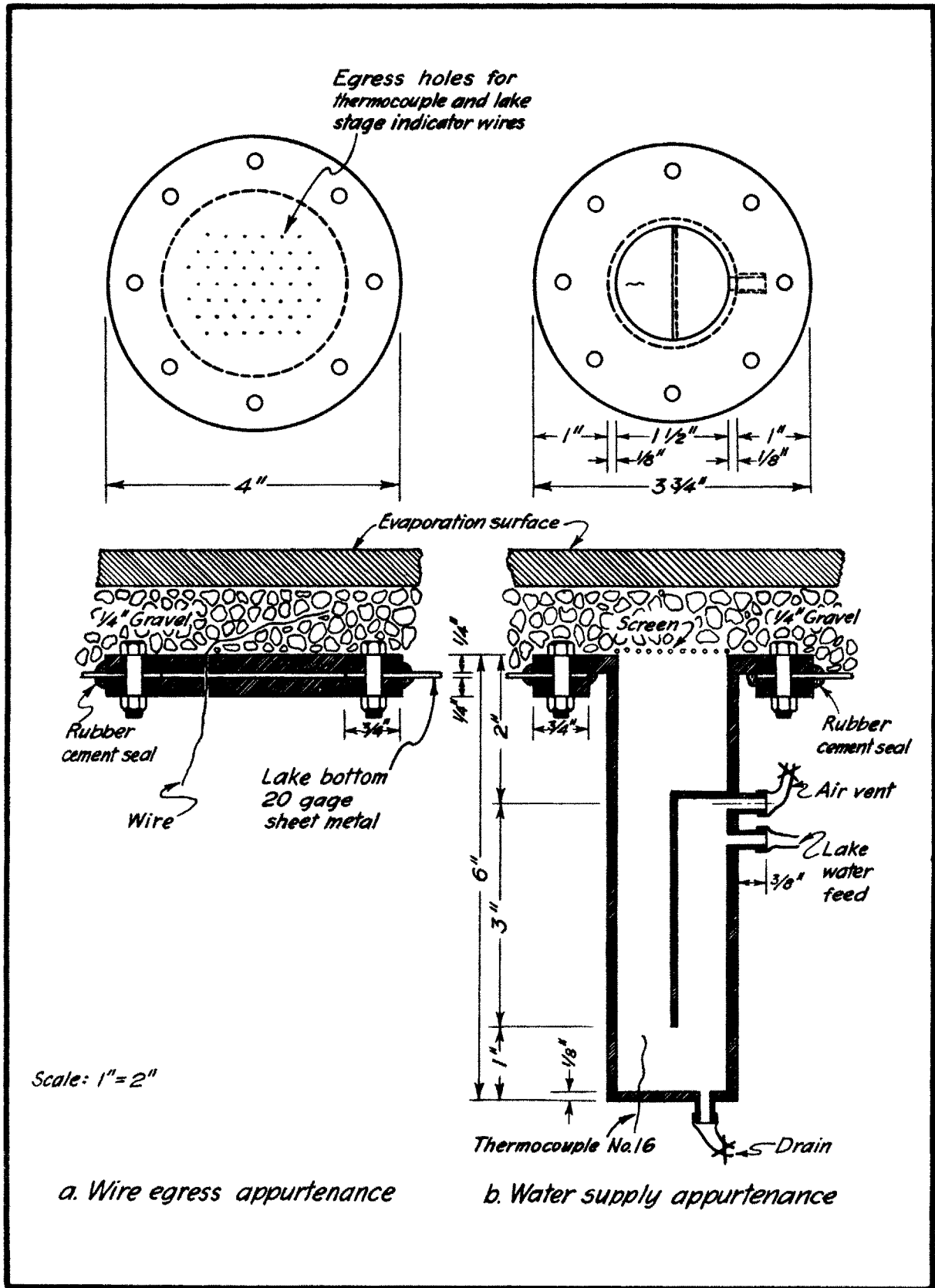
Fig. 19. Lake appurtenances.

of a free-water surface for the evaporation surface was considered but it was
not investigated because of the undeterminable amount of water which might
have been lost as a result of waves and splashing. Also, the rate of evapo-
ration could be determined more easily from a porous evaporation surface than
from a free water surface. Consideration was given to numerous methods of
modeling an evaporation surface and the more promising of these were subjected
to a series of exploratory experiments. Surfaces made from the following
materials were tested:

1. **Fine sand with no binding material.** The surface made up of this
   material appeared to behave satisfactorily when the water was fed to
   the surface by capillary forces. The capillary forces tended to make
   the surface firm but when the free water surface coincided with the
   surface of the sand, the sand was loose. As a result of the loose
   condition of the sand, waves composed of both water and sand traveled
   across the surface when air was blown over the surface. This method
   of construction of the evaporating surface was deemed unsatisfactory
   because of its behavior when the water level was at the surface.

2. **Fine gravel with a clay binder.** Although a surface made from fine
   gravel with a clay binder appeared satisfactory, a great deal of
   consideration was not given to this surface because of the uncertain-
   ty of the area from which evaporation would take place.

3. **Gravel with a cement binder.** This surface appeared firm under
   operation but it too was rejected because of the uncertainty of the
   area from which evaporation would take place.

4. **Glass beads with a plastic binder.** For this investigation, a small
   quantity of plastic was dissolved in ethylene-dichloride. This
   solution was then poured over small glass beads. After the ethylene-
   dichloride had evaporated, a coating of plastic which served as a
   binder was left on the beads. The result was a firm porous surface
   from which evaporation could take place. This investigation was not
   carried further because it was felt that a plaster of Paris surface

could be constructed with less difficulty. This particular process merits consideration for the development of a porous surface.

5. **Plaster of Paris.** The evaporating surface material adopted was plaster of Paris ($CaSO_4 \cdot \frac{1}{2}H_2O$). This material was manufactured by the U. S. Gypsum Company and sold as "Red Top Gauging Plaster". Because of the large area of the modeled lake, the evaporating surface was divided into four sections.

A ratio of 10 parts to 6 parts by weight of air dry plaster of Paris to distilled water was used. The plaster of Paris was added slowly to the water and mixed thoroughly. The mixture had to be mixed and poured within 15 minutes, otherwise setting of the plaster of Paris was encountered. A 1/2-in. plywood form was made for each section of the modeled lake surface.

The wooden forms were placed on a glass plate which was covered with a plastic sheet. The plastic sheet prevented the glass from bonding with the plaster of Paris. The plate glass insured a smooth flat evaporating surface, Figs. 20 and 21. As a consequence of this fabricating technique for the evaporating surface and that for the terrain surface, r_m and r'_m were adjudged to have approximately the same values as r_p and r'_p. The thickness of the plaster of Paris coincided with that of the form; that is, 1/2 in. In order to provide a means for the escape of air from the underside of the evaporating surface, the underside of each section was sloped toward holes which extended through the surface.

A limited number of tests using pans about 6 in. in diameter indicated that evaporation from a free water surface was not noticeably different than that from a saturated plaster of Paris surface. As stated, these tests were limited in number and further investigation of this aspect may be warranted.

In preparation for the placement of the evaporation surface in the pan, provisions were made for the various phases of the instrumentation which were incorporated in the modeled lake. Holes were drilled through the plaster of
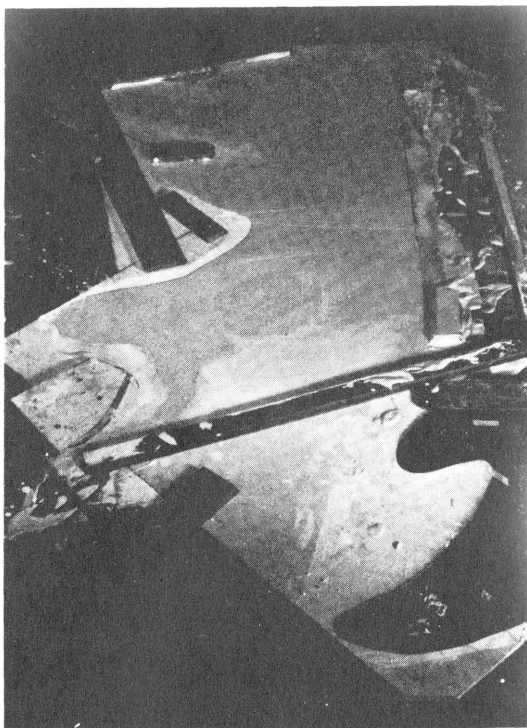
Fig. 20. Fabrication of a section of
the plaster of Paris
evaporation surface.
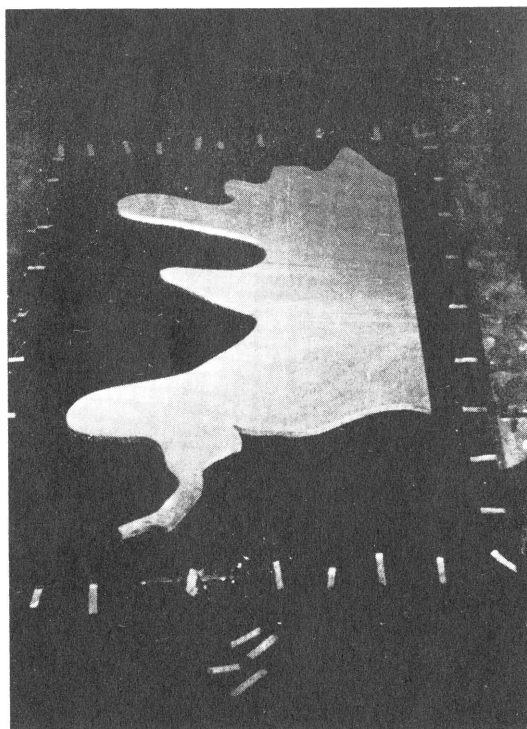
Fig. 21. Fabricated section of the
plaster of Paris evapo-
ration surface.

Paris evaporation surface to accommodate the thermocouples situated on the
surface. A hole was also cut through the evaporation surface for the lake
stage indicator. To prevent warping of the evaporation surface, a continuous
support of 1/4-in. gravel was placed beneath the plaster of Paris, Fig. 22.
The intake tower which was present in the prototype was not duplicated on the
evaporation surface of the model.

After being placed in operation, the evaporation surface appeared to
function as anticipated. But after a period of time, small dry spots de-
veloped on the plaster of Paris, Figs. 23 and 24. The exact cause of the dry
spots is unknown although it has been postulated that this condition was the
result of a change in structure of the plaster of Paris brought about by the
water. The water in the course of passing through the evaporation surface
dissolved some of the calcium sulphate (plaster of Paris). This calcium
sulphate is believed to have been deposited at the surface when the water
evaporated which clogged the pores. An attempt was made to eliminate these
dry areas by successive application of sulphuric acid, hydrochloric acid,
nitric acid, methyl alcohol, and carbon tetrachloride but to no avail. The
application of a vacuum to the evaporation surface also failed to achieve
satisfactory results. Temporary relief from these dry spots was achieved only
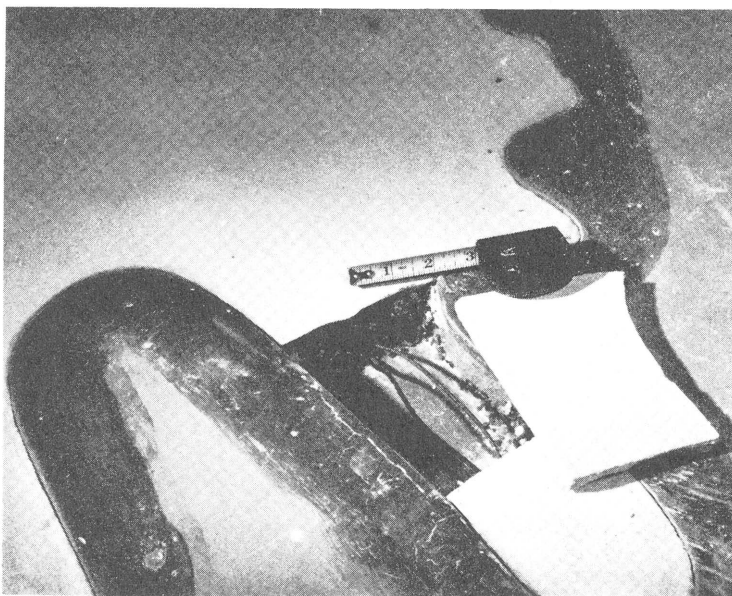
Fig. 22. Assembly of the
modeled lake.
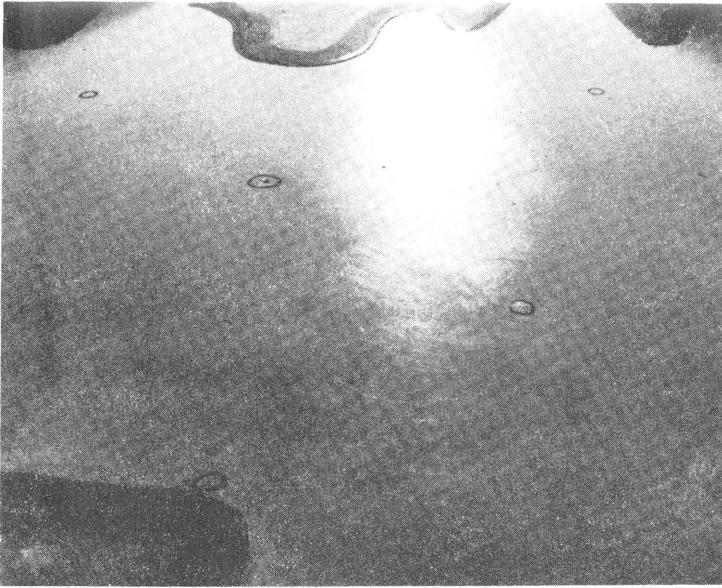
Fig. 23. Evaporation surface. Reflection of light indicates a section of the evaporation surface moist with water.

Fig. 24. Evaporation surface. Dark areas within the reflected light zone indicate dry spots on the evaporation surface.

after sanding the surface with a coarse sandpaper. This sanding roughened the surface to some extent.

Distilled water was used exclusively during this study. The object in using distilled water was to lessen the quantity of dissolved solids and air from that amount which would normally be found in tap water. The dissolved solids if present would affect the rate of evaporation and dissolved air would

interfere with the transmission of the water through the evaporation surface.
The free water surface in the pan was kept approximately 1/8-in. below the
plaster of Paris surface. Capillary forces carried the water to the surface of
the plaster of Paris.

Lake Stage Indicator

The lake stage indicator was an electrical point gage which utilized the
water of the lake as an electrical conductor, Figs. 25 and 26. The device
served to indicate when the level of the water was at a particular elevation
or higher. As the water level of the lake was raised, the water made contact
with the various platinum tips which would light the neon bulbs in series with
the tips.

At the start of a test, the water level of the lake was raised until the
water made contact with the uppermost platinum tip. During the course of a
test the water level was maintained between that uppermost tip and the lowest
tip. At the conclusion of the test the water level was brought back to the
position occupied at the beginning of the test. The level of the water in the
modeled lake fluctuated within a region occupied by the plaster of Paris.
Since capillary action kept the plaster of Paris completely saturated, the
water which evaporated between replenishments was taken from that area of the
modeled lake having a free water surface. The area of free water surface was
considerably less than the area of the lake; therefore, the stage of the
modeled lake was sensitive to changes in the water content of the lake. An
increase of 10 cc in water content of the lake was sufficient to raise the free
water surface approximately 1/16-in. The accuracy of the lake stage indicator
was estimated to be $\pm$ 3 cc. This variation from the true value is acceptable
in light of the total evaporation which varied from 68 cc to 583 cc with an
average evaporation per test of 285 cc.

Water Supply

Two methods of controlling the supply of water to the lake were
incorporated in the model. One method was automatic and the other was manual,
Fig. 27. The automatic system kept the level of the water in the pan at an
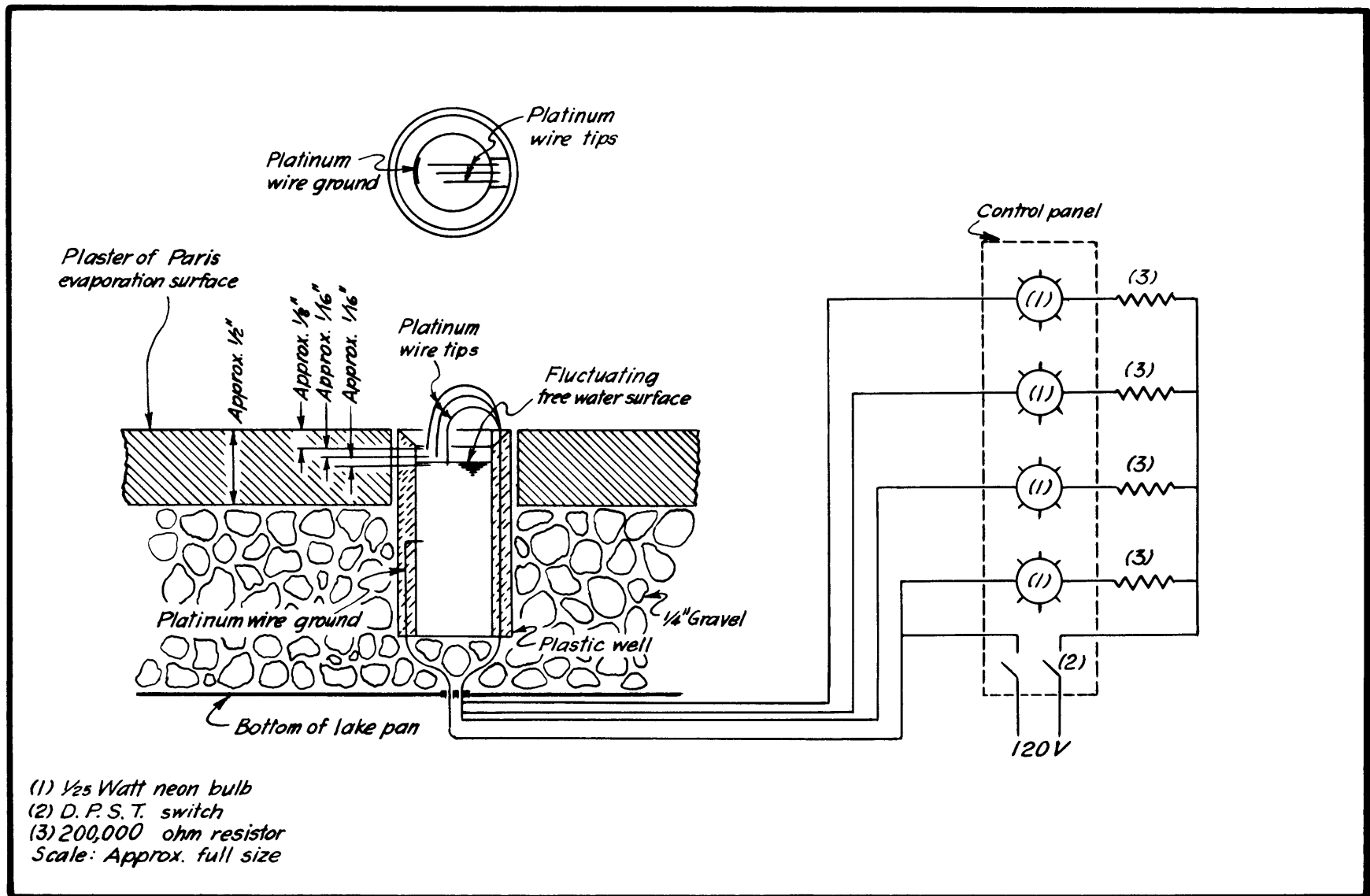
Fig. 25. Schematic diagram of lake stage indicator.

Platinum wire tips

Platinum wire ground

Control panel

Plaster of Paris evaporation surface

Approx. 1/2"
Approx. 1/8"
Approx. 1/16"
Approx. 1/16"

Platinum wire tips

Fluctuating free water surface

(3)
(3)
(3)
(3)

Platinum wire ground

1/4" Gravel

Plastic well

Bottom of lake pan

(2)

120V

(1) 1/25 Watt neon bulb
(2) D. P. S. T. switch
(3) 200,000 ohm resistor
Scale: Approx. full size
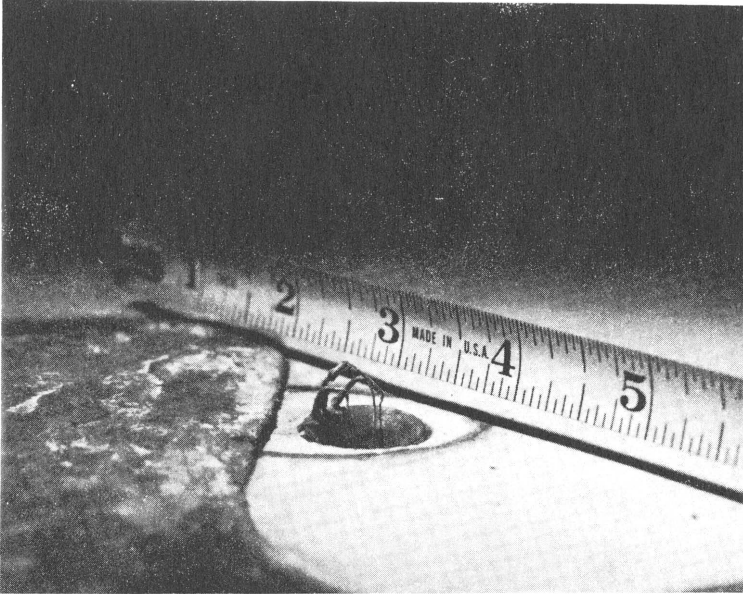
Fig. 26. Lake stage indicator.

elevation such that the evaporation surface was always moist. It was feared that if the evaporation surface were to become dry, air would collect below the surface which might present a problem when remoistening the surface. Keeping the surface moist also lessened the amount of preparatory work that had to be performed for each test.

After the evaporation surface had been completely assembled, the automatic water supply was placed in operation and functioned continuously from that time until the model was taken from the tunnel. The automatic water supply could not be readily adapted to measure the small quantity of water evaporated during the tests; therefore, a manual water supply was incorporated in the system.

Basically all that the manual water supply consisted of was a burette and a lake stage indicator, Fig. 28. When the water level of the lake fell below some predetermined elevation as indicated by the lake stage indicator, water was permitted to flow to the lake by the proper manipulation of the valve on the burette. The burette was mounted so that the force of gravity was utilized in moving the water from the burette to the lake.

Anemometry

During the development of the instrumentation, two different circuits were tried in an attempt to find one suitable for the measurement of the mean
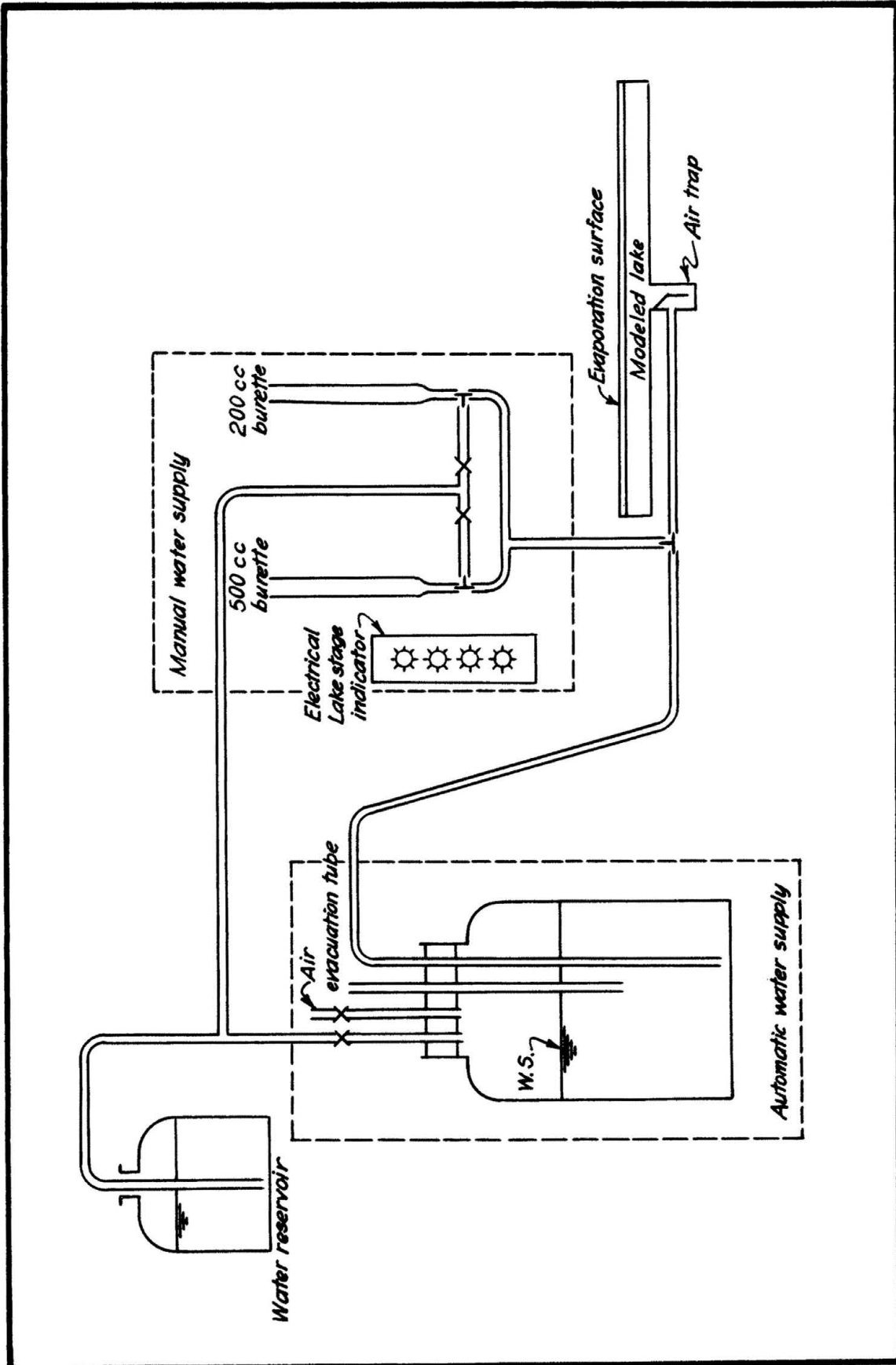
Fig.27. Schematic diagram for water supply system.
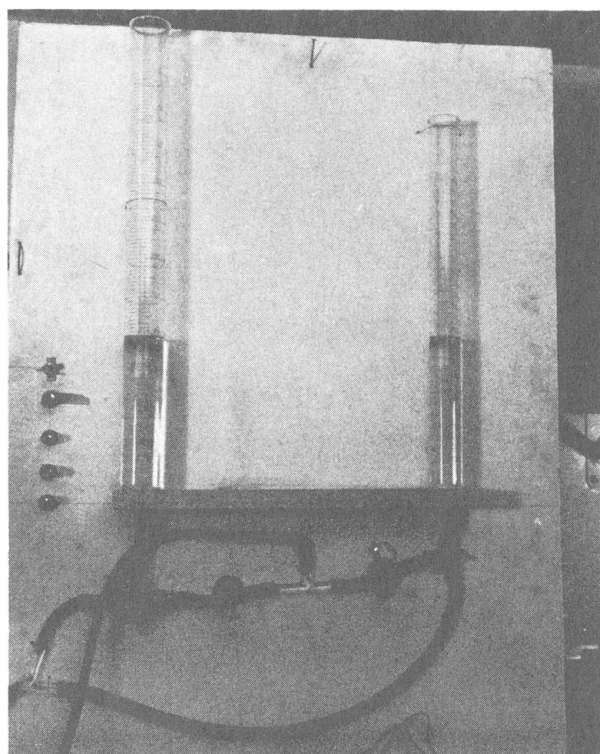
Fig. 28. Manual water supply for the modeled lake. The four bulbs and electrical switch to the left in the picture are a part of the lake stage indicator.

velocity. The last circuit was the only one which proved satisfactory.

The first circuit was the constant voltage type, Fig. 29. In the course of zeroing the tip (bringing the tip to its operating temperature by the passage of current) R_1 and R_2 were manipulated until M_2 read zero. Meter M_1 was placed in the circuit for qualitative readings of current only. After the tip was zeroed, none of the elements of the circuit were varied in the course of operation. When the sensing element was placed in an air stream, heat was removed from the tip by the moving air. This cooled the tip which in turn caused the resistance of the wire to drop. Less resistance in the circuit caused more current to flow. This additional current caused M_2 to deflect. M_2 was selected of such a size and so wired that at the maximum air velocity used in this study the meter would record full scale deflection. This hot wire anemometer circuit was very sensitive when operated in the range of velocities of a few feet per second. But at high velocities, that is above 15 feet per second, the sensitivity was very poor and because of this fact, it was rejected.
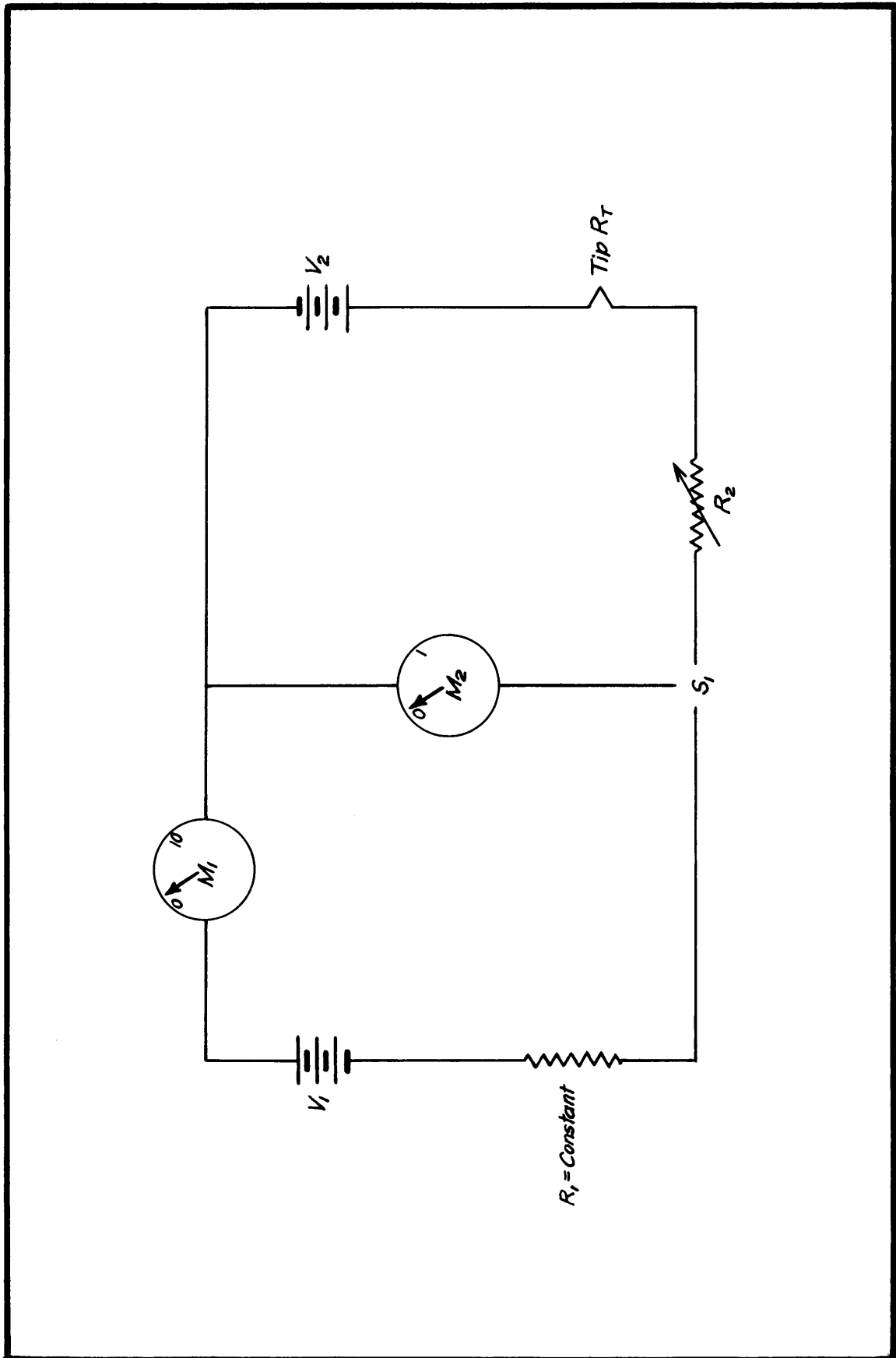
Fig. 29. Schematic diagram of constant voltage hot wire anemometer circuit.

The circuit adapted for the Lake Hefner model study is shown schemetically in Fig. 30 and is termed a constant temperature hot wire anemometer. It derives its name from the fact that the sensing element is maintained at a set temperature regardless of the wind velocity. Based on the fact that a change in temperature of the sensing element of the hot wire anemometer results in a change in the resistance of the wire, a Wheatstone bridge was used to detect variations in the resistance (temperature) of the wire. If the resistance (temperature) of the tip were too low, it was raised by passing more current through the wire. Proper manipulation of R_5 and R_6 caused just enough current to pass through the tip to maintain the resistance (temperature) at some prescribed value.

The following is a review of the elements which made up the circuit (refer to Fig. 30 for location of electrical elements):

V_1 3 type C dry cells in series resulted in a $4\frac{1}{2}$ volt D.C. power supply for the hot wire anemometer circuit.

M_1 0-100 D.C. milliampere meter. This meter operated in the range from 0 to 75 milliampere. The difference between the amount of current indicated by this meter and the current necessary to "zero" the tip was plotted against the true velocity of the air relative to the tip to arrive at a calibration curve for each tip.

M_2 Galvanometer. This galvanometer indicated when the Wheatstone bridge was balanced.

R_G Variable resistance 0-10,000 ohms. This resistance was placed in series with the galvanometer to protect the galvanometer from being overloaded.

R_1 Constant resistance 1040 ohms. This resistance formed a part of one leg of the Wheatstone bridge.

R_2 Constant resistance 1040 ohms. This resistance formed a part of one leg of the Wheatstone bridge.

R_3 Constant resistance 16 ohms. This resistance formed a part of one leg of the Wheatstone bridge.
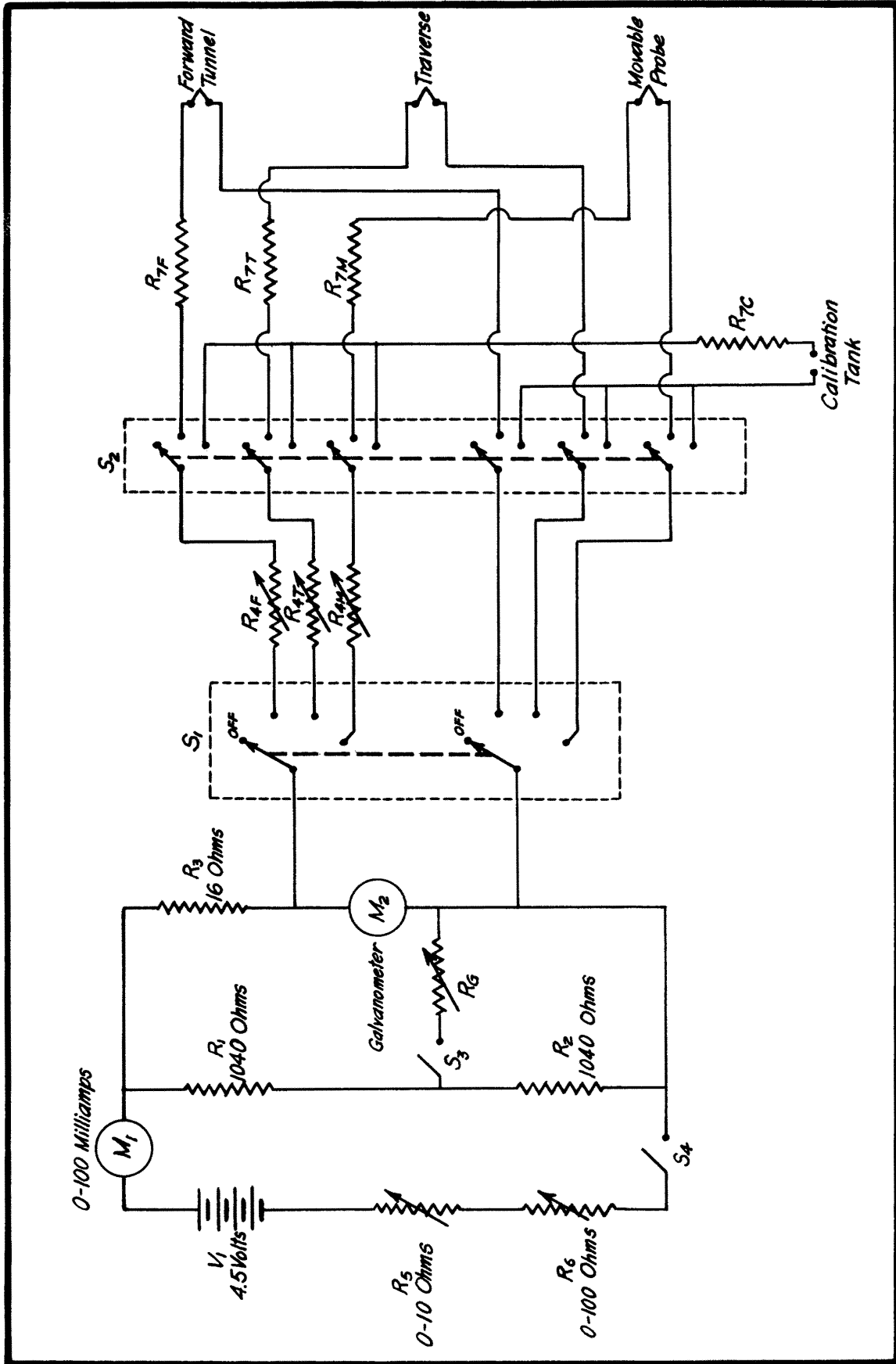
Fig. 30. Schematic diagram of constant temperature hot wire anemometer circuit.

R_{4F} Variable precision resistor placed in series with the forward tunnel sensing element. The resistor was used to compensate for the variation of the resistance between the electrical cable to the calibration tank and the electrical cable to the forward tunnel position.

R_{4M} Variable precision resistor placed in series with the movable probe sensing element. This resistor was used to compensate for the variation of resistance between the electrical cable to the calibration tank and the electrical cable to the movable probe position.

R_{4T} Variable precision resistor placed in series with the traverse sensing element. This resistor was used to compensate for the variation of resistance between the electrical cable to the calibration tank and the electrical cable to the traverse position.

R_5 0-10 ohm variable resistor. This resistor was used to make the final adjustments in the balancing of the Wheatstone bridge.

R_6 0-100 ohm variable resistor. This resistor was used to make the course adjustments in the balancing of the Wheatstone bridge.

R_{7F} Resistance of the wire leading to the forward tunnel position.

R_{7M} Resistance of the wire leading to the movable probe.

R_{7T} Resistance of the wire leading to the traverse mechanism.

R_{7C} Resistance of the wire leading to the calibrating table.

The attempt to make $R_{7F} = R_{7R} = R_{7T} = R_{7C}$ was unsuccessful because of the small variations in the resistance of the various wires and connections.

S_1 Single pole, 11 position, two deck switch. Silver plated contacts.

S_2 Four pole, 3 position, two deck switch. Silver plated contacts.

S_3 SPST switch. This switch was used to place the galvanometer in or out of the circuit.

S_4 SPST switch. This switch was used to turn the hot wire anemometer circuit on or off.

The sensing element for the hot wire anemometer was a piece of tungsten wire approximately 0.0003 in. in diameter and 1/8 in. long. This wire was supported between the pointed ends of two steel probes. To insure a satisfactory mechanical and electrical connection between the tungsten wire and the steel probes, each end of the tungsten wire was copper plated and then tin-lead soldered to the steel probes. A protective cap was provided for each tip. This cap served three purposes, Fig. 31:

1. Prevented physical damage to the tip.

2. Kept the tip free of lint and dust.

3. Prevented the circulation of air around the tip (except free convection) during the zeroing process of the tip.
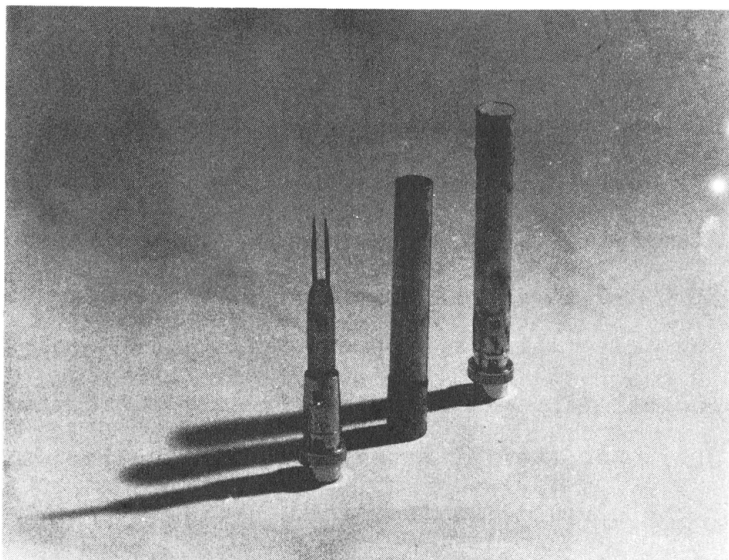
Fig. 31. Sensing element and cover of the hot wire anemometer.

Each sensing element used in the hot wire anemometer was calibrated separately because the tungsten wire was not uniform and the fabrication technique was not developed to the extent that each tip was identical. On the basis of experience at Colorado A & M College and advice from Mr. P. G. Hubbard (Research Engineer, Iowa Institute of Hydraulic Research, State University of Iowa, Iowa City, Iowa), the sensing elements were operated at a temperature such that the resistance of the wire was approximately one and one-half times

the cold resistance. Since the average cold resistance of the tips was 6 ohms, an attempt was made to operate the tips at a temperature such that the resistance of the wire was 9 ohms. A current of 44 milliamperes accomplished this end.

The sensing elements were calibrated by revolving them at known speeds in a cylindrical tank, Fig. 32. The calibrating procedure was as follows:

1. The sensing element, capped, was placed on the rotating arm of the calibration tank. The cap prevented the tip from being affected by any air currents which might be present inside the calibration tank.

2. S_1, Fig. 30, was set to correspond to the position that the tip would occupy when velocity measurements were made with it; that is, forward tunnel, traverse, or movable probe. The description of the rest of the procedure will be based on S_1 set at forward tunnel.

3. S_2 was set to "calibration tank."

4. S_4 was switched to the "on" position and R_5, R_6 and R_{4F} were adjusted simultaneously until the galvanometer showed no deflection and M_1 read 44 milliamperes.

5. The cap was removed from the tip.

6. The rotating arm of the calibration tank was set in motion and R_5 and R_6 were adjusted until the galvanometer read zero. The current drawn by the circuit was indicated by meter M_1. This meter was read and the value of the current flow recorded.

7. The speed of the rotating arm could be changed by changing the position of the belt on one or both of the two pulleys -- the pulley on the motor and the pulley on the rotating arm. In order to establish a tip calibration curve over a wide range of velocities, step number six was repeated for all possible combinations of the two pulleys even though this resulted in duplication for certain speeds. This duplication served as a check on the various points making up the calibration curve.

8. The velocity of the rotating arm was determined from a knowledge of

the time required for the arm to rotate a specific number of whole revolutions and of the radius of the circle described by the rotating tip. A stop watch was used to ascertain the transpired time.
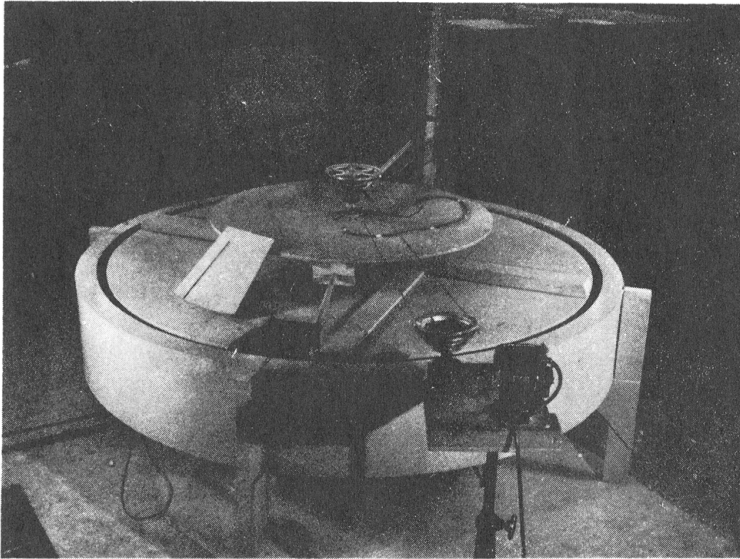
Fig. 32. Calibration tank for the hot wire anemometer.

The velocity of the rotating arm was not the true velocity of the tip relative to the air since the air within the tank was set in motion by the revolving arm and tip. Therefore, a correction arrived at by successive approximations was applied to the absolute velocity of the tip to arrive at the true velocity of the tip relative to the air.

The velocity of the air circulating in the tank for various speeds of the rotating arm of the calibration tank was determined independently five times. In adjusting the early calibration curves for the velocity of the air within the tank, an average of the three sets of data taken up to that time was used. After determining the correction for the air velocity within the tank by two additional tests, the arithmetic average of the five sets of data was used to arrive at the true velocity of the tip with respect to the air. There was no significant difference between the correction based on the average of the three and the correction based on the average of five sets of data.
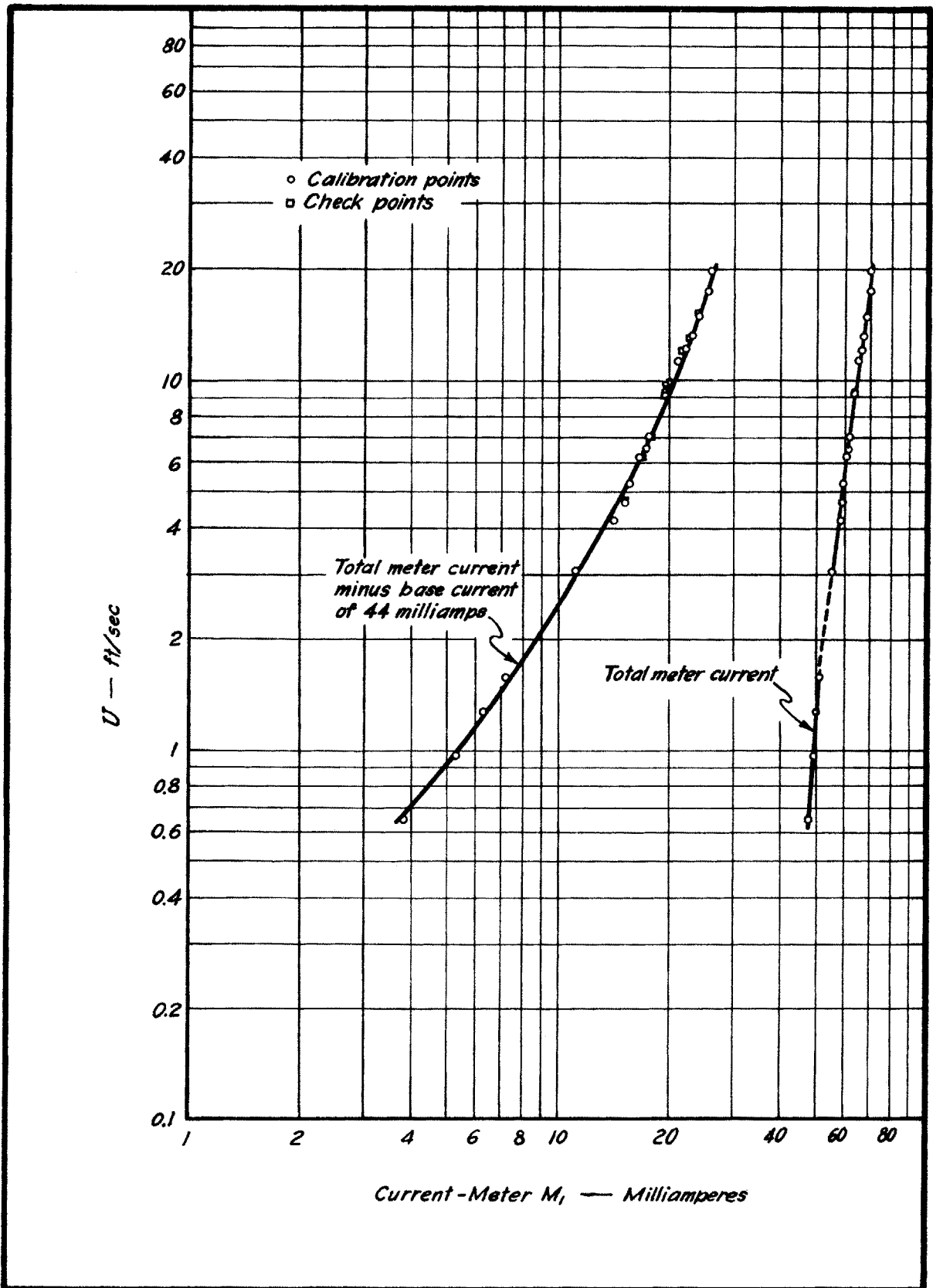
Fig. 33. Typical calibration curve for the hot wire anemometer.

were used for the copper and two different sizes were used for the constantan;
namely:

Single strand -- Enamel insulation

Copper -- B & S Gage No. 30

Constantan -- B & S Gage No. 30

Multistrand -- Rubber insulation

Copper -- Leeds & Northrup No. 22-32-6

Constantan -- Leeds & Northrup No. 22-40-2

The 1938 calibration was applicable for all wires.

The copper-constantan junctions were one of three types depending on their
purpose and location. For purposes of strength, the copper-constantan
junctions were silver soldered rather than tin-lead soldered. The constantan-
constantan junctions were also silver soldered but all the copper-copper
junctions were tin-lead soldered.

The thermocouple circuit used for this study is indicated schematically
in Fig. 34. The "common" constantan junction was placed in a thermally
insulated box so as to eliminate any secondary junction effects. The reference
junction was a water and ice solution contained in a one pint thermos bottle.

A Leeds and Northrup potentiometer was used to measure the thermocouple
electromotive force. The switches used in the thermocouple circuit were of
the silver contact type and were placed in a 1/2-in. thick plywood box --
again to eliminate secondary thermal effects.

Particulars concerning the various thermocouples are given in Table IV,
Appendix B. "Thermocouple No." refers to the number of the thermocouple.
"Name and location" refers to the name given to the thermocouple and its
location. "Junction" refers to the type of junction used; that is:

a   stands for a junction made up of single copper and a single
     constantan wire.

b   stands for a junction made up of two copper and two constantan
     wires (made from multistrand wire only).

f   stands for a junction made up of all the copper and all the

85
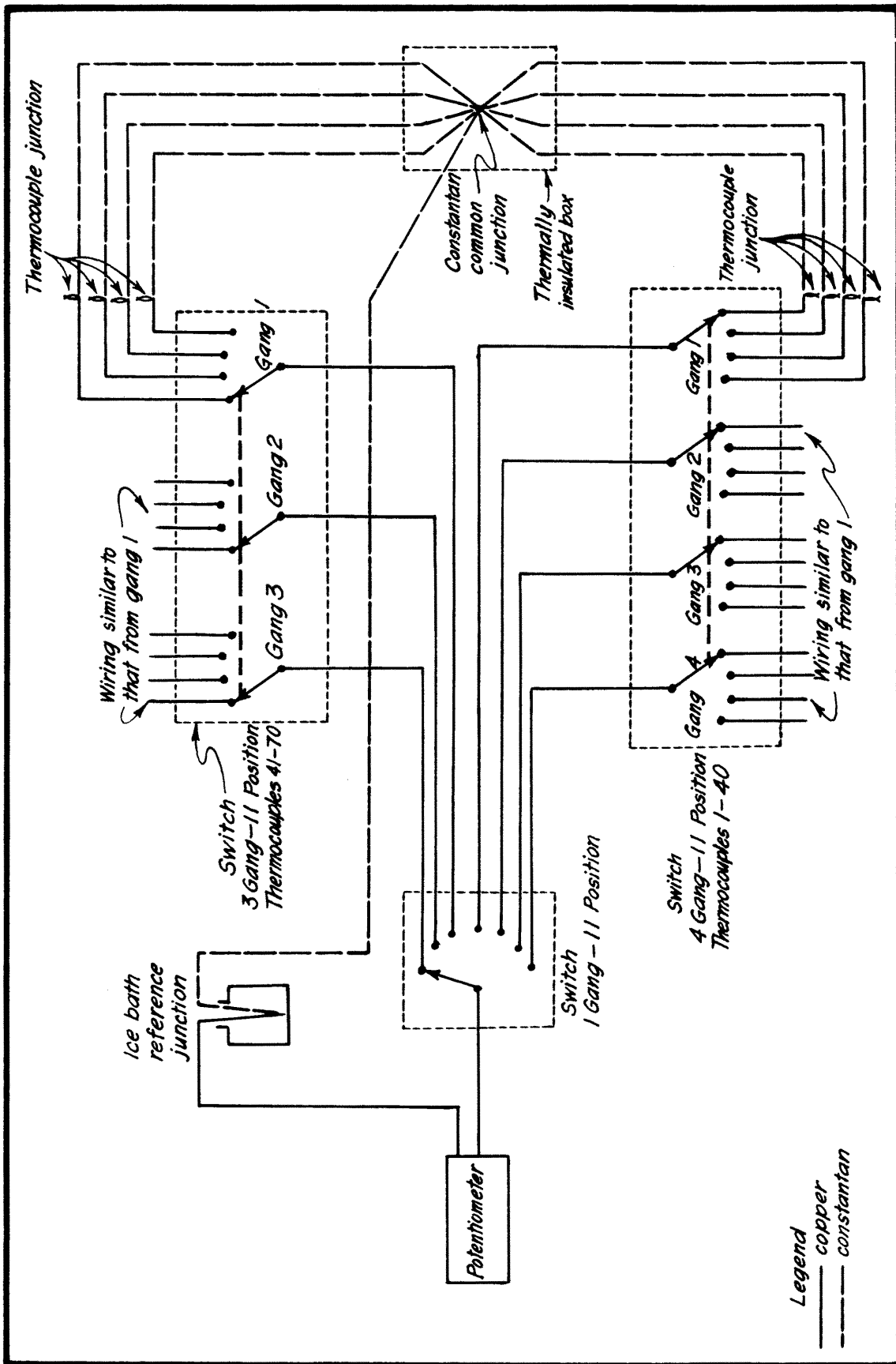
Fig. 34. Schematic diagram of thermocouple circuit.

constantan wires contained in the multistrand wires.

"Wire" refers to the wire used; that is:

g   stands for the single strand wire.

h   stands for the multistrand wire.

Thermocouple Nos. 1 through 28 were used to measure the temperature at various places which might have a bearing on the evaporation surface. The positions of these thermocouples are represented in Fig. 35. The word "surface" used in connection with the thermocouples refers to a thermocouple whose junction was just at the surface of the plaster of Paris from which the evaporation was taking place. The word "bottom" refers to thermocouples located on the bottom of the pan, Fig. 36a.

Thermocouple Nos. 1, 2, 3, 5, 11, 12, 13, and 15 were positioned to agree with the location of the meteorological stations at Lake Hefner.

Thermocouple Nos. 5 through 10 were positioned so that the temperature gradient existing within the modeled lake could be measured, Fig. 36b.

Thermocouple No. 16 refers to the thermocouple placed in the water supply appurtenance attached to the pan. The horizontal location of the water supply appurtenance is indicated in Fig. 35.

Thermocouple Nos. 41 and 51 made up the psychrometer which formed a part of the instrument group called forward tunnel. No. 41 was the dry thermocouple and No. 51 was the wet thermocouple. (For further details see section on forward tunnel).

Thermocouple Nos. 42 and 52 made up the psychrometer on the traverse mechanism. Thermocouple No. 42 was the dry thermocouple and No. 52 was the wet thermocouple. (For further details see section on traverse mechanism).

Thermocouple No. 43 was used to measure the air temperature at the rear tunnel location. (For further details see section on rear tunnel).

Thermocouple No. 44 indicated the temperature of the air which passed over the modeled terrain surface to the north of the lake. This thermocouple was installed so that the junction rested on the surface of the terrain. The horizontal position of this thermocouple is indicated in Fig. 35.
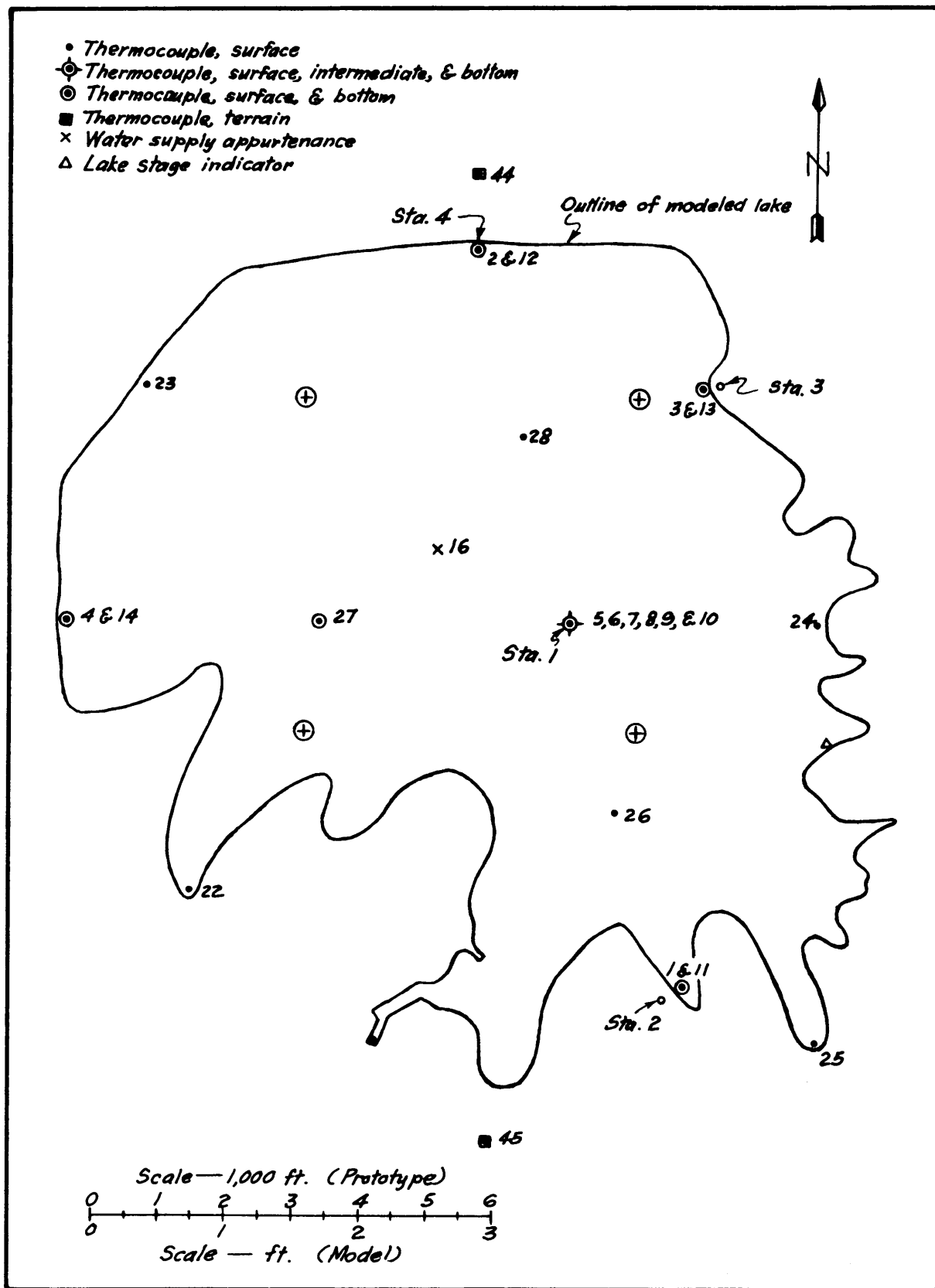
Fig. 35. Thermocouple locations on lake.
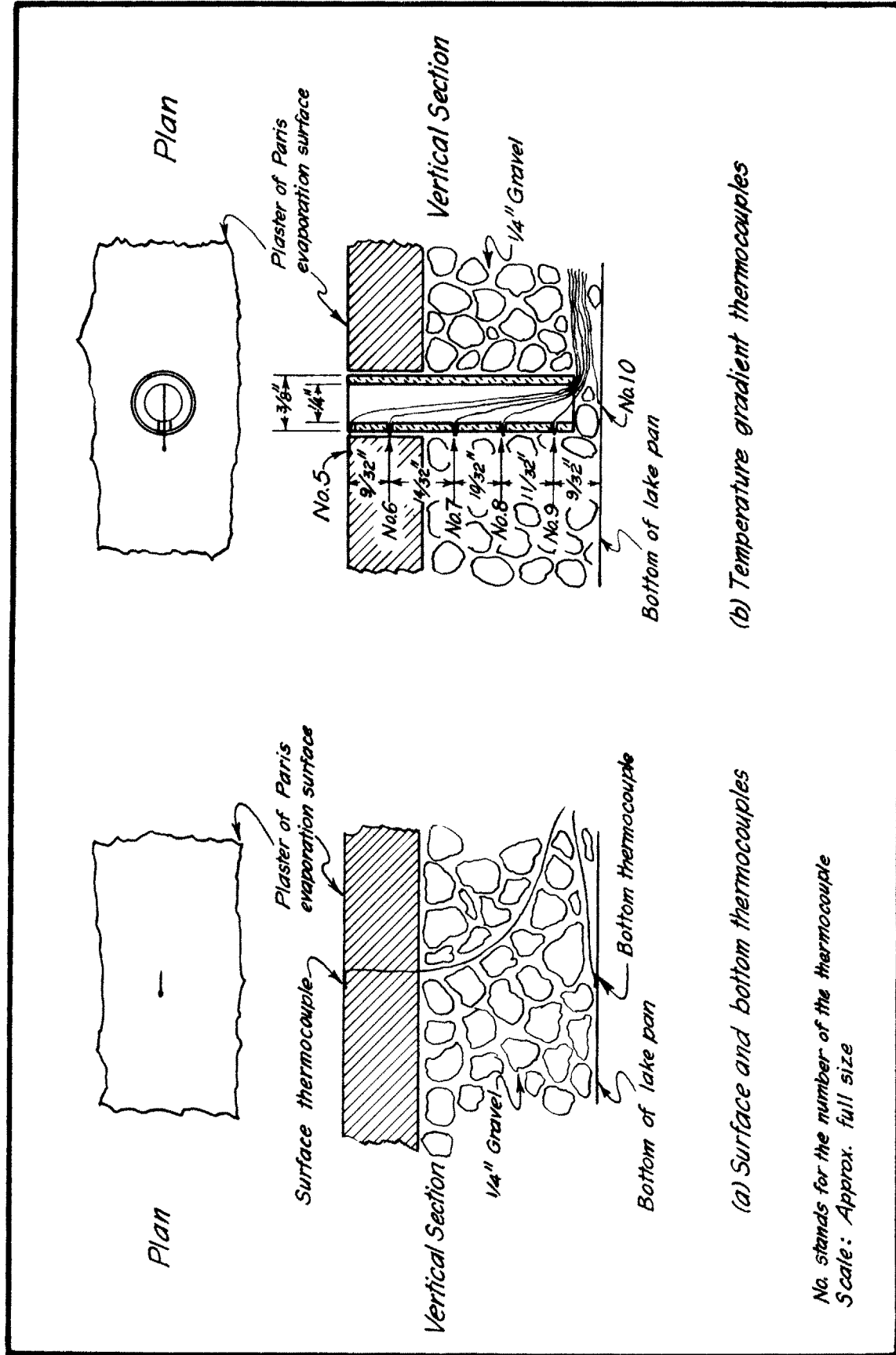
Fig. 36. Details of lake thermocouples.

(a) Surface and bottom thermocouples

(b) Temperature gradient thermocouples

No. stands for the number of the thermocouple
Scale: Approx. full size

Thermocouple No. 45 indicated the temperature of the air which passed over the modeled terrain surface to the south of the lake. This thermocouple was installed in a manner similar to that for No. 44. Fig. 35 indicates the horizontal position of this thermocouple.

Thermocouple No. 46 was located outside the instrument shelter. This thermocouple indicated the temperature of the air which surrounded the instrument shelter and the test section of the wind tunnel.

Thermocouple No. 47 was incased in a 1/4-in. plastic box located inside of the instrument shelter. The junction of the thermocouple was wrapped around the bulb of a mercurial thermometer which was completely enclosed in the plastic box, Fig. 37. A comparison of the temperatures as indicated by the thermocouple and the mercurial thermometer acted as a check on the operation of the thermocouple system. Agreement between the two implied:

1. The reference junction was at the proper temperature.

2. The potentiometer was in adjustment and was operating properly.

3. The switches were functioning as anticipated.

It was realized that the temperature measurements made by means of the thermocouples could still be in error even though there existed a temperature agreement between thermocouple No. 47 and the mercurial thermometer.
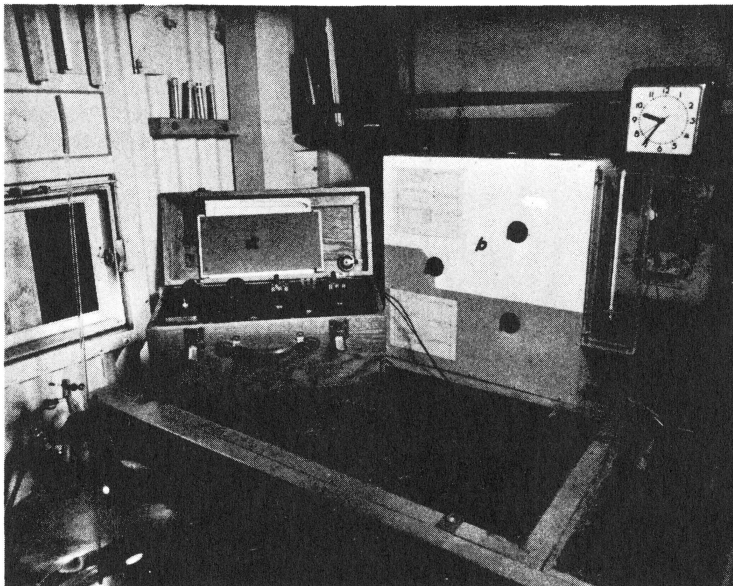
Fig. 37. Thermocouple instrumentation - left to right
a. Leeds and Northrup potentiometer
b. Thermocouple switch box
c. Mercurial thermometer and thermocouple No. 47 enclosed in plastic case.

The thermometer used in conjunction with thermocouple No. 47 was a mercury-in-glass thermometer. The range of the thermometer, graduated in one degree divisions, was from -20 to + 150°C. The calibration of the thermometer was checked and the thermometer was found to indicate temperatures approximately 0.7°C higher than the true temperature.

Thermocouple No. 48 was one part of the instrumentation on the movable probe. This thermocouple indicated the temperature of the air in the vicinity of the movable probe. (For further details see section on movable probe).

Thermocouple Nos. 61 through 68 were used to measure the temperature of the air along the walls of the tunnel. The thermocouple junctions were located at the wall surface, Fig. 38.

The initial adjustment of the thermocouple instrumentation drifted. If this drift had not been corrected frequently, the temperature might have been improperly recorded by ±1.0°F.

Hygrometry

Two types of psychrometers were used during the course of this work. One type was the ordinary sling psychrometer which utilized two mercurial thermometers. The other type was the thermocouple psychrometer. The latter consisted of two thermocouples. One of the thermocouples measured the temperature of the air and served the same function as the dry thermometer of a sling psychrometer. The other thermocouple of the pair was termed the wet thermocouple and served the same purpose as the wet thermometer of the sling psychrometer. The wet thermocouple was a thermocouple wrapped with a cotton thread. This cotton served as a wick for transporting water to all portions of the covered thermocouple. Water was fed to the wick through a small plastic tube from a water supply reservoir. The temperature reading given by the wet thermocouple was sensitive to the rate at which water was fed to the wick. If the rate was too great, the temperature of the water would influence the reading. If the rate was too small or stopped altogether, the temperature reading would indicate a higher humidity than actually present. Experience indicated that good readings were obtained from the thermocouple psychrometer when a non-dripping drop of

West wall—
elevation

No.62

No.64

3 7/8"

2 1/2"

2'-3"

2'-3"

4"

2 1/4"

No.61

No.63

5 1/4"

6"

Nos. 61 & 62

Nos. 63 & 64

Plan

No.45

No.44

Wind direction

Nos. 67 & 68

Nos. 65 & 86

No.68

No.66

3 3/4"

3 7/8"

2'-3"

2'-3"

East wall—
elevation

3 7/8"

3 15/16"

No.67

No.65

5 1/4"

6"

No. Stands for the number of the thermocouple.
Scale:
  Vertical 1"= 1'
  Horizontal 1"= 5'
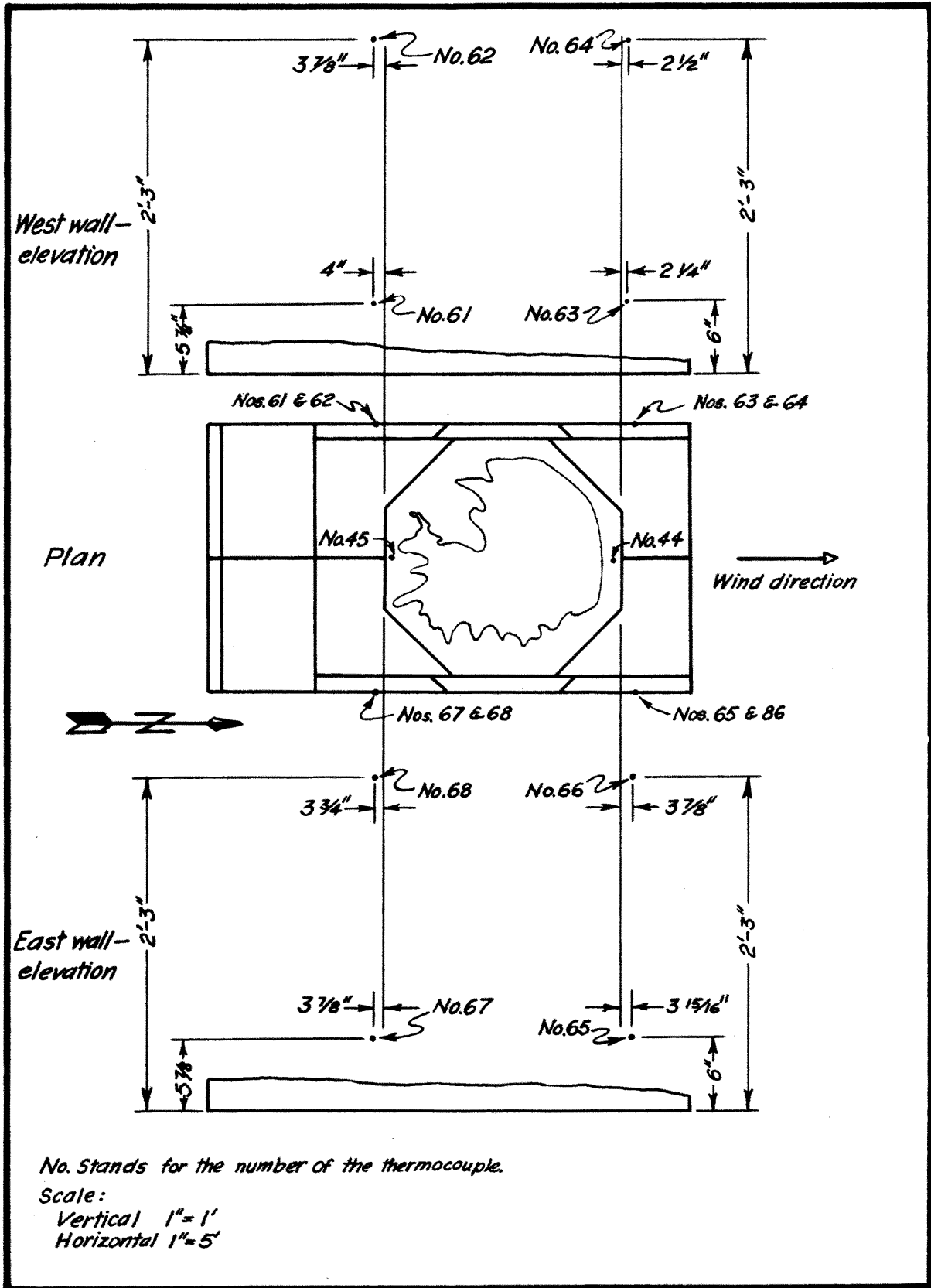
Fig. 38. Thermocouple locations on tunnel walls.

water was maintained on the wet thermocouple. Ventilation of the wet thermocouple was deemed satisfactory when the air speed was equal to or greater than 2 ft/sec (2:51).

The sling psychrometer was used as a check of the humidity as indicated by the forward tunnel psychrometer. When everything functioned properly, the readings of the forward tunnel psychrometer were in fair agreement with those of the sling psychrometer.

Two thermocouple psychrometers were mounted in the tunnel. One was placed at the forward tunnel position and the other on the traverse mechanism.

The dry bulb temperature readings of the sling psychrometer when compared with those of the forward tunnel dry thermocouple differed by an average of $\pm 0.7^{\circ}F$. The wet bulb temperature readings differed by an average of $\pm 1.0^{\circ}F$.

Forward Tunnel

The instrumentation designated forward tunnel was used to measure the ambient velocity, temperature, and humidity of the air, Figs. 39 and 40. This instrumentation was located longitudinally in the tunnel approximately 15 in. from the upwind edge of the modeled lake. Also it was mounted approximately midway between the walls and midway between the surface of the model and the ceiling.

The three elements comprising the instrumentation were:

1. A sensing element of the hot wire anemometer. This was used to measure the velocity of the air. The ambient air velocity within the tunnel for a particular test was established and maintained by the combined use of this anemometer and the throttle on the engine. Frequent measurement of the air velocity at this point during a test served to indicate changes in the ambient air velocity.

2. Dry thermocouple - No. 41. This thermocouple was used to measure the temperature of the ambient air.

3. Wet thermocouple - No. 51. This thermocouple acted as the wet bulb thermometer of a psychrometer. The temperature readings indicated by this thermocouple and the dry thermocouple were used to determine the
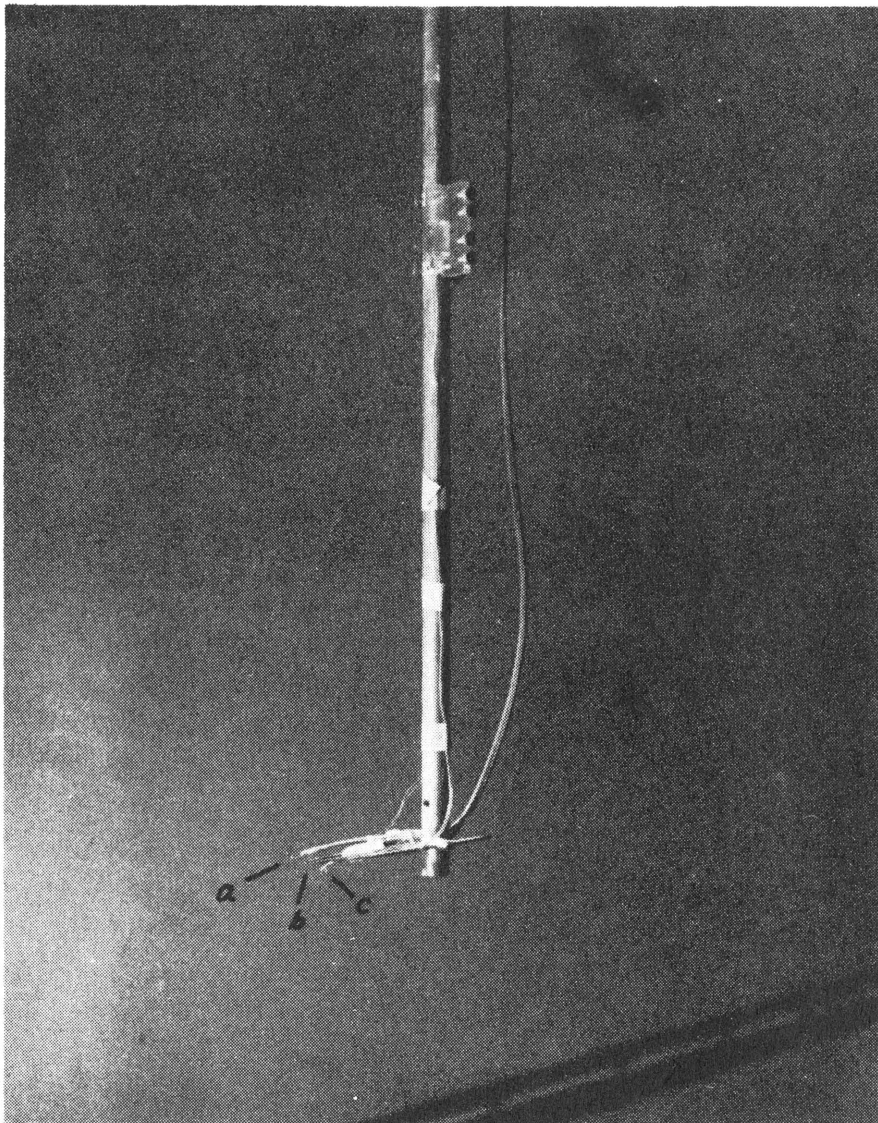
Forward tunnel sensing
elements and support -
left to right
a. Dry thermocouple No. 41
b. Hot wire anemometer
c. Wet thermocouple No. 51
Water reservoir for wet
thermocouple mounted on
vertical rod.
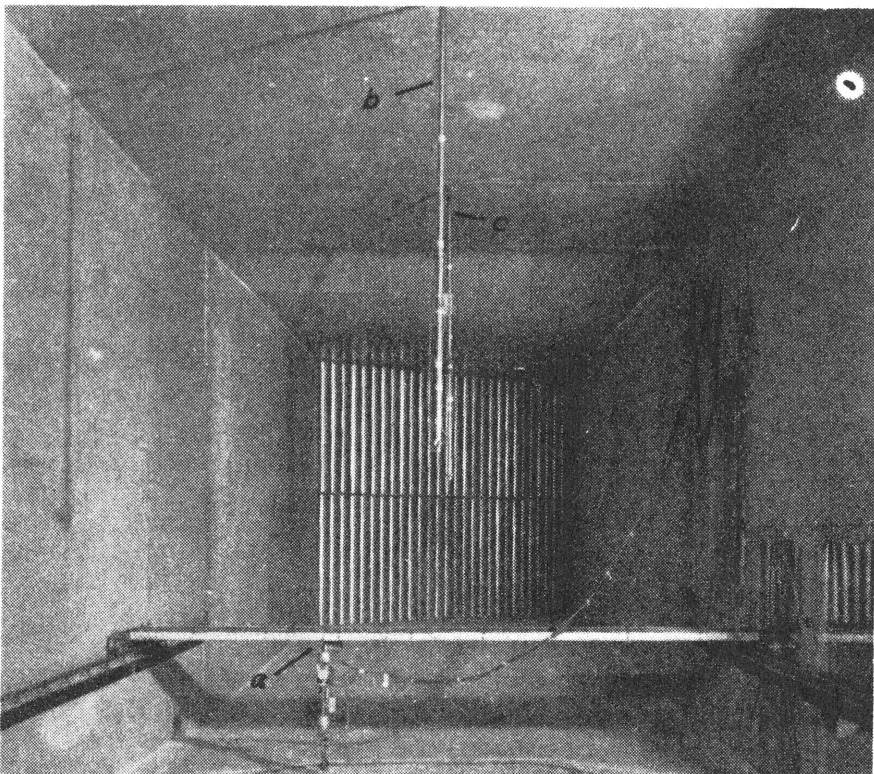
Lake Hefner model -
looking downwind
a. Traverse
b. Forward tunnel
   instrumentation support
c. Rear tunnel instru-
   mentation support.

humidity and temperature of the ambient air.

The vapor concentration of the ambient air was determined by the readings taken from the forward tunnel psychrometer.

Traverse Mechanism

In order that the necessary meteorological measurements could be made above the modeled lake and terrain, a traversing mechanism was built to support the necessary instrumentation. The supporting beam of the traverse mechanism was a steel beam (1.5 in. deep and 19.5 in. wide) which spanned the width of the tunnel. Wheels were mounted on each of the corners of the beam so that the beam could be moved the length of the tunnel on the steel rails which were mounted along each wall, Fig. 40. The steel beam was streamlined upstream with a piece of half round wood and downstream with a curved feathered surface. The traverse mechanism consisted of two interconnected carriages each controlled electrically. The first carriage ran along the underside of the steel beam and was used for transverse positioning of the sensing elements. The second carriage ran along vertical rails which were secured to the first carriage. The latter carriage was used for vertical positioning of the sensing elements. A vernier and revolution counter attached to the electric motor controlling the second carriage served to indicate the distance that the sensing elements were moved vertically to within 0.001 in., Fig. 41.

The traverse mechanism carried three sensing elements:

1. A sensing element of the hot wire anemometer. This was used to measure the velocity profile of the air.

2. Dry thermocouple No. 42. This thermocouple was used to measure the temperature of the air.

3. Wet thermocouple No. 52. This thermocouple acted as the wet bulb thermometer of a psychrometer. The temperature readings indicated by this thermocouple and the dry thermocouple were used to determine humidity and temperature gradients.

During this work the vertical position of the sensing elements on the traverse were not referenced to a common datum. The recorded elevations refer
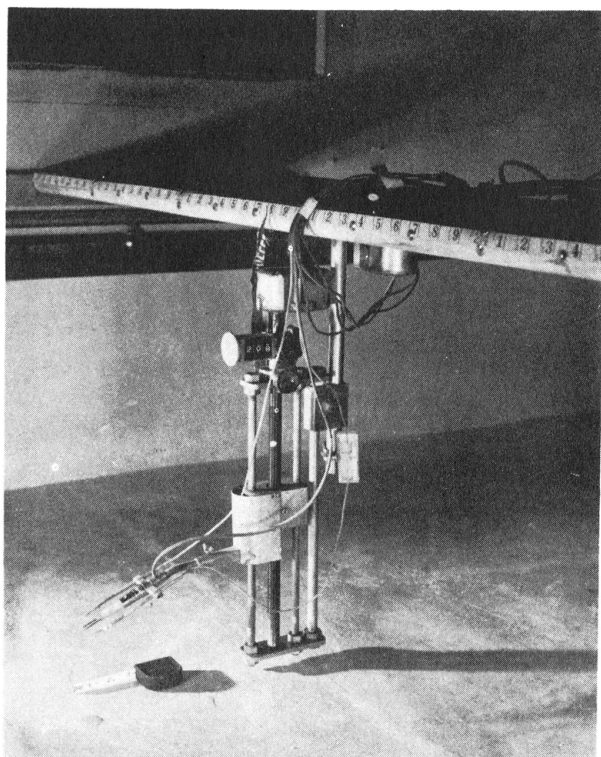
Fig. 41. Traverse mechanism.

to the height above the point at which measurements were made. Because the hot wire anemometer could be broken very easily, it was impossible to bring the sensing element to bear on the surface. Therefore, the height of the sensing element above the terrain had to be estimated for referencing purposes. The sensing element was usually brought to within 0.030 in. to 0.050 in. of the surface. Rulers and feeler gages were used as guides for the person estimating the height of the tip above the terrain. The error in the estimation of the height of the tip above the terrain was considered to be less than the surface roughness, 0.020 in. The vernier and revolution counter, discussed previously, were used to ascertain vertically traversed distances.

When the data were analyzed, the portions of the velocity profiles near the surface were found to deviate from anticipated results. An investigation was undertaken which explained, at least in part, the cause of this behavior. Without air circulating in the tunnel, the procedure of making a velocity profile was carried out. Measurement of the air velocity above 0.09 in. indicated that the air was not moving. But below this height, there existed an

apparent air velocity which increased in magnitude as the surface was approached. This phenomenon was attributed to the greater quantity of heat lost by conduction through the air while in the proximity of the surface than that lost by the normal convection currents which occur in undisturbed air. A correction curve was evolved and applied to the applicable data, Fig. 42.

The correction curve was used in the following manner. When the velocity of the air was measured at distances closer to the surface than 0.09 in., the quantity of current drawn by the hot wire anemometer was decreased by the amount of extra current drawn by the hot wire anemometer under still air conditions for a corresponding height as indicated in Fig. 42. Cognizance was taken of the fact that this procedure may be in error due to the fact that the correction to be applied to the hot wire anemometer may not be the same for still and moving air conditions. Because of the uncertainty of this latter correction, no consideration for purposes of computing U_* was given to the data closer than 0.10 in. to the surface.

Location of Traverse Sensing Elements

During the tests on the Lake Hefner model, the sensing elements on the traverse were mounted as follows: The sensing element of the hot wire anemometer was situated midway between the dry thermocouple No. 42 and the wet thermocouple No. 52. The distance between the thermocouples was approximately 2 in. The three sensing elements were placed in the same horizontal and vertical plane with the latter normal to the direction of the wind.

An attempt was made to measure the meteorological factors existing in the model at positions similarly located to the four meteorological stations in the prototype -- namely Stas. 1, 2, 3 and 4.

When positioning the sensing elements on the traverse for measurement of the temperature, humidity, and velocity profiles above Stas. 3 and 4, the sensing element of the hot wire anemometer was placed directly over the position in the model corresponding to the location of the Stas. 3 and 4 in the prototype. The intake tower which was present in the prototype was not duplicated in the model.
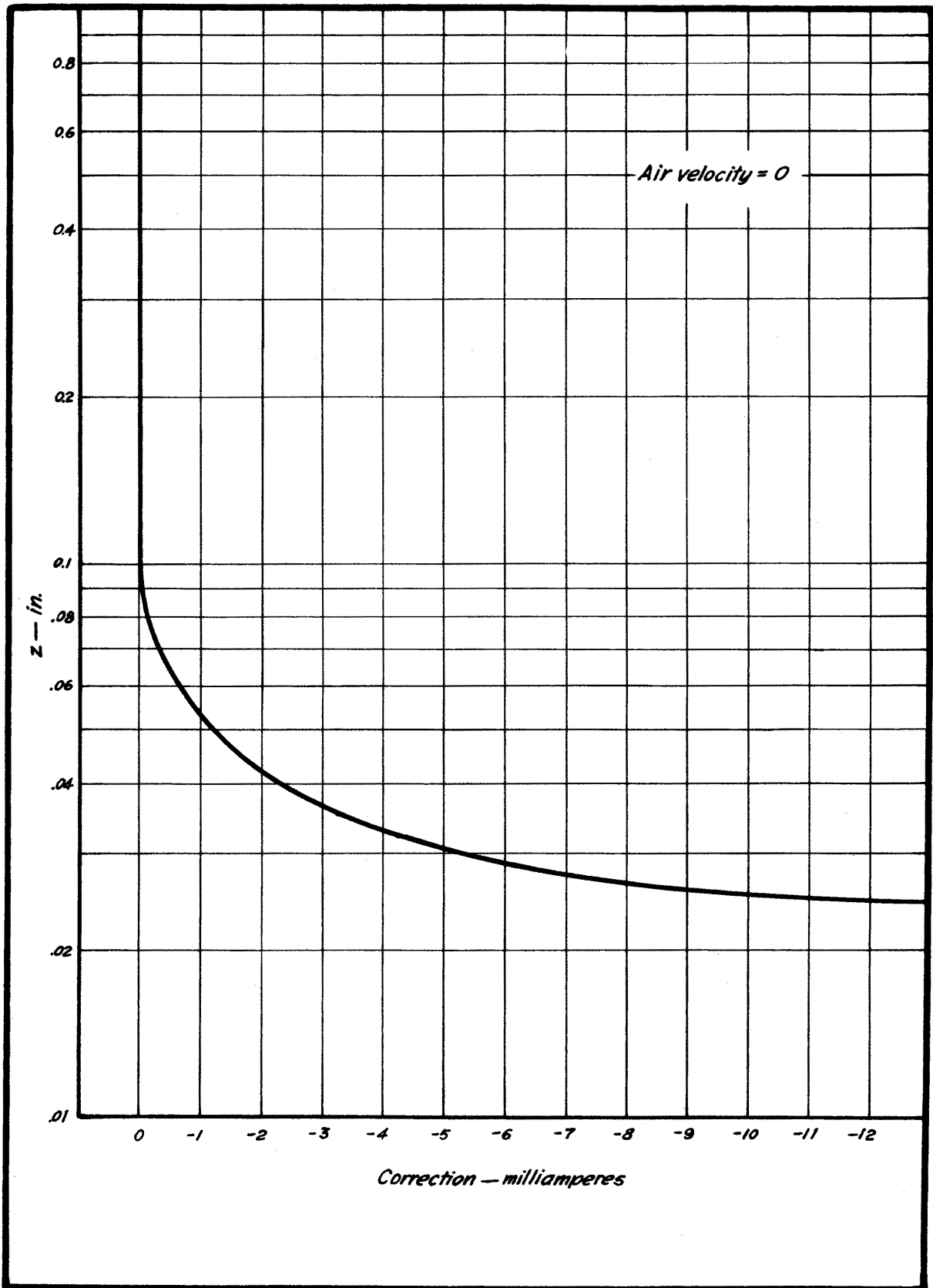
Fig. 42. Surface proximity correction for hot wire anemometer.

The presence of the temperature gradient appurtenance at Sta. 1 and the irregular condition of the terrain caused by the Sta. 2 marker may have created undue turbulence which might have affected the velocity profiles if they were measured directly above Stas. 1 and 2 in the model. For this reason, the measurements which were taken as representative of conditions at the Stas. 1 and 2 were taken at slightly displaced positions, Fig. 43.

Rear Tunnel

That phase of the instrumentation designated rear tunnel was used to measure the temperature of the air downstream from the model, Fig. 44. Its longitudinal location in the tunnel was approximately 4.5 in. from the downstream edge of the modeled lake. The rear tunnel instrumentation was mounted approximately midway between the walls and midway between the surface of the model and the ceiling.

A single sensing element was mounted at this location. This element was thermocouple No. 43 which was used to measure the temperature of the air downstream from the model. Provision was made so that a sensing element of the hot wire anemometer could also be installed at this point but it was never put to use.

Movable Probe

The movable probe was that part of the instrumentation used to measure the air velocity and air temperature at various locations within the tunnel which could not be secured with the traverse mechanism, Figs. 45 and 46. The movable probe consisted of two elements:

1. A sensing element of the hot wire anemometer. This was used to measure the velocity of the air.

2. Dry thermocouple No. 48. This thermocouple was used to measure the temperature of the air.

The rod on which the probe was mounted could be placed at any point within the tunnel. A metallic tape attached to the rod facilitated vertical orientation of the probe.

Sta. 1 (Barge)

Wind direction

N

Data representative of Sta. 1
were taken at this location

Temperature gradient
appurtenance at Sta. 1

2"
(Actual distance on model)

Sta. 2 (South Station)

Data representative of Sta. 2
were taken at this location

Wind direction

N

1"

Sta.2 location marker

2"
(Actual distance on model)
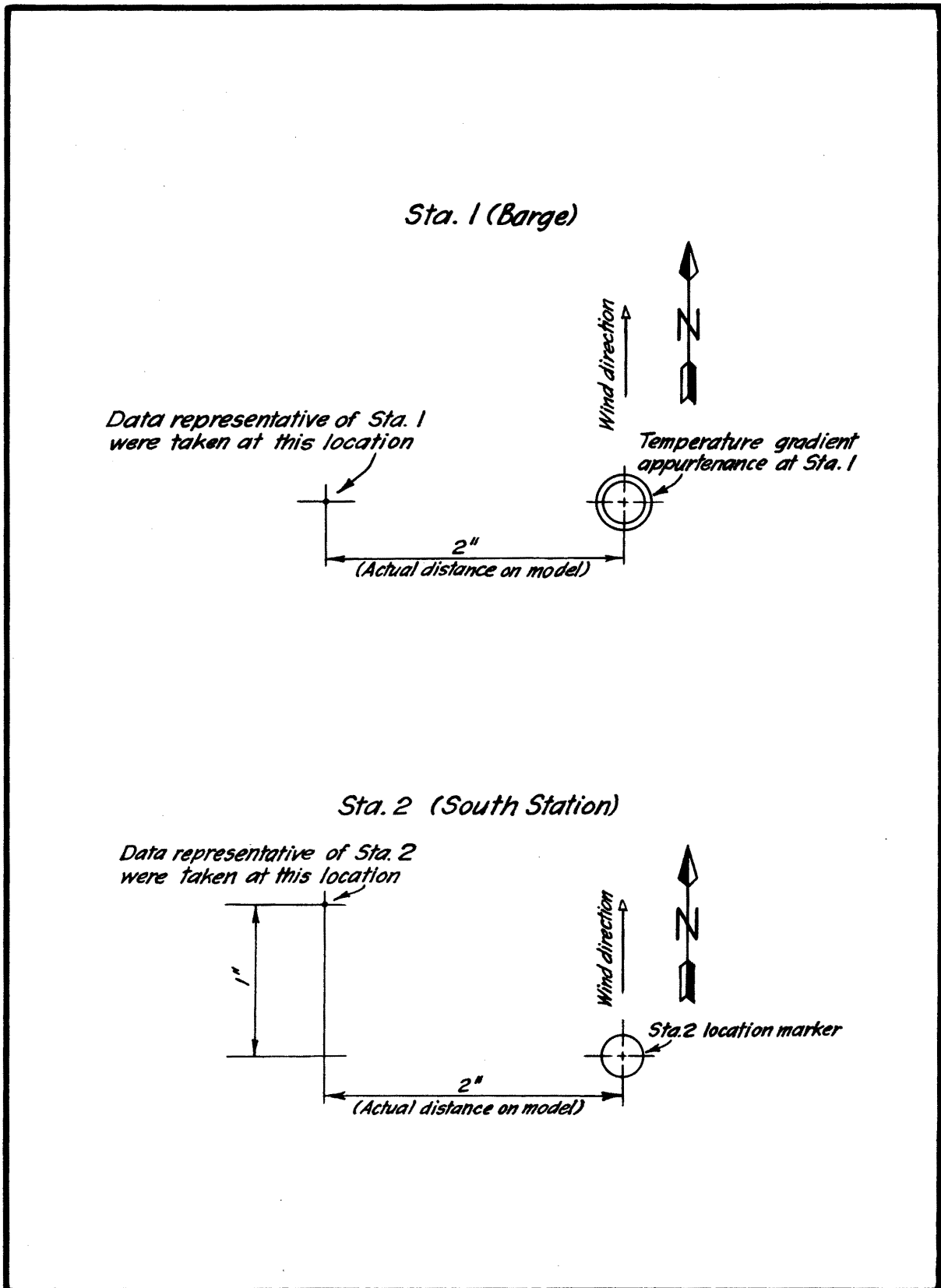
Fig. 43. Displaced positions for Stas. 1 and 2.
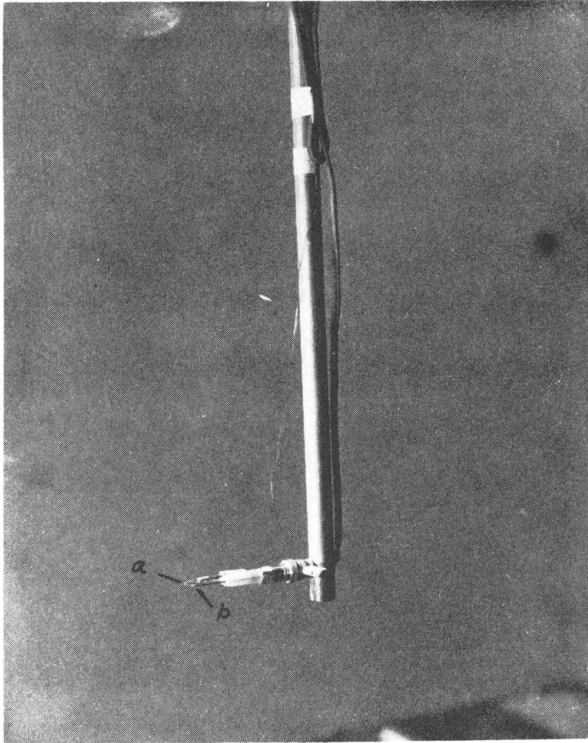
Fig. 44. Rear tunnel sensing
elements and support -
left to right
a. Dry thermocouple No. 43
b. Hot wire anemometer.
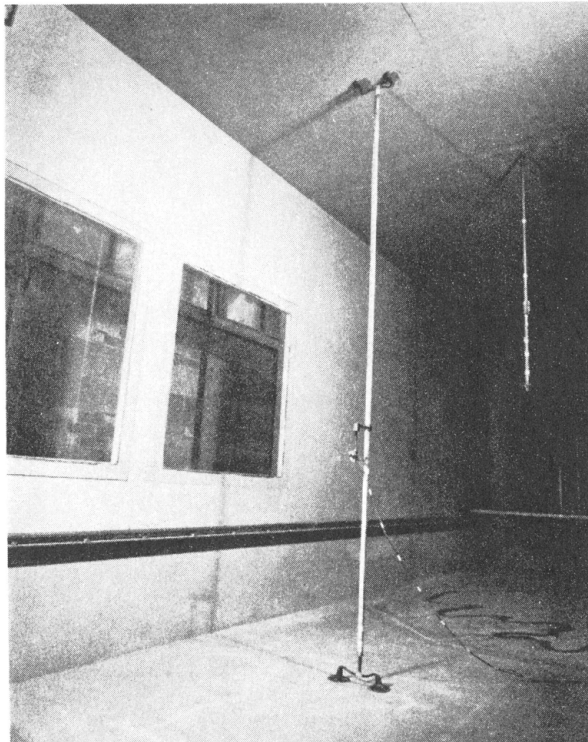
Fig. 45. Movable probe.
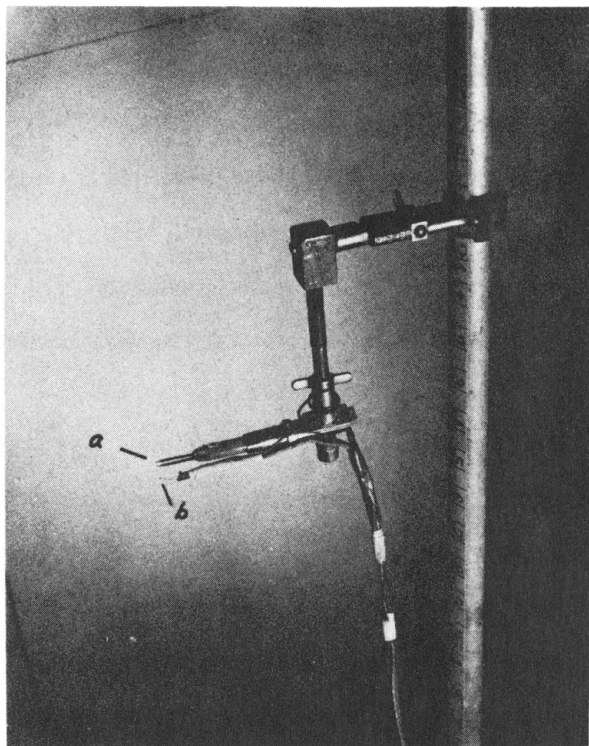
Fig. 46. Movable probe - left to right
    a. Hot wire anemometer
    b. Dry thermocouple
       No. 48.

Testing

Certain work was performed on the model, wind tunnel, and instrumentation prior to the commencement of each day's testing. This included:

1. Instrumentation preparation.

    a. Replenish the supply of ice at the cold junction.

    b. Fill the water supply reservoirs for the thermocouple psychrometers and adjust the rate of flow.

    c. Calibrate the necessary sensing elements of the hot wire anemometer.

2. Preparation of the lake surface. The only means known which would eliminate the dry spots on the evaporation surface was the sanding which provided only temporary relief. Therefore, prior to the testing for any day, the dry spots were eliminated temporarily by sanding.

After the completion of the preparatory work, air was circulated over the model at the same velocity as that which would prevail during the test. The air was circulated for about an hour prior to testing to permit the model to reach thermal equilibrium.

The data gathering program for this study of Lake Hefner was divided into tests and runs, both of which were numbered consecutively, Part I and Part II - Appendix D. The run data were a supplement to the main or test data. The following procedure was followed in securing the data for a particular test and the accompanying runs:

1. Just prior to the commencement of any test, the ambient air velocity within the tunnel was measured with the forward tunnel anemometer. If the velocity deviated considerably from the predetermined value at which the test was to be conducted, the velocity was changed by the proper manipulation of the throttle on the engine. If the velocity were adjusted, a sufficient length of time was permitted to transpire so as to enable the surface to reach thermal equilibrium under the new conditions. If the velocity of the air deviated but a small amount from that desired, it was not corrected.

2. The temperatures as indicated by each of the thermocouples were recorded. These readings indicated, besides other things, the temperature existing at various points on the surface and bottom of the modeled lake. This constituted the data for a run, Part II - Appendix D.

3. The temperature and humidity of the ambient air was measured with the sling psychrometer. These data were used only as a check on the thermocouple data.

4. The instrumentation mounted on the traverse mechanism was used to secure data on the temperature, humidity, and velocity profiles existing above various points. The traverse mechanism was moved so that the sensing element of the hot wire anemometer was directly above and very close to the desired point. The actual height of the

sensing element of the hot wire anemometer above the point was estimated.

5. The water supply for the lake was switched from automatic to manual and a note made of the time.

6. The air velocity and wet and dry bulb temperatures as indicated by the traverse instrumentation were measured while the instrumentation was at the estimated height above the terrain. The time of this measurement usually coincided with the switching of the water supply from automatic to manual. After these measurements were recorded, the sensing elements on the traverse mechanism were raised a predetermined height and the same measurements repeated. This procedure was repeated until the sensing elements on the traverse mechanism were more than 5 in. above the surface. These data constituted part of the test data, Part I - Appendix D.

7. The forward tunnel psychrometer was read each time a measurement was made with the traverse psychrometer. This constituted a part of the test data, Part I - Appendix D.

8. Usually the temperature and humidity of the ambient air were measured in the middle of a test by the use of the sling psychrometer to check the thermocouple data.

9. Water was added to the lake whenever the water level of the modeled lake dropped below some predetermined level as indicated by the lake stage indicator. After all the measurements for the velocity, temperature, and humidity were made, the level of the water in the lake was brought up to the level at which the test commenced. The water supply was then switched from manual to automatic and the time recorded. The manual water supply burette indicated the total quantity of water evaporated during a particular test. These data were a part of the test data, Part I - Appendix D.

10. The sling psychrometer was again used to measure the temperature and humidity of the ambient air. This same set of readings was used to

represent the conditions in the tunnel at the conclusion of one test
and the beginning of another. Again, these data were used only as a
check on the thermocouple data.

11. The temperatures as indicated by all the thermocouples were read.
These readings represented the conditions in the tunnel at the
conclusion of one test and the beginning of another. This constituted
the data for another run, Part II - Appendix D.

12. Usually all the tests on a particular day were conducted at the same
ambient air velocity. Therefore, the tests made in addition to the
first one were usually repeats of the first test or were tests
conducted at the different locations. If it were the latter case, the
traverse mechanism was moved so that the sensing elements were in the
proper position at the new location. The second, third, etc., tests
were made by repeating steps 1 - 11.

13. When feasible, the sensing elements of the hot wire anemometer were
spot-checked after the day's testing.

The data gathered as a result of the testing were placed in two groups --
runs and tests. The main data which concerned the evaporation and temperature,
humidity and velocity profiles were placed into the group called tests. Each
test contains the complete data concerning the evaporation and temperature,
humidity, and velocity profiles taken at a particular location for a certain
ambient air velocity. The tests have been numbered consecutively based on
their chronological order. These data have been included in Part I -
Appendix D in detail.

Each run contains the data of the temperatures existing in and around the
model as indicated by all the thermocouples incorporated in the model. A
steady state condition, so far as temperature was concerned, was assumed to
exist in the model during a particular test. Though this was not an actuality,
temperature changes during a test were of such a small nature that the
arithmetic average of the various temperatures at the beginning and end of a
test was considered to be representative of conditions during the test.

Therefore, the data comprising a test are supplemented by the data of the run preceding the test and the run following the test. The runs have been numbered in a fashion which permits association with the proper test; that is:

Run #6a refers to the temperature data taken prior to test #6.

Run #6b-7a refers to the temperature data taken after test #6 and prior to test #7.

Run #7b-8a refers to the temperature data taken after test #7 and prior to test #8.

Run #8b refers to the temperature data taken after test #8.

The run data, in detail, have been included in Part II - Appendix D.

A summary of the significant test and run data for the 29 tests can be found in Table III - Appendix B.

Barometric Pressure

An off-airways climatological station is maintained on the campus of Colorado A & M College. The barometric pressures existing during the various tests were taken from the barograph records of this station. Because of the proximity of the wind tunnel to the weather station (approximately 0.2 mile) and the negligible difference in elevation between the two places, the barometric pressures recorded at the weather station were considered to be the same as those existing at the wind tunnel. In the process of evaluating the model data the barometric pressure was considered to be constant at a value of 25.0 in. mercury. This procedure was deemed acceptable in light of the small differences of pressure between the actual pressure and 25 in. The actual barometric pressures are presented in this report so that the effect of the different pressures may be evaluated if desired, Table V - Appendix B.

Longitudinal Pressure Drop in the Tunnel

To measure the air pressure drop along the longitudinal axis of the tunnel, three piezometers, spaced 4 ft apart, were installed in the ceiling of the tunnel above the modeled lake. They were made from 1/16 in. brass tubing

having an inside diameter of 3/64 in.

Flexible tubing connected the piezometers to a form of a Wahlen gage which was used to measure the difference in pressure between the various piezometers. The Wahlen gage was capable of measuring pressure differences as small as 0.00028 lb/in.^{2}, Fig. 47. As a result of tests performed with this apparatus, the drop in pressure was found to be insignificant.
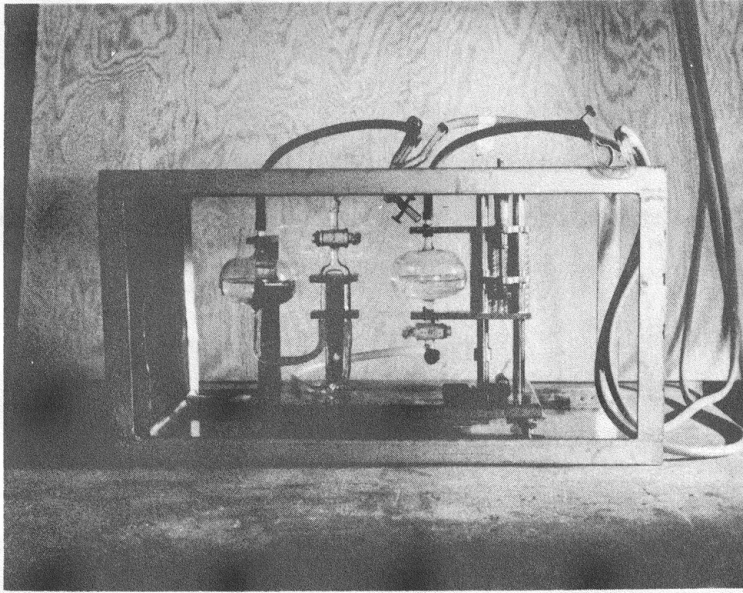
Fig. 47. Wahlen gage.

Appendix B

TABLES

This section of the appendix is devoted to the presentation of tables containing data for both the model and the prototype.

Table I

Prototype Data for Adiabatic Wind Profiles over

Lake Hefner Measured at Sta. 1 (18:49)

$U_{26.2}$	$\dfrac{U_{26.2}}{U_{6.56}}$	U_*	z_0	ϵ_w	$\dfrac{U_* z_0}{\nu}$	$(U_*/U_{26.2})^2$	Surface
$\dfrac{ft}{sec}$		$\dfrac{ft}{sec}$	ft	ft			
			(10^{-2})			(10^{-3})	
3.28	1.239	0.1805	1.90	0.571	21.4	3.06	rough
6.56	1.241	0.371	2.06	0.620	47.5	3.20	rough
9.84	1.243	0.561	2.16	0.650	75.2	3.25	rough
13.10	1.245	0.747	2.26	0.679	105.2	3.26	rough
19.68	1.250	1.140	2.52	0.757	178.2	3.35	rough
32.8	1.259	1.940	3.08	0.925	371.0	3.50	rough
39.4	1.265	2.385	3.44	1.037	510.0	3.66	rough
49.2	1.269	3.05	3.77	1.135	704.0	3.75	rough

Table II

Summary of 3-hour Prototype Data

Day	E $\dfrac{\text{lb}}{\text{ft}^2\text{-sec}}$ $\times 10^{-6}$	$\sqrt{A}$ ft	ΔC $\dfrac{\text{lb}}{\text{ft}^3}$ $\times 10^{-4}$	ν_e $\dfrac{\text{ft}^2}{\text{sec}}$ $\times 10^{-4}$	N $\times 10^6$	U_* $\dfrac{\text{ft}}{\text{sec}}$	R_* $\times 10^7$
Part I Prototype Data -- Period January 6-20, 1951							
6		10,000		2.52		1.945	7.72
7	6.26	10,000	2.12	2.51	1.179	1.135	4.53
8	7.77	10,000	2.26	2.59	1.327	1.197	4.62
9		10,000		2.56		2.04	7.98
10		10,000		2.52		2.33	9.27
11		10,000		2.55		1.843	9.16
12		10,000		2.61		1.429	5.49
13		10,000		2.54		1.020	4.01
14		10,000	1.076	2.53		1.682	6.65
15	3.67	10,000	1.253	2.57	1.141	1.477	5.76
16		10,000		2.64		2.28	8.65
17		10,000		2.66		1.682	6.30
18		10,000		2.65		1.410	5.32
19		10,000		2.71		1.830	6.76
20		10,000		2.42		3.11	12.85
Part II Prototype Data -- Period April 1-15, 1951							
1	9.27	10,000	2.38	2.59	1.501	1.610	6.22
2	7.22	10,000	2.53	2.61	1.092	1.505	5.77
3	1.324	10,000	3.18	2.65	1.569	0.890	3.36
4	8.43	10,000	2.40	2.78	1.261	1.748	6.25
5	-4.03	10,000	-5.20	2.73	2.84	1.870	6.85
6	1.686	10,000	0.877	2.58	0.744	2.38	9.25
7	13.43	10,000	0.0296	2.62	1.729	3.15	12.03
8	12.82	10,000	4.20	2.58	1.182	1.850	7.17
9	12.16	10,000	4.45	2.62	1.044	1.742	6.65
10	5.96	10,000	2.62	2.61	0.870	1.803	6.91
11	19.02	10,000	3.68	2.52	2.05	3.01	11.93
12	19.14	10,000	3.55	2.51	2.15	2.41	9.62
13	10.84	10,000	4.01	2.60	1.041	1.264	4.87
14	11.20	10,000	3.58	2.73	1.141	1.899	6.95
15	16.13	10,000	3.94	2.62	1.566	1.481	5.65
Part III Prototype Data -- Period July 1-15, 1951							
1	20.42	10,000				1.152	4.17
2	8.80	10,000	3.72	2.76	0.822	1.067	3.71
3	2.77	10,000	1.663	2.88	0.565	1.565	5.30
4	8.19	10,000	4.39	2.95	0.653	1.274	4.44
5	12.58	10,000	2.89	2.88	1.478	1.593	5.40
6	14.75	10,000	3.58	2.95	1.393	1.640	5.55
7	17.05	10,000	4.06	2.96	1.436	1.637	5.53
8	20.60	10,000		2.97		1.798	6.06
9	15.41	10,000	4.43	2.97	1.172	1.535	5.18
10	14.63	10,000	4.04	2.97	1.219	1.520	5.12
11	14.57	10,000	4.09	2.97	1.201	1.441	4.86
12	13.31	10,000	4.42	2.98	1.013	1.313	4.41
13	9.52	10,000	4.63	2.92	0.705	1.116	3.83
14	11.57	10,000	4.34	2.88	0.925	1.218	4.22
15	13.49	10,000	3.76	2.93	1.176	1.270	4.33

Table III

Summary of Model Data for 1952

Test No.	Mo. & Day	Sta.	Time of Day of Test	A ft²	E $\frac{lb}{ft^2\text{-}sec}$ ×10⁻⁵	T_o °F	C_o $\frac{lb}{ft^3}$ ×10⁻⁴	T_{AD} °F	T_{AW} °F	C_A $\frac{lb}{ft^3}$ ×10⁻⁴	ΔC $\frac{lb}{ft^3}$ ×10⁻⁴	ν_e $\frac{ft^2}{sec}$ ×10⁻⁴	$N = \frac{E\sqrt{A}}{\Delta C \nu_e}$ ×10²	$U_{52.5}$ $\frac{ft}{sec}$	$U_{26.2}$ $\frac{ft}{sec}$	U_* $\frac{ft}{sec}$	$R_* = \frac{U_*\sqrt{A}}{\nu_e}$ ×10³
1	9-27	2	0929-1026	25.01	1.460	54.1	6.72	73.9	53.2	3.28	3.44	3.30	6.42	8.95	7.92	0.586	8.88
2	10-8	2	1530-1643	25.01	0.607	56.6	7.32	72.7	52.9	3.36	3.96	3.28	2.34	1.97	1.40	0.329	5.01
3	10-20	2	1352-1445	25.01	0.693	49.4	5.70	56.2	43.8	2.73	2.97	3.10	3.76	1.67	1.21	0.273	4.40
4	10-20	2	1513-1604	25.01	0.708	49.2	5.66	55.9	44.7	3.05	2.61	3.10	4.38	2.00	1.47	0.296	4.77
5	10-21	2	1328-1434	25.01	1.296	51.4	6.12	70.1	48.7	2.29	3.83	3.25	5.21	4.12	3.54	0.330	5.09
6	10-22	2	1334-1420	24.59	1.072	52.8	6.42	66.7	49.0	2.84	3.58	3.22	4.61	4.32	3.42	0.536	8.25
7	10-22	1	1445-1530	24.52	1.093	52.8	6.42	66.0	48.3	2.70	3.72	3.21	4.53	4.32	3.73	0.352	5.42
8	10-22	3	1545-1623	24.42	1.110	52.7	6.40	64.2	48.1	2.91	3.49	3.19	4.93	4.91	4.22	0.414	6.41
9	10-23	2	1351-1439	24.50	0.709	52.3	6.31	70.3	50.1	2.70	3.61	3.26	2.98	2.14	1.76	0.216	3.28
10	10-23	1	1455-1545	24.50	0.765	53.3	6.53	69.4	49.2	2.51	4.02	3.25	2.90	2.52	2.16	0.203	3.10
11	10-23	3	1606-1642	24.43	0.798	53.8	6.65	67.1	48.2	2.54	4.11	3.22	2.98	1.90	1.57	0.195	2.99
12	10-25	2	1402-1451	25.01	1.750	51.3	6.10	74.0	49.4	1.88	4.22	3.30	6.29	6.88	6.10	0.456	6.91
13	10-25	1	1511-1554	25.01	1.980	51.7	6.18	72.3	47.3	1.45	4.73	3.28	6.39	4.08	2.42	0.957	14.59
14	10-28	2	1330-1427	25.01	1.150	48.0	5.43	66.5	47.2	2.27	3.16	3.22	5.50	5.20	4.28	0.527	8.17
15	10-28	2	1535-1609	25.01	2.400	49.0	5.62	66.9	46.3	1.93	3.69	3.22	10.10	12.87	11.46	0.812	12.61
16	10-29	2	1405-1446	25.01	1.130	48.5	5.52	63.2	45.6	2.23	3.29	3.18	5.41	4.61	3.71	0.511	8.06
17	10-29	4	1540-1621	25.01	1.050	49.1	5.64	61.4	46.1	2.66	2.98	3.16	5.58	6.47	5.59	0.508	8.06
18	11-3	2	1429-1456	24.99	1.210	42.6	4.47	52.0	41.8	2.71	1.76	3.05	11.33	14.80	13.10	1.017	16.78
19	11-3	1	1551-1619	24.99	1.310	42.7	4.49	52.5	41.1	2.45	2.04	3.06	10.49	13.70	12.10	0.914	14.93
20	11-3	4	1638-1700	25.01	1.340	42.3	4.43	50.4	39.5	2.28	2.15	3.04	10.27	12.50	10.60	1.096	18.07
21	11-4	2	1343-1407	25.01	1.213	47.7	5.37	67.6	47.7	2.26	3.11	3.23	6.05	5.23	4.60	0.358	5.55
22	11-4	1	1431-1458	24.96	1.303	48.7	5.57	69.5	47.5	1.91	3.66	3.25	5.49	5.27	4.67	0.352	5.41
23	11-4	4	1513-1533	24.96	1.203	49.5	5.72	68.5	48.6	2.44	3.28	3.24	5.66	5.10	4.47	0.371	5.71
24	11-4	3	1548-1612	24.99	1.189	50.0	5.82	67.0	47.2	2.19	3.63	3.22	5.09	3.65	3.20	0.264	4.10
25	11-4	3	1630-1646	24.99	1.341	50.2	5.87	63.3	45.9	2.31	3.56	3.18	5.92	3.47	3.05	0.242	3.80
26	11-6	2	1408-1439	25.01	0.531	41.1	4.24	47.6	34.8	1.32	2.92	3.00	3.03	1.07	0.78	0.169	2.82
27	11-6	1	1451-1524	25.01	0.370	40.9	4.21	48.2	33.8	0.974	3.24	3.01	1.90	1.07	0.66	0.236	3.91
28	11-6	4	1540-1613	25.01	0.396	40.5	4.15	45.9	32.3	0.908	3.24	2.98	2.05	1.28	0.89	0.223	3.74
29	11-6	3	1629-1650	25.00	0.476	39.9	4.06	46.6	32.0	0.723	3.34	3.00	2.38	1.50	1.15	0.200	3.33

Table IV

Thermocouple Details

Thermo-couple number	Name and location	Junction	Wire
1	Sta. 2 (South station) - surface	a	h
2	Sta. 4 (North station) - surface	a	h
3	Sta. 3 (Northeast station) - surface	a	h
4	West - surface	a	h
5	Sta. 1 (Barge) - surface)	b	h
6	Sta. 1 (Barge))	b	h
7	Sta. 1 (Barge) : Water tempera-	b	h
8	Sta. 1 (Barge)) ture gradient	b	h
9	Sta. 1 (Barge))	b	h
10	Sta. 1 (Barge) - bottom)	f	h
11	Sta. 2 (South station) - bottom	f	h
12	Sta. 4 (North station) - bottom	f	h
13	Sta. 3 (Northeast station) - bottom	f	h
14	West - bottom	f	h
15	Same as #10	f	h
16	Water supply	f	h
17-20	Blank		
21	Inlet - surface	a	h
22	Southwest - surface	a	h
23	Northwest - surface	a	h
24	East - surface	a	h
25	Southeast - surface	a	h
26	South-intermediate - surface	a	h
27	West-intermediate - surface	a	h
28	North-intermediate - surface	b	h
29-40	Blank		
41	Forward tunnel psychrometer - dry temperature	a	g
42	Traversing psychrometer - dry temperature	a	g
43	Rear tunnel - air temperature	a	g
44	Air temperature, surface, north of lake	a	g
45	Air temperature, surface, south of lake	a	g
46	Air temperature outside instrument shelter	a	g
47	Encased thermocouple check temperature	f	h
48	Air temperature, roving probe	a	h
49-50	Blank		
51	Forward tunnel psychrometer - wet temperature	a	g
52	Traversing psychrometer - wet temperature	a	g
53-60	Blank		
61	Air temperature, tunnel wall, S.W., low	b	h
62	Air temperature, tunnel wall, S.W., high	b	h
63	Air temperature, tunnel wall, N.W., low	b	h
64	Air temperature, tunnel wall, N.W., high	b	h
65	Air temperature, tunnel wall, N.E., low	b	h
66	Air temperature, tunnel wall, N.E., high	b	h
67	Air temperature, tunnel wall, S.E., low	b	h
68	Air temperature, tunnel wall, S.E., high	b	h

Table V

Barometric Pressures - Fort Collins, Colorado

Units - Inches of Mercury

Date					Time of Day						
	8:00	9:00	10:00	11:00	12:00	13:00	14:00	15:00	16:00	17:00	18:00
9-27-52	25.080	25.075	25.070	25.040	25.010	24.995	24.975	24.970	24.960	24.960	24.960
10-8-52	25.165	25.170	25.180	25.175	25.170	25.160	25.135	25.130	25.120	25.120	25.120
10-20-52	25.220	25.220	25.220	25.210	25.200	25.180	25.180	25.180	25.180	25.180	25.180
10-21-52	25.180	25.185	25.190	25.190	25.185	25.165	25.155	25.145	25.145	25.150	25.155
10-22-52	25.280	25.300	25.320	25.325	25.325	25.320	25.300	25.295	25.295	25.295	25.295
10-23-52	25.285	25.285	25.285	25.285	25.275	25.250	25.220	25.200	25.195	25.180	25.180
10-25-52	25.170	25.180	25.180	25.175	25.170	25.150	25.130	25.125	25.120	25.125	25.135
10-28-52	25.405	25.400	25.375	25.360	25.325	25.290	25.270	25.260	25.250	25.200	25.200
10-29-52	25.180	25.180	25.160	25.150	25.130	25.100	25.065	25.060	25.050	25.020	25.020
11-3-52	25.440	25.440	25.440	25.430	25.420	25.400	25.370	25.350	25.340	25.230	25.325
11-4-52	25.180	25.180	25.165	25.150	25.120	25.090	25.075	25.055	25.045	25.045	25.050
11-6-52	25.315	25.320	25.320	25.315	25.295	25.260	25.240	25.230	25.225	25.220	25.220

Appendix C

DATA TRANSFORMATION

As a result of this study and others, data for correlation purposes were
available from four sources. Many of these evaporation data were not in a form
consistent with the dimensional analysis of Chapter II. Therefore, these data
were transformed to forms which were. The object of this Chapter is to present
in detail the steps followed in accomplishing this end. Each of the four
sources of data will be treated in turn.

Data Based on the von Kármán Extension of Reynolds Analogy

In Chapter II relationships between the parameters N and R_* were
derived for various ranges of values of R_* when evaporation occurred from
smooth and rough plane boundaries. The object of this section is to evaluate
further these relationships between N and R_* in light of the known
prototype data (18) and model characteristics.

Case I -- Evaporation equation for $10^3 \leqq R_* \leqq 10^5$ -- smooth boundary (model
range).

$$\frac{1}{N} = \frac{6.23}{(R_*)^{8/9}\left(\frac{x}{\sqrt{A}}\right)^{4/45}} - \frac{3.77}{R_*\left(\frac{x}{\sqrt{A}}\right)^{1/10}} \tag{22}$$

Since R_* for the model data fell in this range, the quantity x in Eq. 22
was considered to be the distance from the upstream edge of the modeled terrain
to Sta. 2. This distance was 7.8 ft. The parameter $\sqrt{A}$ was taken as the
square root of the area of the modeled lake. The area of the modeled lake was
25.01 square feet and the square root of this was 5.00 ft. When x and $\sqrt{A}$
were considered equal to 7.8 ft and 5.00 ft respectively, Eq. 22 reduced to

$$\frac{1}{N} = \frac{5.99}{(R_*)^{8/9}} - \frac{3.61}{R_*} \, . \tag{22a}$$

Case II -- Evaporation equation for $R_* \geqq 10^5$ -- smooth boundary.

$$\frac{1}{N} = \frac{0.174}{R_* \log\left(\frac{3280}{z_{ol}}\right)} \left\{ 4.68 \left\{ 0.574 + \log\left[\log\left(\frac{3280}{z_{ol}}\right)\right] + \log R_* \right\}^{2.64} \right.$$

$$\left. -8.70 \left\{ 0.574 + \log\left[\log\left(\frac{3280}{z_{ol}}\right)\right] + \log R_* \right\}^{1.32} \right\} \qquad (24)$$

A more direct relationship between N and R_* could be evolved if a representative value of z_{ol} were substituted into Eq. 24. The following procedure was followed in the determination of this value of z_{ol}.

Since Sta. 2 was the upwind station for the prevailing wind, it was selected as the significant land station for purposes of computing z_{ol} and for extrapolation of Sta. 1 data to a land station.

Prior to the determination of z_{ol}, a correlation had to be evolved between the wind velocity at Sta. 1 and Sta. 2 so that the average wind velocity at Sta. 2 could be determined on the basis of the 16-month average velocity at Sta. 1 which was 19.4 ft/sec at an elevation of 26.2 ft. This correlation was attained in the following manner:

a. The 1/2-hour prototype data were reviewed and those satisfying the following were selected for further analysis.

(1) The predominant wind direction at all of the four stations for a particular 1/2-hour period was southerly.

(2) The velocity at Sta. 1 at an elevation of 52.5 ft was 54.1 ft/sec.

b. The velocities for Stas. 1 and 2 at an elevation of 26.2 ft were selected from the data satisfying conditions (1) and (2) under a. From these figures an average velocity for Sta. 1 was determined and an average velocity for Sta. 2 was determined. Both average velocities were for an elevation of 26.2 ft and satisfied the restrictions under a. This value of $U_{26.2\text{-Sta. }1}$ and $U_{26.2\text{-Sta. }2}$ determined one point on the plot of $U_{26.2\text{-Sta. }1}$ versus $U_{26.2\text{-Sta. }2}$, Fig. 1.

c. Five additional points for Fig. 1 were determined when Steps a and b were repeated for velocities of 40.6, 27.01, 13.51, 6.76, and 3.38 ft/sec instead of the velocity of 54.1 ft/sec.

d. The 16-month average velocity of 19.4 ft/sec for Sta. 1 at an elevation of 26.2 ft corresponded to a velocity of 16.2 ft/sec for Sta. 2 at an elevation of 26.2 ft based on Fig. 1.

To attain an average value of $z_{o\ell}$, $z_{o\ell}$ was considered to have that value of roughness which corresponded to the average wind velocity for Sta. 2; namely, 16.2 ft/sec. Fig. 2 was prepared in an endeavor to correlate $z_{o\ell}$ and $U_{26.2-Sta. 2}$. This was accomplished as follows:

e. After the data had been separated according to Step a, $z_{o\ell}$ for each velocity profile for Sta. 2 was determined. The arithmetic average of these values of $z_{o\ell}$ combined with the average velocity at Sta. 2 located one point on the plot of $z_{o\ell}$ versus $U_{26.2-Sta. 2}$, Fig. 2.

f. Five additional points for Fig. 2 were obtained by repeating Step e for the different velocities listed under Step c.

g. According to Fig. 2, the value of $z_{o\ell}$ which corresponded to a velocity of 16.2 ft/sec was 0.22 ft.

The adoption of the value of 0.22 ft for $z_{o\ell}$ simplified the relationship of Eq. 24 between N and R_* to

$$\frac{1}{N} = \frac{0.0417}{R_*}\left[4.68(1.194 + \log R_*)^{2.64}\right.$$
$$\left.-8.70(1.194 + \log R_*)^{1.32}\right] . \tag{24a}$$

Case III -- Evaporation equation for $R \geqq 10^5$ -- rough boundary.

$$N = \frac{2.875 R_*}{\left[1.89 + 1.62 \log \left(\frac{\sqrt{A}}{\epsilon_w}\right)\right]^{2.5}} \log\left(\frac{3280}{z_{o\ell}}\right) . \tag{26}$$

Here as in Case II a more direct relationship between N and R_* was evolved by substituting into Eq. 26 average values of $z_{o\ell}$ and r' . As in Case II, $z_{o\ell}$ was assigned the value of 0.22 ft. By definition, r' was equal to $\frac{\sqrt{A}}{\epsilon_w}$.

For the prototype, the $\sqrt{A}$ was assumed to be constant at a value of 10,000 feet since A was taken as equal to 10^8 square feet (2,290 acres). The selection of a significant average value of ϵ_w for insertion into Eq. 26 was, in light of present day knowledge, a difficult task. This was the case because the wind not only causes the water surface to move but it also creates waves. Therefore, the application of Eq. 6

$$\frac{U_z}{U_*} = 5.75 \log \left(\frac{30z}{\epsilon}\right) \tag{6}$$

to the velocity profiles over water in an endeavor to determine ϵ_w may not be justified. Be that as it may, the average value of ϵ_w was taken as 0.754 ft corresponding to a velocity of 19.4 ft/sec. This value of the roughness parameter was based on the figures for $U_{26.2-Sta.\ 1}$ and ϵ_w in Table I - Appendix B. Using these approximations for $z_{o\ell}$ and r', Eq. 26 reduced to

$$N = 0.0546\ R_* . \tag{26a}$$

Prototype Data

The actual data from the prototype study of Lake Hefner were available in three forms:

1. The 1/2-hour data cards. The meteorological conditions at the four Lake Hefner meteorological stations were recorded for each 1/2-hour interval on I.B.M. punch cards. A set of these cards was made available to Colorado A & M College.

2. The 3-hour average data. For purposes of averaging the data, each day was broken down into eight 3-hour periods. The arithmetic average of the various readings for the six 1/2-hour intervals comprising a 3-hour period was considered as being representative of that 3-hour period. A set of these data was also made available to Colorado A & M College.

3. U. S. Geological Survey Circular #229 data (18). The agencies participating in the Lake Hefner prototype study subjected the data to

rigorous analysis. The significant findings and results of these
analyses were presented in this circular.

These three forms of prototype data were analyzed at Colorado A & M
College in light of the work being done on the Lake Hefner model. The
remainder of this section will be devoted to a discussion of the approach
adopted at Colorado A & M College in analyzing these forms of prototype data.

The 1/2-Hour Data Cards

The data contained on the 1/2-hour data cards were subjected to minor
analyses. Some of the velocity data for south winds at Sta. 2 were used to
determine a relationship between $U_{26.2-Sta. 1}$ and $U_{26.2-Sta. 2}$, Fig. 1.
They were also used to obtain a relationship between $U_{26.2-Sta. 2}$ and $z_{o\ell}$,
Fig. 2.

The 3-Hour Average Data

The staff at Colorado A & M College concluded that the meteorological
conditions recorded at the four meteorological stations were well represented
by the 3-hour average data. Certain parts of these data were subjected to
detailed analysis in an endeavor to substantiate the soundness of the
assumptions made while treating the equation in the U. S. Geological Survey
Circular #229 (18). An analysis of all the data was not attempted because such
work would have only duplicated that performed by the agencies participating in
the Lake Hefner project.

An attempt was made to secure representative samples of consecutive proto-
type data which was taken during three different seasons of the year -- winter,
spring, and summer. A season representative of the autumn was not chosen
because the belief was held that spring and autumn conditions would be similar.

The personnel who gathered the Lake Hefner data assigned a quality grade
to the water budget evaporation data for each day. If conditions were such
that nothing took place which might affect the precision of the measurements,
the data were rated high. If something occurred, such as a rain storm, whose
effect might not be fully accounted for, then the data were rated lower
depending on the severity of conditions. The periods of data representing the

three seasons were chosen in such a manner that the average grade of the consecutive data contained within a given period was the highest obtainable within that season. The periods chosen were:

January 6 - 20, 1951, inclusive	Winter
April 6 - 20, 1951, inclusive	Spring
July 1 - 15, 1951, inclusive	Summer

The significant variables for the analysis of the prototype data were the same as those for the model; namely, U_z , U_* , $\sqrt{A}$, E , ν_e , and ΔC . In the prototype, it was not feasible to measure E for periods of time of less than one day. Therefore, the values of the variables U_z , U_* , $\sqrt{A}$, E , ν_e , and ΔC were derived in such a fashion as to reflect the average conditions for a day. Each of these variables will be discussed separately in the paragraphs that follow. As an introduction to this discussion, it might be well to remind the reader that each day was divided into eight 3-hour periods. In the prototype data analysis, each of the above mentioned variables except E was determined for each 3-hour period. The numerical value of each parameter for a particular day was considered to be the arithmetic average of the eight values of each parameter for that day.

U_z - velocity of the air at elevation z above the terrain -- feet/ second. The velocity profiles measured at the four meteorological stations for each 3-hour period were well represented by a linear relationship between the velocity and the logarithm of height. This linear relationship was used in the determination of the velocity at various elevations. The meteorological station located at the center of the lake, Sta. 1, recorded the wind direction. The wind direction over the lake for each 3-hour period was considered to be the same as the prevailing wind at Sta. 1 for that same period. The velocity profile at the up-wind station was considered to be representative of the velocity profile over the lake for each 3-hour period. If the prevailing wind was from the south or southeast, the wind profile at the south meteorological station, Sta. 2, was used. If the prevailing wind was from the east or northeast, the wind profile at the northeast meteorological station, Sta. 3, was

used. If the prevailing wind was from the north, the wind profile at the north meteorological station, Sta. 4, was used. At no time during the three fifteen-day periods considered was the prevailing wind for any three-hour period from the northwest, west, or southwest.

U_* - shear velocity of the air -- feet/second. The shear velocity for each 3-hour period, U_* , was determined by the solution of the two simultaneous equations formed when the velocities at two different levels were substituted into Eq. 1. The wind profile used in the determination of U_* for each three-hour period was taken as the up-wind profile for that period.

$\sqrt{A}$ - length parameter -- feet. The area of Lake Hefner, A , was considered to be constant at 10^8 square feet (2,290 acres). The area of the lake varied with the stage of the lake but the amount of variation was small and was therefore neglected. The length parameter $\sqrt{A}$ was computed by taking the square root of the area A which resulted in $\sqrt{A}$ being equal to 10,000 ft.

E - rate of evaporation -- pounds/feet^2-second. In the Lake Hefner records, the evaporation was recorded as so many inches of water per day. Simple numerical constants were used to convert these figures to the units of E , lb/ft^2-sec.

ν_e - molecular diffusion coefficient for water vapor -- feet^2/second. The kinematic viscosity of air ν for each 3-hour period was determined from a consideration of temperature and barometric pressure. The Prandtl number σ was considered to have a constant value of 0.6 which permitted the computation of ν_e by the relationship $\nu_e = \nu/0.6$. The barometric pressure used in the determination of ν was considered to be constant at 28.7 in. of mercury, (3:392). The 3-hour average temperature recorded at the meteorological station located at the center of the lake, Sta. 1 at an elevation of 6.56 ft was considered as being representative of the temperature for purposes of evaluating ν .

$\Delta C = C_o - C_A$ - difference in absolute humidity between the air in contact with the evaporation surface and the ambient air -- pounds/feet^3.

120

C_O - represented the absolute humidity of the air in contact with the lake -- pounds/feet^3. The air was considered to be completely saturated and at the same temperature as the evaporation surface. Therefore, the absolute humidity of the air was that corresponding to a saturated atmosphere at a temperature equal to that of the surface from which evaporation was taking place (9:83). The 3-hour average water surface temperature measured at Sta. 1, was used to evaluate C_O for each 3-hour period.

C_A - represented the absolute humidity of the ambient air -- pounds/feet^3. C_A for each 3-hour period was based on the 3-hour average readings as recorded by the psychrometer located at the 52.4 ft level at the up-wind meteorological station. The barometric pressure used in the computation of C_A was considered to be constant at a value of 28.7 in. of mercury.

The variables U_*, $\sqrt{A}$, ν_e, E, and ΔC were combined into the dimensionless parameters, N and R_*, for comparison purposes. The data are summarized in Table II - Appendix B and represented graphically in Fig. 7. U. S. Geological Survey Circular #229 Data (18).

As a result of the Lake Hefner prototype study the following relationship was evolved as the best correlation between evaporation, wind speed, and vapor pressure difference:

$$\frac{E'}{\Delta e} = 0.001167 \ U_{26.2\text{-Sta. 1}} \qquad (32)$$

where

E' - evaporation of water -- inches/feet^2-day,

$U_{26.2\text{-Sta. 1}}$ - wind speed at an elevation of 26.2 feet measured at Sta. 1 -- feet/second,

Δe - difference in water vapor pressure between that at the surface of the water and that of the air -- millibars.

The dimensional analysis indicated that for purposes of correlating evaporation, the variables U_*, $\sqrt{A}$, ν_e, E, and ΔC should be placed in the following dimensionless form:

$$\frac{E\sqrt{A}}{\Delta C \ \nu_e} = \phi_3\left(\frac{U_*\sqrt{A}}{\nu_e}\right). \qquad (33)$$

When Eq. 32 was transformed so as to be expressed in terms of the dimensionless parameters of Eq. 33, it assumed the form

$$N = 0.0203 \; R_* \; .\tag{27}$$

One must remember that Eq. 27 was derived from the equation for Lake Hefner, that is Eq. 32, and is only valid within the scope of the approximations used for the transformation of Eq. 32 to that of Eq. 27.

The steps followed in the process of transforming Eq. 32 to Eq. 27 are presented in the paragraphs that follow:

The conversion of E' to the units of E was accomplished by the introduction of the following constants:

$$E' = E \; \frac{(12)(24)(60)(60)}{62.4}\tag{34}$$

where

E' - evaporation of water -- inches/feet^2-day,

E - evaporation of water -- pound/feet^2-second.

Since the velocity $U_{26.2\text{-Sta. 1}}$ in Eq. 32 was based on the velocity of the air measured at Sta. 1 which was located at the center of Lake Hefner, $U_{26.2\text{-Sta. 1}}$ was converted to the velocity at a land station so as to be consistent with the analysis used on the actual prototype data. This was performed by means of the approximate linear relationship between $U_{26.2\text{-Sta. 1}}$ and $U_{26.2\text{-Sta. 2}}$ given in Fig. 1. Expressed in approximate functional form, this relationship was

$$U_{26.2\text{-Sta. 1}} = 1.137 \; U_{26.2\text{-Sta. 2}} \; .\tag{35}$$

The relationship between $U_{26.2\text{-Sta. 2}}$ and U_* was considered to be that expressed by

$$\frac{U_{26.2\text{-Sta. 2}}}{U_*} = 5.75 \; \log \left(\frac{z}{z_{o\ell}} \right) \; .\tag{1a}$$

In the course of evaluating Eq. 1a , z was taken as 26.2 feet which corresponded to the height at which the velocity was measured and $z_{o\ell}$ was considered to have the same value as that used for the evaluation of the von Kármán extension of Reynolds analogy; namely, 0.22 ft. These specific values

of z and $z_{o\ell}$ reduced Eq. 1a to

$$U_{26.2-Sta. 2} = 11.92 \, U_* \, . \tag{36}$$

Eqs. 35 and 36 were then combined with the result that

$$U_{26.2-Sta. 1} = 13.54 \, U_* \, . \tag{37}$$

The approximations and relations used to correlate Δe and ΔC were as follows: Specific humidity q_h may be expressed by the following relations (8:38)

$$q_h = \frac{C}{C + \rho} = \frac{0.622e}{p_a - 0.378e} \tag{38}$$

where

q_h - specific humidity -- pound/pound,

C - absolute humidity -- pounds/feet^3,

ρ - density of dry air -- pounds/feet^3,

e - water vapor pressure -- millibars,

p_a - total atmospheric pressure -- millibars.

Since p_a was of the order of 100 times that of $0.378e$, the omission of the term $0.378e$ was considered to be permissible without the introduction of a large error. Eq. 38 was rewritten as

$$e = \frac{Cp_a}{(C + \rho) \, 0.622} \, . \tag{39}$$

By definition

$$\Delta e = e_0 - e_{26.2} \, . \tag{40}$$

The vapor pressure of saturated air at the temperature of the water surface was e_0. Eq. 39 rewritten in terms of e_0 was

$$e_0 = \frac{C_0 p_a}{(C_0 + \rho_0) \, 0.622} \tag{41}$$

where

C_0 - absolute humidity of saturated air at the temperature of the water surface -- pounds/feet^3,

ρ_o - density of dry air at the temperature of the water surface -- pounds/feet^3.

The vapor pressure of the ambient air $e_{26.2}$ was determined by the psychrometer at the 26.2 ft-level at Sta. 1. Eq. 39 rewritten in terms of $e_{26.2}$ was

$$e_{26.2} = \frac{c_{26.2}\, p_a}{(c_{26.2} + \rho_{26.2})0.622} \tag{42}$$

where

$c_{26.2}$ - absolute humidity of the air as indicated by the psychrometer at Sta. 1 at the height of 26.2 feet -- pounds/feet^3,

$\rho_{26.2}$ - density of dry air as indicated by the temperature at an elevation of 26.2 feet at Sta. 1 -- pounds/feet^3.

Utilizing Eqs. 41 and 42, Eq. 40 was written in terms of absolute humidity as

$$\Delta e = e_o - e_{26.2}$$

$$= \frac{p_a}{0.622}\left[\frac{c_o\,(c_{26.2} - \rho_{26.2}) - c_{26.2}\,(c_o - \rho_o)}{\rho_o\,\rho_{26.2} + \rho_{26.2}\,c_o + \rho_o\,c_{26.2} + c_o c_{26.2}}\right] \tag{43}$$

Eq. 43 was simplified through the adoption of the following assumptions:

a. For practical purposes ρ_o and $\rho_{26.2}$ were considered to be equal. Data presented in reference (18:8) indicated that the difference in temperature between the air temperature at the 26.2-ft level and the water surface temperature was no greater than 3°C based on the average monthly temperatures. Most of the time this difference was between 1°C and 2°C. At a yearly average temperature of 15°C, a 3°C difference in air and water temperature accounts for less than 1 percent variation between ρ_o and $\rho_{26.2}$. Because ρ_o and $\rho_{26.2}$ were so nearly alike in value, they were considered to be equal; that is,

$$\rho_o = \rho_{26.2} = \rho.$$

b. The density of dry air ρ is of the order of 70 times greater than C_o and $C_{26.2}$. The quantity ρ^2 considered equal to $\rho_o \rho_{26.2}$ was likewise of the order of 70 times greater than $\rho_{26.2} C_o$ and $\rho_o C_{26.2}$ and of the order of 4900 times greater than $C_o C_{26.2}$. Therefore, the sum of the values of $\rho_{26.2} C_o$, $\rho_o C_{26.2}$, and $C_o C_{26.2}$ could be omitted because it was small when compared with ρ^2.

On the basis of these approximations, Eq. 43 reduced to

$$\Delta e = \frac{p_a}{0.622} \left(\frac{C_o - C_{26.2}}{\rho} \right).$$
(44)

Eq. 44 was further simplified by assuming average values for p_a and ρ. Based on the U. S. Standard Atmosphere (3:101) and on an elevation of 1194 feet, p_a had the value of 971 millibars. The average air temperature measured at the meteorological station located at the center of the lake at the 26.2 ft-level was taken as 15°C (18:8-Fig. 5). The value of ρ was assumed to be 0.0733 lb/ft^3 based on a temperature of 15°C and a barometric pressure of 971 millibars; therefore,

$$\Delta e = 21300 \, (C_o - C_{26.2}) = 21300 \, \Delta C.$$
(45)

These transformations permitted Eq. 32 to be rewritten as

$$\frac{E}{\Delta C} = 0.0203 \, U_*.$$
(46)

The introduction of the ratio of $\sqrt{A}/\nu_e$ to both sides of Eq. 46 completes the steps necessary to place Eq. 32 in the form of the dimensionless parameter N and R_*; that is,

$$N = 0.0203 \, R_*.$$
(27)

Model Data

The testing of the Lake Hefner model resulted in the accumulation of a considerable amount of data. These data had to be transformed so as to assume forms which would be significant for comparison purposes. The significant variables were U_z, U_*, $\sqrt{A}$, E, ν_e, and ΔC. The experimental data for each test are included in detail form in Appendix D. The transformed data have

been summarized in Table III - Appendix B. The data from each of the 29 tests performed on the Lake Hefner model were treated as follows:

U_z - velocity of the air at elevation z above the terrain -- feet/second. For each velocity profile a plot of velocities versus logarithm of heights greater than 0.10 in. above the terrain were best represented by a linear relationship. This linear relationship was used in the determination of the velocity at various elevations.

U_* - shear velocity of the air -- feet/second. The shear velocities U_* represented by the various velocity profiles, were determined by the simultaneous solution of Eq. 1 utilizing values of U_z corresponding to two different elevations.

$\sqrt{A}$ - length parameter -- feet. The total area of the evaporation surface was 25.01 sq ft. The net area from which evaporation took place was determined by deducting the estimated dry-spot area from the total area of 25.01 sq ft. The length parameter $\sqrt{A}$ was computed by taking the square root of the net area.

E - rate of evaporation -- pounds/feet^2-second. The total amount of water evaporated during a test was measured quantitatively by means of a burette. E was determined by dividing the total quantity of water evaporated by the length of time of the test and by the net evaporating area.

ν_e - molecular diffusion coefficient for water vapor -- feet^2/second. The kinematic viscosity of air ν was determined from a consideration of temperature and barometric pressure. The Prandtl number σ was considered to have a value of 0.6 which permitted the computation of ν_e by the relationship $\nu_e = \nu/0.6$. The barometric pressure used in the determination of ν was taken as the average barometric pressure at Fort Collins, 25.0 in. of mercury. The temperature T_{AD} which governed the value of ν was taken as the arithmetic average of the dry bulb temperatures recorded during a test at the forward tunnel position.

$\Delta C = C_o - C_A$ - difference in absolute humidity between the air in contact with the evaporation surface and the ambient air -- pound/feet^3.

C_0 - represented the absolute humidity of the air in contact with the evaporation surface -- pounds/feet^3. This air was considered to be completely saturated and at the same temperature T_0 as the evaporation surface. Therefore, the absolute humidity of the air was that corresponding to a saturated atmosphere at the temperature of the evaporation surface (9:83). Just prior to and following a test, the temperatures existing at 13 points on the evaporation surface were measured by means of thermocouples (thermocouples 1 through 5 and 21 through 28). The arithmetic average of these 26 temperature readings (2 times 13) was considered to be representative of the evaporation surface temperature T_0 for purpose of computing C_0 .

C_A - represented the absolute humidity of the ambient air -- pounds/feet^3. It was based on the temperature and humidity as indicated by the forward tunnel psychrometer and the average barometric pressure at Fort Collins, 25.0 in. mercury (3:392). The dry bulb temperature, T_{AD} used for computational purposes of C_A , was considered to be the arithmetic average of the dry bulb temperature recorded at the forward tunnel position during a test. The wet bulb temperature T_{AW} was considered to be the arithmetic average of the wet bulb temperatures recorded at the forward tunnel position during a test.

In view of the aforementioned interpretations given to the data, the results were placed in the form of the significant parameters. The variables U_z and U_* could be used for velocity profile correlations. The parameters N equal to $\dfrac{E\sqrt{A}}{\Delta C\, \nu_e}$ and R_* equal to $\dfrac{U_*\sqrt{A}}{\nu_e}$ could be determined for evaporation comparisons.

Data of Albertson (1)

The data of Albertson (1) concerning evaporation from a plane boundary were in a form consistent with the dimensional analysis and therefore could be plotted directly on Fig. 7. The range of $\dfrac{x}{\sqrt{A}}$ for these data was from 0.25 to 24.

Appendix D
DETAILED MODEL DATA

In this section of the report the detailed data are presented. These data are divided into two main sections, Part I - Model Tests and Part II - Model Runs. The reader is referred to Appendix A and in particular to the section titled "Testing" of that Appendix for a description of the methods and equipment used in collecting these data.

Part I - Model Tests

128

Time of day	Height above terrain Inches	Forward tunnel psychrometer $T_{AD}-°F$ Thermo. #41	$T_{AW}-°F$ Thermo. #51	Traverse psychrometer °F Thermo. #42	°F Thermo. #52	Traverse wind velocity ft/sec	Quantity of water evaporated cc
		Test No. 1		Date Sept. 27, 1952		Sta. 2	
9:28	0.020	69.5	51.4	66.7	53.2	3.6	0
9:30	0.025	70.2	51.7	66.8	53.2	3.6	20
9:34	0.030	70.5	51.2	67.0	53.1	3.6	40
9:36	0.035	70.8	52.3	65.3	53.2	4.0	60
9:37	0.045	71.1	51.8	65.3	53.3	4.4	80
9:38	0.055	71.7	52.6	67.6	53.3	4.8	100
9:40	0.065	71.8	52.4	68.0	53.7	5.9	135
9:43	0.075	71.9	53.2	69.5	52.7	6.4	140
9:44	0.085	72.6	52.8	69.5	52.2	7.0	160
9:46	0.095	73.0	53.1	70.2	52.2	7.0	180
9:48	0.120	72.2	53.3	70.2	52.2	7.0	180
9:50	0.145	73.1	52.7	70.7	52.2	7.8	180
9:52	0.170	73.1	53.2	70.7	52.1	7.8	200
9:54	0.195	74.3	53.4	71.4	52.1	8.6	230
9:55	0.245	73.3	52.8	71.4	51.8	8.6	250
9:57	0.295	73.5	52.9	71.7	51.4	8.6	280
9:58	0.345	74.1	52.7	71.1	51.5	9.5	300
10:00	0.395	74.3	53.1	71.8	51.5	9.5	320
10:02	0.495	74.4	53.2	71.8	52.3	10.5	330
10:04	0.595	74.7	53.2	73.5	52.3	10.5	350
10:05	0.695	74.8	53.6	72.9	52.4	10.5	360
10:06	0.895	74.9	53.6	73.3	52.4	10.5	380
10:07	1.095	75.1	53.3	73.3	52.6	10.5	400
10:09	1.345	76.1	53.7	73.8	52.6	12.0	410
10:10	1.595	76.2	54.0	74.0	53.1	12.0	420
10:13	1.845	75.3	53.6	74.3	52.7	12.0	430
10:15	2.095	75.6	54.4	74.3	53.2	12.0	440
10:16	2.595	76.1	53.6	75.3	53.3	12.0	460
10:18	3.095	76.5	54.2	76.5	53.6	12.0	480
10:19	3.595	77.0	54.7	76.6	54.1	12.0	500
10:21	4.095	77.1	54.5	76.6	53.7	12.0	525
10:23	4.595	77.9	55.0	77.9	54.6	12.0	550
10:26	5.095	77.9	54.6	77.9	52.7	12.0	565
		Test No. 2		Date Oct. 8, 1952		Sta. 2	
15:30	0.010	75.4	56.4	71.0			0
15:37	0.015	74.9	54.6	69.8	58.2		22
15:40	0.020	74.5	55.2	69.9	57.7		27
15:42	0.025	75.0	55.2	70.0	57.1		38
15:44	0.035	74.5	54.6	70.1	56.9		48
15:46	0.045	74.4	54.6	70.4	56.6		59
15:47	0.055	73.8	52.7	69.9	56.0	0.59	67
15:50	0.065	73.7	53.5	69.9	56.0	0.74	82
15:52	0.075	73.9	53.3	69.9	55.6	0.94	86
15:56	0.085	73.9	53.4	69.7	55.0	0.96	95
15:58	0.110	73.5	53.2	70.8	54.5	1.0	107
16:01	0.135	73.4	52.9	70.6	50.1	1.2	125
16:03	0.160	72.9	53.2	70.6	49.1	1.4	137
16:05	0.185	72.7	53.1	70.5	49.1	1.4	148
16:07	0.235	72.8	52.9	70.4	49.1	1.8	156

Time of day	Height above terrain Inches	Forward tunnel psychrometer $T_{AD}-{}^{\circ}F$ Thermo. #41	$T_{AW}-{}^{\circ}F$ Thermo. #51	Traverse psychrometer ${}^{\circ}F$ Thermo. #42	${}^{\circ}F$ Thermo. #52	Traverse wind velocity ft/sec	Quantity of water evaporated cc
		Test No. 2 (Cont.)					
16:08	0.285	72.9	52.7	70.4	49.1	1.8	158
16:10	0.335	72.7	52.7	70.4	49.2	1.8	165
16:12	0.385	72.4	52.8	70.0	49.0	2.2	170
16:13	0.485	72.7	52.4	70.4	49.0	2.4	179
16:15	0.585	72.6	52.3	70.4	49.2	2.4	187
16:17	0.685	72.2	52.3	70.4	49.2	2.6	201
16:20	0.885	72.1	52.1	70.2	49.1	2.9	206
16:22	1.085	71.7	51.5	70.3	48.7	2.9	215
16:24	1.335	71.8	51.9	70.8	48.7	3.1	223
16:26	1.585	72.1	52.1	70.4	49.2	3.6	233
16:28	1.835	71.6	52.1	70.4	48.7	3.6	239
16:31	2.085	71.3	52.0	70.3	48.7	3.6	250
16:33	2.588	71.3	52.2	70.2	49.1	3.6	266
16:35	3.088	70.9	52.0	70.3	49.2	3.9	270
16:37	3.588	70.8	52.2	70.3	49.2	3.9	277
16:38	4.088	70.7	51.9	69.9	49.1	3.9	286
16:40	4.588	70.5	51.1	69.9	49.1	3.9	289
16:43	5.088	70.5	50.9	69.9	49.0	3.9	302
	Test No. 3		Date Oct. 20, 1952			Sta. 2	
13:52	0.020	55.4	43.6	55.6	49.1		0
13:58	0.025	55.8	43.6	56.8	49.0		32
14:00	0.030	56.3	44.1	56.8	49.0		44
14:04	0.035	57.4	44.9	57.1	49.0		57
14:05	0.045	56.4	44.5	57.0	48.8		65
14:07	0.055	57.3	44.2	57.2	48.3		85
14:08	0.065	55.9	43.7	56.7	48.2	0.48	96
14:11	0.075	56.6	44.4	56.8	48.0	0.51	96
14:12	0.085	56.7	44.4	56.8	47.5	0.70	102
14:13	0.095	57.3	44.4	57.2	47.4	0.86	108
14:14	0.120	57.2	44.3	57.0	46.8	1.1	108
14:15	0.145	57.3	44.6	57.3	45.8	1.1	117
14:17	0.170	57.4	44.6	57.3	45.4	1.2	123
14:19	0.195	56.6	44.3	56.6	45.3	1.4	128
14:20	0.245	57.3	44.2	57.2	45.1	1.4	140
14:22	0.295	57.5	44.5	57.2	45.3	1.7	148
14:23	0.345	57.3	44.1	56.8	45.1	1.9	148
14:25	0.395	57.3	44.0	56.8	45.1	1.9	158
14:27	0.495	56.3	43.6	56.3	44.7	2.0	164
14:28	0.595	56.3	43.2	56.3	44.8	2.0	170
14:30	0.695	55.5	43.4	55.8	44.6	2.4	177
	0.895	55.4	43.4	56.2	44.5	2.4	185
14:32	1.095	55.6	43.4	55.6	44.5	2.4	185
14:33	1.345	55.5	43.2	55.8	44.4	2.6	194
14:35	1.595	55.4	43.1	55.4	44.0	2.6	202
14:37	1.845	55.0	43.1	55.0	44.2	2.9	214
14:38	2.095	55.2	43.0	55.2	44.2	2.9	214
14:39	2.595	55.0	43.1	55.0	44.1	3.1	223
14:41	3.095	54.7	43.0	55.3	44.0	3.1	227

Time of day	Height above terrain Inches	Forward tunnel psychrometer $T_{AD}-°F$ Thermo. #41	$T_{AW}-°F$ Thermo. #51	Traverse psychrometer °F Thermo. #42	°F Thermo. #52	Traverse wind velocity ft/sec	Quantity of water evaporated cc
Test No. 3 (Cont.)							
14:43	3.595	55.3	43.1	55.3	44.0	3.1	235
14:44	4.095	55.0	43.1	55.0	43.7	3.1	242
14:45	4.595	55.0	43.1	55.0	43.9	3.2	250
	5.095	54.9	43.0	54.9	43.5	3.2	250
Test No. 4			**Date Oct. 20, 1952**			**Sta. 2**	
16:04	0.020	55.0	43.2	54.5	48.0		246
16:03	0.025	54.7	43.2	54.5	47.6		240
16:02	0.030	55.0	43.4	55.3	47.8		231
16:00	0.035	55.0	45.0	55.6	47.8		225
15:57	0.045	55.4	46.8	55.8	47.4		209
15:55	0.055	55.7	45.4	56.0	47.2	0.41	203
15:54	0.065	55.7	45.0	55.8	46.8	0.65	198
15:53	0.075	55.5	44.7	56.3	46.8	0.68	193
15:51	0.085	55.8	44.7	56.3	46.6	0.94	184
15:47	0.095	56.0	44.6	56.4	45.9	1.3	172
15:46	0.120	56.0	44.6	56.8	45.8	1.5	167
15:45	0.145	56.1	44.9	56.8	45.9	1.5	162
15:44	0.170	56.0	45.0	56.8	45.8	1.6	158
15:43	0.195	56.2	44.9	56.8	45.7	1.6	146
15:42	0.245	56.0	44.9	57.0	45.6	1.7	146
15:40	0.295	56.3	45.0	57.0	45.6	1.9	134
15:39	0.345	56.3	44.9	57.1	45.8	2.0	134
15:38	0.395	56.3	44.8	56.9	45.8	2.0	127
15:37	0.495	55.9	44.9	56.7	45.4	2.4	124
15:35	0.595	56.2	44.6	56.8	45.6	2.4	124
15:33	0.695	56.3	44.6	56.4	45.4	2.7	112
15:32	0.895	56.2	44.8	56.4	45.4	2.7	106
15:31	1.095	56.2	45.0	56.3	45.4	2.9	98
15:29	1.345	56.0	44.6	56.0	45.4	3.1	90
15:28	1.595	56.2	44.7	56.4	45.3	3.1	83
15:26	1.845	56.1	44.7	56.3	45.2	3.2	77
15:24	2.095	55.8	44.7	56.0	45.0	3.4	69
15:22	2.595	56.2	44.7	56.2	45.3	3.4	55
15:18	3.095	56.0	44.6	56.0	44.8	3.4	40
15:17	3.595	56.0	44.7	56.0	45.0	3.4	40
15:16	4.095	56.0	44.5	56.0	44.8	3.4	26
15:15	4.595	55.8	44.4	55.8	44.6	3.7	26
15:13	5.095	55.7	44.1	55.9	44.4	3.7	0
Test No. 5			**Date Oct. 21, 1952**			**Sta. 2**	
13:28	0.020	70.4	49.2	66.0	53.0		0
13:31	0.025	69.4	48.7	65.8	52.3		28
13:32	0.030	70.0	48.6	66.2	52.0		44
13:34	0.035	69.9	48.8	66.2	51.9		55
13:36	0.045	70.2	49.2	66.4	51.9	0.92	64
13:39	0.055	69.9	49.0	66.4	51.4	1.5	105

Time of day	Height above terrain Inches	Forward tunnel psychrometer T_{AD}-°F Thermo. #41	T_{AW}-°F Thermo. #51	Traverse psychrometer °F Thermo. #42	°F Thermo. #52	Traverse wind velocity ft/sec	Quantity of water evaporated cc
		Test No. 5 (Cont.)					
13:41	0.065	69.8	49.2	66.3	51.5	2.1	112
13:43	0.075	69.9	48.4	66.4	51.0	2.3	121
13:44	0.085	69.7	48.8	66.2	50.9	2.8	137
13:45	0.095	70.0	48.6	66.3	50.9	3.0	148
13:47	0.120	71.0	48.1	67.1	50.2	3.2	162
13:49	0.145	69.9	48.6	66.3	49.7	3.5	176
13:50	0.170	70.3	48.6	66.4	49.0	3.8	186
13:52	0.195	69.7	48.2	66.8	49.1	3.8	206
13:55	0.245	69.4	48.6	67.2	49.2	4.0	221
13:57	0.295	69.9	48.3	67.7	49.1	4.1	233
13:59	0.345	70.6	48.6	67.8	49.2	4.1	250
14:00	0.395	70.3	48.6	67.7	49.2	4.3	259
14:01	0.495	69.4	47.7	67.4	48.7	4.5	277
14:02	0.595	70.5	49.0	68.6	50.7	4.5	287
14:23	0.695	70.3	48.6	68.0	50.1	4.5	493
14:25	0.895	69.9	48.4	68.6	51.8	4.6	509
14:27	1.095	70.9	48.2	68.8	50.3	4.9	519
14:29	1.345	71.1	48.3	69.0	50.0	5.2	539
14:30	1.595	70.3	50.1	69.3	48.6	5.3	550
14:32	1.845	70.4	48.6	69.8	49.9	6.0	566
14:34	2.095	69.9	48.7	68.9	50.1	6.0	582
							750

	Test No. 6			Date Oct. 22, 1952		Sta. 2	
13:34	0.015	67.7	49.1	66.1	52.7		0
13:36	0.020	67.2	48.7	65.6	52.8		12
13:37	0.025	66.8	48.7	65.9	52.7		22
13:39	0.030	64.9	49.1	65.4	52.7		32
13:40	0.040	66.3	49.1	65.8	52.2		46
13:42	0.050	66.8	48.3	65.5	51.8	0.74	52
13:43	0.060	66.2	48.7	65.4	51.6	1.3	58
13:44	0.070	67.5	49.2	65.8	51.3	1.9	66
13:45	0.080	67.2	48.7	65.8	51.4	2.2	79
13:46	0.090	65.8	48.6	65.2	50.5	2.6	87
13:47	0.115	65.2	48.2	65.3	48.6	3.1	94
13:48	0.140	65.3	48.7	65.1	49.0	3.4	102
13:50	0.165	67.2	49.5	65.9	49.3	3.4	116
13:51	0.190	66.4	49.1	65.3	49.1	3.8	121
13:52	0.240	66.3	48.6	65.7	49.1	3.8	127
13:54	0.290	66.3	49.8	66.2	49.4	4.3	141
13:55	0.340	66.9	49.1	66.3	49.4	4.5	148
13:57	0.390	66.7	50.0	66.1	49.5	4.7	163
13:59	0.490	66.5	50.4	66.3	49.1	4.7	178
14:00	0.590	68.1	50.6	66.5	49.6	4.7	185

Time of day	Height above terrain Inches	Forward tunnel psychrometer T_{AD}-°F Thermo. #41	T_{AW}-°F Thermo. #51	Traverse psychrometer °F Thermo. #42	°F Thermo. #52	Traverse wind velocity ft/sec	Quantity of water evaporated cc
Test No. 6 (Cont.)							
14:01	0.690	67.1	49.2	66.3	49.2	4.0	192
14:02	0.890	67.3	48.6	65.8	49.0	4.7	205
14:04	1.090	66.2	49.1	66.2	48.9	4.9	213
14:07	1.340	66.9	48.7	65.8	49.0	4.9	238
14:09	1.590	66.6	48.7	65.5	49.0	5.0	250
14:11	1.840	67.6	48.7	66.1	48.7	5.0	262
14:12	2.090	66.8	48.6	66.4	49.0	3.9	270
14:13	2.590	66.7	48.4	66.7	48.9	4.5	281
14:14	3.090	66.7	48.4	67.1	49.1	4.7	287
14:16	3.590	66.6	48.4	66.8	48.8	4.9	297
14:17	4.090	65.8	48.6	66.6	48.9	6.2	306
14:18	4.590	67.3	49.1	67.2	49.1	6.1	317
14:20	5.090	67.2	48.7	67.4	49.3	6.1	330
Test No. 7			**Date Oct. 22, 1952**			**Sta. 1**	
14:45	0.020	66.7	48.7	58.8	51.3		0
14:47	0.025	66.9	49.0	58.7	51.1		17
14:49	0.030	67.1	48.7	59.0	51.0		22
14:51	0.035	66.7	48.3	58.6	51.0		34
14:52	0.045	64.9	48.5	58.7	50.8	0.80	40
14:53	0.055	66.6	48.6	59.5	50.5	1.3	53
14:54	0.065	66.3	49.0	59.6	50.7	1.9	61
14:55	0.075	67.2	48.6	59.7	50.4	2.3	68
14:57	0.085	65.8	48.6	59.6	50.3	2.7	76
14:58	0.095	66.5	49.1	60.5	50.5	3.0	88
14:59	0.120	67.2	48.7	61.9	50.4	3.4	98
15:00	0.145	66.8	48.3	62.2	49.8	3.8	104
15:02	0.170	66.3	48.5	62.4	49.9	4.5	114
15:03	0.195	66.2	48.6	62.5	49.7	4.3	128
15:05	0.245	66.3	48.2	63.2	49.5	4.5	137
15:06	0.295	66.2	48.0	62.4	49.0	4.5	143
15:07	0.345	65.3	48.2	63.1	49.3	4.7	150
15:08	0.395	65.6	48.1	63.3	49.2	4.5	162
15:09	0.495	66.4	48.3	63.7	49.2	4.7	170
15:10	0.595	65.8	48.1	64.1	49.0	4.9	176
15:11	0.695	66.3	47.9	64.5	48.9	4.9	187
15:13	0.895	66.2	47.8	64.5	48.6	5.1	194
15:14	1.095	65.4	48.1	64.5	48.6	5.4	200
15:15	1.345	65.9	48.6	65.0	48.6	5.5	209
15:16	1.595	65.8	48.6	65.1	48.6	5.6	218
15:17	1.845	66.3	48.4	65.8	48.7	5.8	227
15:18	2.095	65.5	47.7	65.0	48.2	6.2	234
15:19	2.595	65.3	47.9	64.9	48.2	6.3	240
15:20	3.095	65.4	47.7	65.4	48.2	6.4	250
15:21	3.595	65.2	48.5	65.0	48.3	6.8	261
15:23	4.095	65.0	47.7	64.6	48.1	6.8	270
15:24	4.595	65.3	47.8	65.0	48.2	7.2	278
15:26	5.095	65.4	47.5	64.9	48.2	7.2	293
15:30	5.095	65.0	47.6	64.5	47.8	7.2	328

Time of day	Height above terrain Inches	Forward tunnel psychrometer		Traverse psychrometer		Traverse wind velocity	Quantity of water evaporated
		T_AD-°F Thermo. #41	T_AW-°F Thermo. #51	°F Thermo. #42	°F Thermo. #52	ft/sec	cc
Test No. 8				**Date Oct. 22, 1952**		**Sta. 3**	
15:45	0.020	64.6	47.6	61.7	52.2		0
15:47	0.025	64.7	47.7	60.8	52.4		25
15:48	0.030	64.5	49.8	60.8	52.5		25
15:50	0.035	64.9	47.3	60.5	52.4	0.69	36
15:53	0.045	64.4	47.7	60.8	52.2	1.1	64
15:55	0.055	64.5	47.6	60.7	52.2	1.7	77
15:56	0.065	64.5	47.7	60.8	51.8	2.4	82
15:57	0.075	64.6	47.7	60.9	51.5	2.9	91
15:58	0.085	64.1	47.5	60.8	51.3	3.2	96
15:59	0.095	64.5	47.5	60.9	51.1	3.8	102
16:00	0.120	64.0	47.3	60.9	49.7	4.0	109
16:00	0.145	64.5	47.8	61.2	49.6	4.5	116
16:01	0.170	64.3	47.7	61.4	49.5	4.7	120
	0.195	64.2	47.8	61.6	49.4	4.7	128
16:02	0.245	64.1	47.8	61.5	49.5	4.9	134
16:03	0.295	64.1	47.8	61.8	49.1	5.1	140
16:04	0.345	64.5	47.9	62.0	49.1	4.9	147
16:05	0.395	64.4	47.8	61.9	49.0	5.0	152
16:06	0.495	64.0	47.9	62.6	48.9	5.0	157
16:07	0.595	64.4	47.7	62.8	49.0	5.0	162
16:08	0.695	64.3	47.8	62.8	48.6	5.1	172
16:09	0.895	63.9	48.1	62.9	48.5	5.8	177
16:10	1.095	64.0	47.8	63.2	48.3	5.8	189
16:11	1.345	64.1	48.1	63.3	48.1	6.1	195
16:12	1.595	63.9	48.1	63.5	48.1	6.1	201
16:15	1.845	63.9	48.1	63.7	48.0	6.4	224
16:16	2.095	63.6	48.1	63.6	48.0	6.4	231
16:17	2.595	63.7	48.4	63.7	47.7	7.2	239
16:18	3.095	63.6	48.6	63.7	47.6	7.2	250
16:20	3.595	63.9	48.7	63.8	47.7	7.7	256
16:21	4.095	63.5	49.2	64.0	47.6	8.0	266
16:22	4.595	63.6	49.5	64.0	47.7	8.0	272
16:23	5.095	63.6	50.0	64.0	47.6	8.0	280
Test No. 9				**Date Oct. 23, 1952**		**Sta. 2**	
13:51	0.020	70.0	50.0	64.9	53.3		0
13:52	0.025	70.0	49.9	65.0	52.9		6
13:53	0.030	70.3	49.9	65.1	52.9		9
13:54	0.035	69.9	49.9	64.9	52.8		12
13:55	0.045	69.9	49.7	65.0	52.8		17
13:56	0.055	69.9	50.0	65.4	52.7		23
13:58	0.065	70.3	49.8	65.5	52.5		28
13:59	0.075	69.7	49.9	65.4	52.2	0.57	34
14:00	0.085	70.3	50.0	65.6	51.9	0.68	39
14:01	0.095	70.3	50.0	65.8	51.7	0.80	44
14:02	0.120	70.0	49.7	65.8	52.4	0.85	52
14:03	0.145	70.1	50.0	65.9	50.4	1.2	55
14:04	0.170	70.6	50.2	66.2	49.6	1.5	64
14:06	0.195	70.0	50.1	66.2	49.4	1.8	70

Time of day	Height above terrain Inches	Forward tunnel psychrometer T_{AD}-°F Thermo. #41	T_{AW}-°F Thermo. #51	Traverse psychrometer °F Thermo. #42	°F Thermo. #52	Traverse wind velocity ft/sec	Quantity of water evaporated cc
Test No. 9 (Cont.)							
14:07	0.245	70.8	50.3	66.5	49.2	2.1	76
14:08	0.295	70.6	50.1	66.3	49.2	2.1	81
14:10	0.345	70.0	50.2	66.6	49.2	2.1	87
14:12	0.395	70.2	49.9	66.8	49.1	2.3	92
14:13	0.495	70.5	50.4	67.2	49.4	2.4	98
14:14	0.595	70.3	50.3	67.0	49.3	2.5	107
14:15	0.695	70.6	50.9	67.7	49.6	2.7	111
14:16	0.895	70.3	50.7	67.6	49.3	2.7	116
14:17	1.095	70.5	55.8	68.1	50.0	2.8	122
14:21	1.345	70.4	52.4	67.9	49.5	2.9	134
14:23	1.595	71.0	54.7	68.1	49.8	2.9	139
14:24	1.845	70.0	54.9	68.5	49.8	3.1	147
14:26	2.095	70.7	54.6	72.6	49.7	3.1	155
14:28	2.595	70.8	54.2	69.0	49.5	3.3	168
14:32	3.095	70.4	53.3	69.5	49.9	3.4	186
14:35	3.595	70.8	50.5	70.0	50.4	3.4	198
14:37	4.095	70.9	50.4	70.4	50.3	3.6	207
14:38	4.595	70.8	50.4	70.4	50.5	3.6	215
14:39	5.095	70.8	50.2	70.6	50.5	3.6	227
Test No. 10		Date Oct. 23, 1952				Sta. 1	
14:55	0.030	70.8	50.4	59.5	53.6		0
14:58	0.035	70.7	50.3	59.6	53.7		14
14:59	0.040	70.9	51.3	59.7	53.6	0.30	18
15:00	0.045	70.7	50.3	59.9	53.7	0.33	23
15:02	0.055	70.3	50.3	60.0	53.6	0.38	30
15:07	0.065	70.4	50.0	60.2	53.3	0.65	60
15:08	0.075	69.9	49.7	60.5	53.2	0.68	66
15:10	0.085	69.9	49.8	60.8	53.3	0.92	72
15:12	0.095	69.8	49.6	62.5	53.1	1.2	78
15:14	0.105	69.7	49.4	62.6	52.7	1.2	92
15:16	0.130	69.4	49.0	62.9	52.4	1.5	100
15:17	0.155	69.4	49.1	63.3	51.2	1.8	105
15:18	0.180	69.3	49.1	63.5	50.6	2.1	110
15:19	0.205	69.1	49.1	63.4	50.5	2.3	113
15:20	0.255	69.3	49.0	64.3	50.2	2.4	118
15:21	0.305	69.4	49.1	64.4	50.0	2.5	123
15:22	0.355	69.4	49.1	65.1	50.0	2.5	129
	0.405	69.4	49.0	65.1	49.8	2.7	129
15:23	0.505	69.0	48.7	65.9	49.4	2.8	138
15:24	0.605	69.1	48.7	66.0	49.4	2.9	143
15:25	0.705	69.3	49.1	66.0	49.2	2.9	143
15:26	0.905	68.9	48.7	66.3	49.0	2.9	149
15:27	1.105	69.0	48.7	66.7	48.9	2.9	155
15:30	1.355	69.5	48.7	67.3	48.7	2.9	171
15:37	1.605	68.8	48.7	67.1	48.7	2.9	212
15:38	1.855	68.6	48.6	67.2	48.6	2.9	218
15:39	2.105	68.8	48.6	67.3	48.6	2.9	221
15:40	2.605	68.5	48.2	67.7	48.6	2.9	227

Time of day	Height above terrain Inches	Forward tunnel psychrometer T_{AD}-°F Thermo. #41	T_{AW}-°F Thermo. #51	Traverse psychrometer °F Thermo. #42	°F Thermo. #52	Traverse wind velocity ft/sec	Quantity of water evaporated cc
Test No. 10 (Cont.)
15:41	3.105	68.6	48.6	67.6	48.6	3.4	232
15:42	3.605	68.6	48.7	67.6	48.7	3.6	237
15:43	4.105	68.5	48.8	67.7	48.8	3.6	243
15:44	4.605	68.6	48.7	68.1	48.7	3.6	250
15:45	5.105	68.5	49.0	67.8	49.1	3.6	255
Test No. 11   Date Oct. 23, 1952   Sta. 3
16:06	0.015	67.7	48.1	62.2	55.0		0
16:07	0.020	67.5	48.2	61.8	55.1		0
16:08	0.025	67.8	48.2	61.9	55.1		7
16:09	0.030	67.8	48.2	62.0	55.1		7
16:10	0.040	67.9	48.3	62.1	54.5		16
16:11	0.050	67.6	48.2	61.8	54.1	0.26	22
16:13	0.060	67.6	48.3	62.0	53.7	0.41	27
16:14	0.070	67.6	48.2	61.9	53.2	0.59	32
16:15	0.080	67.6	48.3	61.9	52.8	0.80	40
16:16	0.090	65.7	48.2	62.0	52.8	0.94	47
16:17	0.115	67.6	48.1	62.4	52.4	1.2	54
16:18	0.140	67.6	48.2	62.6	51.7	1.4	60
16:19	0.165	67.4	48.4	62.6	50.8	1.7	65
16:20	0.190	67.7	48.2	63.0	50.4	1.8	72
16:23	0.240	67.3	48.2	63.1	50.1	1.8	84
16:25	0.290	67.2	48.2	63.4	49.9	2.1	92
16:26	0.340	67.3	48.6	63.7	49.7	2.1	92
16:27	0.390	67.2	48.6	63.7	49.8	2.1	100
16:28	0.490	67.2	48.3	64.0	49.5	2.1	105
16:29	0.590	67.3	48.6	64.5	49.1	2.1	110
16:30	0.690	66.9	48.2	64.5	49.0	2.1	113
16:31	0.890	67.1	48.6	65.0	48.6	2.3	122
	1.090	66.7	48.6	64.7	48.6	2.3	122
16:32	1.340	66.9	48.3	65.3	48.3	2.3	130
16:33	1.590	67.1	48.1	65.5	48.1	2.4	135
16:34	1.840	66.0	48.1	64.0	47.6	2.9	135
16:35	2.090	66.0	48.2	64.5	47.7	2.9	142
16:36	2.590	66.3	47.8	64.4	47.3	2.9	150
16:37	3.090	66.2	47.9	65.0	47.6	3.1	158
16:38	3.590	65.8	47.9	64.6	47.0	3.1	164
16:39	4.090	65.9	48.0	64.6	47.3	3.1	170
16:41	4.590	65.9	48.1	65.2	47.6	3.1	182
16:42	5.090	65.9	48.7	65.4	47.7	3.1	191
Test No. 12   Date Oct. 25, 1952   Sta. 2
14:02	0.015	73.9	48.1	67.1	58.7		0
14:04	0.020	74.3	48.6	66.8	58.7		15
14:06	0.025	73.8	49.0	66.6	58.5		30
14:07	0.030	74.9	48.8	66.7	58.3		55
14:09	0.040	73.5	48.7	71.3	52.7	1.3	77

Time of day	Height above terrain Inches	Forward tunnel psychrometer TAD-°F Thermo. #41	TAW-°F Thermo. #51	Traverse psychrometer °F Thermo. #42	°F Thermo. #52	Traverse wind velocity ft/sec	Quantity of water evaporated cc
		Test No. 12 (Cont.)					
14:10	0.050	73.4	48.7	71.2	52.5	2.1	94
14:11	0.060	74.3	49.4	72.1	51.8	2.8	105
14:12	0.070	74.5	49.0	72.2	52.2	3.4	123
14:13	0.080	74.4	49.8	71.8	51.8	3.8	142
14:14	0.090	74.4	49.7	72.1	51.8	4.6	152
14:15	0.115	73.9	49.5	72.2	51.8	5.4	165
14:16	0.140	73.6	49.9	71.8	51.3	6.1	180
14:17	0.165	73.5	49.7	72.0	51.0	6.1	200
14:19	0.190	73.4	50.1	72.1	50.4	6.4	218
14:20	0.240	74.0	50.2	72.4	50.6	6.7	232
14:21	0.290	73.6	50.0	72.4	50.5	6.7	250
14:22	0.340	74.4	49.6	72.3	50.1	6.8	250
14:23	0.390	73.9	50.9	72.6	50.5	7.1	271
14:25	0.490	73.9	50.9	71.7	50.0	7.2	288
14:26	0.590	73.4	51.6	72.2	50.1	7.7	297
14:27	0.690	74.0	53.2	72.5	50.5	7.7	315
14:29	0.890	74.8	54.0	72.6	50.2	8.1	332
14:30	1.090	73.0	49.6	72.6	49.7	8.7	357
14:32	1.340	73.9	48.0	73.0	49.6	9.7	392
14:33	1.590	74.5	48.2	73.1	49.7	9.8	407
14:35	1.840	75.2	48.1	73.4	49.9	9.8	432
14:37	2.090	73.9	47.9	73.2	49.3	10.3	452
14:38	2.590	74.2	47.7	73.2	51.3	10.3	459
14:39	3.090	73.5	48.1	73.5	49.5	10.6	482
14:41	3.590	73.7	47.9	72.9	48.6	10.8	510
14:43	4.090	73.9	48.1	73.2	49.0	11.0	541
14:44	4.590	73.4	47.9	73.0	48.5	11.3	556
14:51	5.090	73.5	47.9	73.5	48.6	11.0	583
		Test No. 13		Date Oct. 25, 1952		Sta. 1	
15:11	0.050	73.0	50.4	67.2	58.4	1.5	0
15:12	0.055	73.5	47.6	67.1	53.3	1.9	23
15:13	0.060	73.0	47.7	67.1	53.1	2.0	41
15:15	0.065	73.2	47.6	67.1	53.0	2.3	55
15:16	0.075	72.7	47.4	67.2	53.2	3.2	75
15:17	0.085	72.7	47.4	67.0	52.8	4.0	98
15:18	0.095	73.0	47.2	67.1	52.9	4.4	110
15:20	0.105	72.7	47.3	67.1	53.0	5.0	129
15:21	0.115	72.2	47.3	67.2	52.7	5.0	145
15:22	0.125	72.6	47.4	67.2	52.7	5.1	155
15:23	0.150	72.7	47.2	67.1	52.7	6.1	161
15:24	0.175	72.6	47.4	67.8	52.2	3.0	173
15:25	0.220	72.6	47.5	68.2	50.3	3.1	195
15:26	0.200	72.5	47.3	68.1	50.1	3.2	207
15:28	0.275	72.8	47.5	68.5	50.0	3.9	221
15:29	0.325	72.6	47.2	68.5	49.7	4.9	242
15:30	0.375	72.0	47.3	68.6	49.5	4.9	250
15:31	0.425	72.5	47.2	68.6	49.5	5.0	263
15:32	0.525	72.0	47.2	68.7	49.5	5.0	285

Time of day	Height above terrain Inches	Forward tunnel psychrometer TAD-°F Thermo. #41	TAW-°F Thermo. #51	Traverse psychrometer °F Thermo. #42	°F Thermo. #52	Traverse wind velocity ft/sec	Quantity of water evaporated cc
Test No. 13 (Cont.)							
15:34	0.625	72.5	47.4	69.7	49.2	5.1	301
15:36	0.725	72.2	47.4	70.0	49.1	5.3	330
15:37	0.925	72.1	47.2	70.4	49.1	5.7	341
15:38	1.125	72.2	47.3	70.7	48.5	6.1	359
15:40	1.375	72.2	47.2	70.7	48.6	7.7	387
15:41	1.625	72.2	47.4	70.8	48.6	8.1	393
15:42	1.875	71.8	47.2	70.8	48.0	8.1	403
15:43	2.125	71.9	47.3	71.0	48.0	8.7	422
15:45	2.625	71.8	47.3	71.2	47.8	9.3	450
15:46	3.125	71.7	50.9	71.3	47.6	9.3	467
15:48	3.625	71.5	49.8	70.9	47.5	10.8	500
15:50	4.125	71.2	49.5	71.0	47.6	10.8	510
15:52	4.625	71.0	49.1	70.3	47.3	10.8	540
15:54	5.125	71.3	49.1	71.0	47.4	11.2	580
Test No. 14	Date Oct. 28, 1952			Sta. 2			
13:30	0.015	65.0	47.1	61.3	48.7		0
13:33	0.020	64.9	46.4	61.7	48.1		18
13:35	0.025	65.0	46.5	61.8	48.2		30
13:37	0.030	65.5	46.9	62.1	48.2		43
13:38	0.040	65.4	46.8	62.2	48.1	0.43	52
13:39	0.050	65.4	47.0	62.6	48.1	2.3	64
13:41	0.060	65.9	46.6	63.2	47.9	2.7	80
13:43	0.070	65.5	47.2	62.8	47.6	3.3	93
13:45	0.080	65.8	46.8	62.7	47.7	3.5	108
13:46	0.090	65.9	47.1	63.2	47.6	4.2	120
13:48	0.115	65.8	47.3	63.1	46.4	3.5	128
13:49	0.140	66.7	47.0	63.5	46.4	3.7	142
13:52	0.165	66.2	47.1	63.5	46.3	4.3	165
13:53	0.190	66.3	47.4	64.0	46.5	4.4	173
13:55	0.240	66.2	47.1	64.0	46.3	4.6	193
13:57	0.290	66.3	47.6	64.3	46.7	4.6	208
13:59	0.340	67.2	47.6	64.2	46.8	4.6	217
14:00	0.390	66.3	47.2	64.4	46.5	4.6	229
14:01	0.490	66.8	47.2	64.4	46.5	4.8	242
14:02	0.590	66.4	47.4	64.9	46.7	4.9	250
14:05	0.690	67.2	47.6	65.6	46.8	5.3	250
14:06	0.890	66.8	47.5	65.2	46.8	5.9	265
14:07	1.090	67.2	46.9	65.1	46.7	6.1	273
14:08	1.340	67.1	47.4	65.8	46.8	6.1	285
14:12	1.590	67.2	47.8	66.2	46.8	6.3	324
14:14	1.840	66.7	47.7	65.8	46.7	6.5	337
14:15	2.090	67.0	47.7	66.0	46.8	6.5	342
14:18	2.590	67.8	47.7	67.0	47.1	8.2	373
14:20	3.090	67.9	47.3	66.4	47.0	8.4	387
14:22	3.590	67.7	47.3	67.3	46.7	8.4	405
14:23	4.090	67.7	47.2	67.7	47.1	8.6	414
14:25	4.590	67.7	47.3	67.6	47.0	8.8	425
14:27	5.090	67.9	47.5	67.8	47.3	9.4	445

Time of day	Height above terrain Inches	Forward tunnel psychrometer T_{AD}-°F Thermo. #41	T_{AW}-°F Thermo. #51	Traverse psychrometer F Thermo. #42	F Thermo. #52	Traverse wind velocity ft/sec	Quantity of water evaporated cc
Test No. 15				Date Oct. 28, 1952		Sta. 2	
15:35	0.015	67.8	46.9	66.3	51.4		0
15:36	0.020	67.4	46.7	66.2	50.9		10
15:37	0.025	67.3	46.8	65.9	51.0		25
15:40	0.030	67.6	46.8	66.2	50.8	3.0	
15:41	0.040	67.2	46.4	66.2	49.6	5.4	88
15:42	0.050	67.0	46.4	66.2	49.4	6.6	98
15:43	0.060	67.4	46.4	66.3	49.4	8.0	115
15:44	0.070	67.1	46.3	66.2	49.2	8.8	133
15:45	0.080	67.6	46.2	66.2	49.2	9.4	144
15:46	0.090	67.1	46.4	66.2	49.2	9.6	157
	0.115	67.4	46.4	66.2	49.2	11.0	171
	0.140	67.2	46.4	66.4	48.2	11.5	186
	0.165	67.1	46.3	66.2	48.2	11.5	200
	0.190	67.2	46.4	66.3	48.4	11.5	215
15:50	0.240	67.1	46.4	66.4	48.2	12.5	224
15:51	0.290	66.8	46.3	66.1	48.0	12.5	236
15:52	0.340	67.1	46.2	66.2	48.1	12.5	261
15:53	0.390	67.1	46.4	66.2	48.1	13.0	275
15:54	0.490	66.8	46.3	66.3	48.1	13.2	290
15:55	0.590	66.8	46.4	66.3	47.8	14.8	310
15:56	0.690	66.8	46.4	66.1	47.8	14.8	329
15:57	0.890	66.8	46.4	66.3	47.7	15.5	344
15:58	1.090	66.8	46.3	66.3	48.0	15.8	367
15:59	1.340	66.6	46.3	66.2	47.6	16.0	380
16:00	1.590	66.7	46.3	66.3	47.5	16.0	397
16:01	1.840	66.4	46.2	66.0	47.2	16.0	417
16:02	2.090	66.6	46.1	66.0	47.0	16.0	429
16:03	2.590	66.3	46.2	66.3	47.2	16.0	443
16:05	3.090	66.4	46.3	66.2	46.8	16.6	461
	3.590	66.2	46.0	66.2	46.8	17.8	480
	4.090	66.3	46.1	66.2	46.7	19.5	514
	4.590	66.0	46.0	66.0	46.4	19.5	532
16:09	5.090	66.1	46.0	66.1	46.4	20.8	555
Test No. 16				Data Oct. 29, 1952		Sta. 2	
14:05	0.020	62.8	45.4	61.2	48.6		0
14:07	0.025	63.2	45.4	61.4	48.1		7
14:08	0.030	63.4	45.5	61.4	48.2		16
14:09	0.035	63.4	45.5	61.3	48.0		24
14:10	0.045	63.2	45.6	61.4	47.8	0.70	32
14:12	0.055	63.3	45.5	61.4	47.8	1.1	37
14:14	0.065	63.4	45.5	61.6	47.6	2.0	49
14:15	0.075	63.5	45.6	61.4	47.3	2.5	58
14:17	0.085	63.2	45.5	61.4	47.2	2.7	77
14:19	0.095	63.4	45.7	61.8	46.4	2.9	90
14:20	0.120	63.2	45.6	61.8	46.2	3.6	97
14:21	0.145	63.6	45.6	61.4	46.3	3.8	106
14:22	0.170	63.4	45.7	61.8	46.3	4.0	114
14:23	0.195	63.4	45.4	61.8	46.2	4.0	121

Time of day	Height above terrain Inches	Forward tunnel psychrometer T_{AD}-°F Thermo. #41	T_{AW}-°F Thermo. #51	Traverse psychrometer °F Thermo. #42	°F Thermo. #52	Traverse wind velocity ft/sec	Quantity of water evaporated cc
		Test No. 16 (Cont.)					
14:24	0.245	63.2	45.3	61.8	46.0	4.5	130
14:25	0.295	63.2	45.4	61.8	46.0	4.7	138
14:26	0.345	63.2	45.6	61.8	46.0	4.8	145
14:27	0.395	63.2	45.6	61.7	46.3	4.8	157
14:28	0.495	63.2	45.6	61.7	45.9	5.0	187
14:31	0.595	63.4	45.6	61.8	46.2	5.4	187
14:32	0.695	63.2	45.4	61.8	45.9	5.4	195
14:33	0.895	63.2	45.5	62.1	46.2	6.1	204
14:34	1.095	63.2	45.5	61.9	46.1	6.4	214
14:35	1.345	63.2	45.6	62.2	46.1	6.4	224
14:36	1.595	63.2	45.8	62.1	46.4	6.4	232
14:37	1.845	63.1	45.9	62.1	46.2	6.4	242
14:38	2.095	63.1	46.0	62.2	46.4	6.6	250
14:40	2.595	63.0	45.9	62.2	46.7	7.4	260
14:42	3.095	63.1	45.8	62.3	46.4	7.6	270
14:43	3.595	62.7	45.8	62.2	46.3	8.0	279
14:44	4.095	63.0	45.8	62.6	46.6	8.0	287
14:45	4.595	62.8	45.8	62.6	46.2	8.0	297
14:46	5.095	62.8	45.8	62.6	46.4	8.0	316
		Test No. 17		Date Oct. 29, 1952		Sta. 4	
15:40	0.025	61.2	46.2	55.0	48.2		0
15:41	0.030	61.4	46.3	54.9	48.1		8
15:42	0.035	61.4	46.1	54.8	48.2	0.67	17
15:43	0.040	61.5	45.8	55.0	48.0	0.82	23
15:44	0.050	61.4	45.8	55.4	47.7	1.5	32
15:46	0.060	61.0	46.4	55.8	48.1	2.1	46
15:48	0.070	60.6	46.4	55.7	48.1	3.1	68
15:52	0.080	60.4	46.4	55.7	47.8	3.5	102
15:55	0.090	60.4	46.8	55.8	48.2	3.9	111
15:56	0.100	60.3	46.8	56.3	48.4	4.7	115
15:57	0.125	61.0	46.4	56.4	48.0	5.0	119
15:58	0.150	60.4	46.8	56.3	48.2	5.5	130
15:59	0.175	60.3	46.8	56.8	48.2	5.8	142
16:00	0.200	60.1	46.8	56.8	48.1	6.0	153
16:01	0.250	60.4	46.4	57.2	48.1	6.2	153
16:02	0.300	61.4	45.5	58.1	47.3	6.4	159
16:03	0.350	61.6	45.9	58.1	47.2	6.6	164
16:04	0.400	60.9	45.9	58.2	47.2	7.0	170
16:05	0.500	61.1	45.9	58.6	47.2	7.2	174
16:06	0.600	61.3	45.9	58.8	47.2	7.4	179
16:07	0.700	61.3	45.9	59.0	46.9	7.4	188
16:09	0.900	61.4	46.0	59.6	46.8	7.8	199
16:10	1.100	61.4	46.1	59.6	46.8	7.8	204
16:11	1.350	61.6	45.9	60.0	46.8	8.1	209
16:12	1.600	61.8	45.6	60.3	46.3	8.1	218
16:13	1.850	62.2	45.4	60.9	45.9	8.3	227
16:14	2.100	62.3	45.9	61.0	46.2	8.6	235
16:15	2.600	62.6	45.9	61.4	46.2	9.0	250

Time of day	Height above terrain Inches	Forward tunnel psychrometer T$_{AD}$-°F Thermo. #41	T$_{AW}$-°F Thermo. #51	Traverse psychrometer °F Thermo. #42	°F Thermo. #52	Traverse wind velocity ft/sec	Quantity of water evaporated cc
	Test No. 17 (Cont.)						
16:16	3.100	62.8	46.0	62.1	46.0	9.4	250
16:17	3.600	63.1	46.0	62.2	46.3	9.8	259
16:19	4.100	62.6	46.2	61.8	46.3	10.0	266
16:20	4.600	62.6	46.2	61.7	46.4	10.0	275
16:21	5.100	62.6	46.3	61.9	46.8	10.0	292
	Test No. 18	Date Nov. 3, 1952			Sta. 2		
14:29	0.040	51.8	41.5	51.0	43.4	6.8	0
14:31	0.050	51.8	41.8	51.3	43.2	8.3	22
14:32	0.060	52.4	42.1	51.3	43.2	9.6	32
14:33	0.080	52.2	42.0	51.8	43.0	11.3	40
14:35	0.100	52.3	42.2	51.3	43.0	11.8	52
14:37	0.120	51.8	41.2	51.4	42.3	12.5	61
14:38	0.140	51.7	40.9	51.4	41.3	12.4	68
14:39	0.190	51.4	41.6	51.4	42.2	13.9	85
14:40	0.240	51.8	41.3	51.4	41.9	13.9	94
14:42	0.340	51.3	41.3	51.3	41.3	14.8	109
14:43	0.440	51.8	41.6	51.3	41.6	15.6	116
14:45	0.640	51.6	41.6	51.1	41.8	16.3	134
14:46	0.840	51.2	42.0	51.5	42.0	17.0	150
14:48	1.240	51.5	41.8	51.6	42.1	18.0	163
14:50	1.740	52.7	42.2	51.0	42.2	19.1	175
14:52	2.240	52.7	41.8	51.2	41.8	21.3	188
14:53	3.740	52.7	42.6	51.6	42.2	22.2	196
14:56	5.240	52.8	42.2	50.7	42.2	22.2	222
	Test No. 19	Date Nov. 3, 1952			Sta. 1		
15:51	0.050	52.8	42.0	47.5	42.3	3.4	0
15:52	0.060	52.8	41.3	50.0	41.8	5.3	15
15:56	0.070	52.5	41.3	49.5	41.8	5.4	54
15:58	0.090	52.5	41.4	49.5	41.7	9.0	60
15:59	0.110	52.3	41.3	49.6	41.8	10.9	70
16:00	0.130	52.8	41.3	50.0	41.8	11.5	85
16:01	0.150	52.8	41.1	49.8	41.4	11.5	95
16:02	0.200	52.8	41.3	50.0	41.7	12.1	105
16:04	0.250	52.3	41.3	50.0	41.5	12.7	113
16:06	0.350	52.5	41.3	50.3	41.3	13.5	123
16:07	0.450	52.7	41.1	50.0	41.5	13.5	134
16:09	0.650	52.7	41.3	50.4	41.3	14.7	147
16:11	0.850	52.3	40.9	50.8	40.9	15.3	165
16:12	1.250	52.5	40.8	50.2	41.0	16.5	182
16:13	1.750	52.4	40.9	50.4	40.9	17.0	190
16:15	2.250	52.1	40.9	50.1	40.9	17.5	210
16:17	3.750	51.9	40.7	50.1	40.7	19.7	232
16:19	5.250	52.1	40.8	50.0	40.8	20.0	250

Time of day	Height above terrain Inches	Forward tunnel psychrometer T_{AD}-°F Thermo. #41	T_{AW}-°F Thermo. #51	Traverse psychrometer °F Thermo. #42	°F Thermo. #52	Traverse wind velocity ft/sec	Quantity of water evaporated cc
		Test No. 20		Date Nov. 3, 1952		Sta. 4	
16:38	0.100	51.4	40.0	47.7	40.7	6.6	0
16:39	0.110	51.0	40.0	47.7	40.8	7.5	12
16:41	0.120	51.0	39.6	47.6	40.5	8.0	21
16:42	0.140	50.8	39.8	47.6	40.3	9.8	36
16:43	0.160	50.8	39.8	47.3	40.4	9.8	46
16:45	0.180	50.8	39.7	47.4	40.4	10.2	56
16:46	0.200	50.7	39.5	47.2	40.2	10.9	72
16:48	0.250	50.6	39.5	47.2	40.2	11.4	92
16:49	0.300	50.6	39.5	46.9	39.9	12.1	102
16:50	0.400	50.5	39.5	46.9	39.8	12.1	109
16:51	0.500	50.4	39.5	47.0	39.8	13.4	117
16:52	0.700	50.4	39.5	47.3	39.8	14.6	125
16:53	0.900	50.4	39.4	46.9	39.4	15.2	134
16:54	1.300	50.4	39.6	47.6	39.6	16.7	143
16:55	1.800	50.0	39.0	46.4	39.3	17.0	152
16:56	2.300	50.2	39.2	47.5	39.2	17.5	160
16:58	3.800	49.2	39.2	46.5	39.0	19.2	180
17:00	5.300	49.0	38.5	45.4	38.5	21.2	201
		Test No. 21		Date Nov. 4, 1952		Sta. 2	
13:43	0.035	67.6	48.2	63.2	53.4	1.0	0
13:44	0.045	67.3	47.6	63.4	53.0	1.5	10
13:46	0.055	67.6	47.8	63.2	53.0	2.2	20
13:47	0.075	67.3	47.6	64.0	53.2	3.0	35
13:48	0.095	67.6	48.1	64.0	53.1	3.6	47
13:49	0.115	67.4	48.6	64.5	52.7	4.2	55
13:50	0.135	67.1	48.1	64.6	52.7	4.7	60
13:51	0.185	67.5	48.1	65.0	52.3	4.8	72
13:52	0.235	67.2	47.7	64.9	50.5	4.8	80
13:53	0.335	67.6	47.4	65.3	50.4	5.1	92
13:55	0.435	67.2	47.5	65.2	50.4	5.5	102
13:57	0.635	67.6	47.7	65.4	50.4	5.8	110
13:58	0.835	67.8	47.2	66.0	50.2	6.0	119
13:59	1.235	67.6	46.9	65.8	49.5	6.3	130
14:00	1.735	67.6	47.5	67.1	50.0	6.7	138
14:02	2.235	68.0	47.2	67.6	50.0	7.1	162
14:05	3.735	67.9	47.8	67.9	50.2	7.6	180
14:07	5.235	68.2	47.2	69.0	48.6	7.6	198
		Test No. 22		Date Nov. 4, 1952		Sta. 2	
14:31	0.035	69.0	47.2	56.8	51.7		0
14:32	0.045	69.4	47.3	56.8	51.4		12
14:36	0.055	69.4	47.2	56.8	51.4	2.6	44
14:37	0.075	70.0	47.7	57.3	51.4	3.0	60
14:38	0.095	69.5	47.3	58.2	51.8	3.3	72
14:40	0.115	69.5	47.6	59.5	51.8	3.9	84
14:42	0.135	69.1	47.1	61.3	51.8	4.6	96

Time of day	Height above terrain Inches	Forward tunnel psychrometer T_{AD}-°F Thermo. #41	T_{AW}-°F Thermo. #51	Traverse psychrometer °F Thermo. #42	°F Thermo. #52	Traverse wind velocity ft/sec	Quantity of water evaporated cc
		Test No. 22 (Cont.)					
14:43	0.185	69.5	47.4	62.6	51.0	4.8	108
14:44	0.235	69.5	47.8	63.5	50.8	5.0	118
14:45	0.335	69.8	47.7	64.1	50.8	5.1	125
14:46	0.435	69.4	47.3	64.9	50.9	5.8	137
14:47	0.635	69.9	47.8	66.2	50.7	6.0	146
14:48	0.835	69.7	47.6	66.7	50.4	6.2	160
14:50	1.235	69.4	47.7	67.6	50.4	6.2	168
14:51	1.735	69.4	47.6	67.3	50.0	6.4	175
14:52	2.235	69.5	47.1	68.1	50.0	7.1	186
14:55	3.735	69.1	47.6	68.5	49.4	7.6	221
14:58	5.235	69.5	47.6	69.4	49.0	7.6	239
		Test No. 23		Date Nov. 4, 1952		Sta. 4	
15:13	0.040	68.8	47.6	57.7	53.5	1.2	0
15:14	0.050	68.9	48.2	57.3	52.8	1.8	9
15:15	0.060	68.8	48.2	58.1	52.8	2.3	18
15:16	0.080	68.5	47.8	59.6	52.7	3.1	27
15:17	0.100	68.5	48.2	59.6	52.7	3.6	36
15:18	0.120	68.5	48.2	60.4	52.7	4.2	45
15:19	0.140	68.5	48.6	60.9	52.8	4.5	52
15:20	0.190	68.5	48.6	61.5	51.3	4.7	60
15:21	0.240	68.5	48.7	62.1	51.5	4.8	69
15:22	0.340	68.5	49.1	63.1	51.4	5.1	76
15:23	0.440	68.4	48.9	63.5	51.3	5.5	87
15:24	0.640	68.5	49.1	64.5	51.3	5.8	94
15:25	0.840	68.5	48.9	65.3	51.3	6.1	104
15:26	1.240	68.3	49.0	65.8	50.7	6.3	111
15:27	1.740	68.3	48.7	66.4	50.3	6.3	120
15:29	2.240	68.5	49.1	67.5	50.3	7.1	129
15:31	3.740	68.2	49.2	67.6	49.7	7.6	146
15:33	5.240	68.3	49.1	67.9	49.5	7.6	164
		Test No. 24		Date Nov. 4, 1952		Sta. 3	
15:48	0.020	67.7	47.2	59.6	54.2		0
15:51	0.030	67.6	47.2	59.3	53.9		20
	0.040	66.7	47.2	59.1	54.0	0.70	
15:53	0.060	66.7	47.2	60.0	53.6	1.3	42
15:54	0.080	67.1	47.4	59.9	52.8	2.5	58
15:56	0.100	68.0	47.4	60.8	52.7	2.8	70
15:58	0.120	67.2	47.6	60.4	52.3	3.2	84
15:59	0.170	67.6	47.5	62.2	51.8	3.4	92
	0.220	67.2	47.5	61.9	50.8	3.5	98
16:00	0.320	67.3	47.3	62.7	50.8	3.6	106
16:01	0.420	67.1	47.3	62.2	50.5	3.9	113
16:02	0.620	67.2	47.4	63.5	50.3	3.9	121
16:04	0.820	67.2	47.6	64.2	49.9	4.2	131
16:05	1.220	67.1	47.1	64.7	49.7	4.5	140

Time of day	Height above terrain Inches	Forward tunnel psychrometer		Traverse psychrometer		Traverse wind velocity	Quantity of water evaporated
		T_{AD}-°F Thermo. #41	T_{AW}-°F Thermo. #51	°F Thermo. #42	°F Thermo. #52	ft/sec	cc
Test No. 24 (Cont.)							
16:06	1.720	66.2	46.9	64.0	49.1	4.8	146
16:07	2.220	66.1	46.8	64.0	49.0	4.8	156
16:10	3.720	66.0	46.7	64.9	48.2	5.1	178
16:12	5.220	65.7	46.7	63.6	47.6	5.5	194
Test No. 25			Date Nov. 4, 1952			Sta. 3	
16:30	0.020	63.2	46.3	57.6	52.7		0
	0.030	64.5	45.9	57.7	52.3		
16:31	0.040	64.4	46.3	57.6	52.3		16
16:32	0.060	64.0	46.2	57.3	51.9	1.4	23
16:33	0.080	64.0	46.3	58.0	51.8	2.0	31
16:34	0.100	63.7	45.9	58.3	51.7	2.6	44
16:35	0.120	63.1	45.9	57.8	51.5	2.8	50
16:36	0.170	63.2	46.0	58.3	51.1	3.2	57
16:37	0.220	63.5	46.3	58.9	50.4	3.2	65
	0.320	64.0	46.3	58.9	49.9	3.4	76
16:38	0.420	62.8	45.6	58.6	48.9	3.6	84
16:39	0.620	62.7	45.5	59.5	49.1	3.7	90
16:40	0.820	62.3	45.5	58.6	48.6	4.2	98
16:41	1.220	62.8	45.8	60.1	48.6	4.2	98
16:42	1.720	63.5	45.8	61.0	48.6	4.4	108
16:43	2.220	63.2	45.9	60.9	47.9	4.5	114
16:44	3.720	62.4	45.7	58.7	47.0	4.8	120
16:46	5.220	62.2	45.4	60.2	46.3	5.1	146
Test No. 26			Date Nov. 6, 1952			Sta. 2	
14:08	0.040	47.8	34.9	46.2	39.4	0.70	0
	0.050	48.2	34.4	45.0	39.7	0.14	
14:10	0.060	48.1	34.9	45.0	40.1	0.15	12
14:11	0.080	48.4	34.8	45.6	39.7	0.21	17
14:13	0.100	48.1	34.7	45.5	39.0	0.31	24
14:14	0.120	47.8	34.4	45.4	38.0	0.39	30
14:15	0.140	48.2	34.4	45.0	37.6	0.47	34
14:16	0.190	48.0	34.7	44.5	36.6	0.75	44
14:20	0.240	48.1	34.8	44.7	36.3	0.75	53
14:22	0.340	48.1	34.8	44.6	36.1	1.1	59
14:23	0.440	48.0	34.7	44.5	35.6	1.4	63
14:25	0.640	47.8	35.2	44.8	35.6	1.6	67
14:27	0.840	46.0	35.0	45.0	35.7	1.7	76
14:32	1.240	46.4	34.9	44.0	35.4	1.7	83
14:33	1.740	45.9	35.2	44.4	35.5	1.7	89
14:34	2.240	47.4	34.9	43.2	35.4	1.7	102
14:37	3.740	47.4	34.9	43.5	35.3	1.9	102
14:39	5.240	47.6	34.4	43.5	34.8	2.2	112

Time of day	Height above terrain Inches	Forward tunnel psychrometer T_{AD}-°F Thermo. #41	T_{AW}-°F Thermo. #51	Traverse psychrometer °F Thermo. #42	°F Thermo. #52	Traverse wind velocity ft/sec	Quantity of water evaporated cc
	Test No. 27		Date Nov. 6, 1952			Sta. 1	
14:51	0.030	48.3	34.3	42.5	40.9		0
	0.040	48.4	34.2	42.2	41.1		0
14:53	0.050	48.4	34.4	42.2	41.0		5
14:55	0.070	48.4	34.7	42.4	40.9	0.25	13
14:56	0.090	48.2	34.4	42.6	40.9	0.29	25
14:57	0.110	48.2	34.4	42.6	40.8	0.30	25
15:02	0.130	48.2	33.9	42.2	39.8	0.47	25
15:03	0.180	47.9	34.0	42.3	39.1	0.47	25
15:04	0.230	48.1	33.9	42.4	38.8	1.0	25
15:06	0.330	48.2	33.8	42.6	37.6	1.4	30
15:07	0.430	48.1	33.8	42.3	37.0	1.6	33
15:08	0.630	48.1	33.5	42.6	35.9	1.6	39
15:13	0.830	47.9	33.3	41.8	34.8	1.9	50
15:15	1.230	47.9	33.3	42.0	34.4	1.9	57
15:17	1.730	47.8	33.1	41.6	34.4	2.1	64
15:18	2.230	48.0	33.2	41.6	33.6	1.9	64
15:20	3.730	48.4	33.1	41.4	33.8	2.3	70
15:24	5.230	48.4	32.9	40.8	33.3	2.5	83
	Test No. 28		Date Nov. 6, 1952			Sta. 4	
15:40	0.035	46.4	32.6	40.8	40.5		0
15:41	0.045	46.4	32.6	41.2	40.7		
15:42	0.055	45.9	32.6	40.8	40.8	0.23	4
15:47	0.075	45.9	32.6	40.9	40.3	0.28	19
	0.095	45.8	32.5	40.8	39.9	0.41	19
15:50	0.115	45.9	32.7	41.0	39.0	0.41	29
	0.135	45.9	32.6	40.9	38.9	0.65	29
15:55	0.185	45.9	32.4	40.9	38.2	1.0	40
15:56	0.235	46.0	32.3	40.7	37.3	1.1	43
15:57	0.335	46.2	32.4	40.8	36.4	1.1	43
15:59	0.435	46.0	32.2	40.4	35.2	1.7	52
16:00	0.635	45.9	32.0	40.4	34.3	1.7	52
16:01	0.835	45.9	32.0	40.3	34.3	1.6	56
16:02	1.235	45.9	32.2	40.4	33.8	2.1	60
16:06	1.735	45.9	32.0	40.0	32.6	2.3	69
16:08	2.235	45.6	32.0	39.9	32.8	2.3	76
16:10	3.735	45.4	32.0	39.8	32.0	2.7	79
16:13	5.235	45.6	32.0	39.6	32.0	2.3	89

Time of day	Height above terrain Inches	Forward tunnel psychrometer T_{AD}-°F Thermo. #41	T_{AW}-°F Thermo. #51	Traverse psychrometer °F Thermo. #42	°F Thermo. #52	Traverse wind velocity ft/sec	Quantity of water evaporated cc
		Test No. 29	Date Nov. 6, 1952			Sta. 3	
16:29	0.050	47.3		40.4	39.4		0
	0.060	47.2		39.9	39.0		
16:30	0.070	47.2		40.0	38.9	0.31	7
	0.090	46.9		39.4	38.3	0.40	7
16:31	0.110	47.2		39.6	37.4	0.56	10
16:32	0.130	46.8	Less than 32°	39.4	36.2	0.65	16
16:35	0.150	46.8		39.6	36.2	1.0	24
16:37	0.200	46.4		39.0	35.8	1.3	24
	0.250	46.9		38.6	34.9	1.6	30
	0.350	46.8		38.6	34.1	2.3	30
16:39	0.450	46.8		38.6	33.8	2.1	36
	0.650	46.7		38.0	33.4	2.3	36
16:43	0.850	46.4		38.0	32.4	2.3	48
	1.250	46.0		38.0	32.1	2.3	48
16:45	1.750	45.9		37.1	32.0	2.5	52
16:46	2.250	45.9		37.2	32.0	2.7	56
16:47	3.750	45.8		36.7	32.0	2.5	60
16:50	5.250	45.8		37.2	32.0	2.5	68

Part II - Model Runs

Thermocouple Number	Run 1a	Run 1b	Run 2a	Run 2b	Run 3a	Run 3b-4a	Run 4b	Run 5a	Run 5b	Run 6a	Run 6b-7a
1	53.2	54.7	55.8	56.9	49.0	48.6	48.6	48.7	53.2	52.2	51.9
2	53.2	55.7	56.2	58.6	51.3	50.2	50.2	50.3	52.8	54.0	52.2
3	53.2	54.7	55.2	56.9	50.6	49.7	49.8	50.4	52.8	53.5	53.4
4	51.7	54.7	54.5	55.5	48.8	48.0	48.2	49.2	52.4	51.7	51.5
5	54.2	55.0	54.8	56.7	49.4	48.6	48.8	49.6	52.4	52.3	52.2
6	56.7	55.3	54.8	56.7	49.8	49.0	49.2	49.6	51.8	52.8	52.6
7	56.7	55.3	54.8	56.7	49.8	49.2	49.2	49.4	51.7	52.7	52.5
8	59.4	55.3	54.6	56.4	49.9	49.4	49.5	49.4	51.5	52.9	52.6
9	57.7	55.3	54.6	56.4	50.0	49.4	49.6	49.2	51.5	53.1	52.7
10	57.3	55.3	54.8	56.4	50.0	49.4	49.5	49.5	51.7	53.1	52.7
11	54.6	56.1	56.7	58.0	50.3	49.9	50.0	50.4	53.6	53.8	53.6
12	54.7	55.9	56.1	58.6	52.2	51.0	51.0	50.6	53.1	54.4	54.6
13	53.9	54.9	55.4	57.2	51.4	50.4	50.4	50.3	52.7	53.8	53.6
14	53.2	54.9	54.9	56.2	49.8	49.4	49.2	49.5	52.0	52.7	52.7
15			54.9	56.8	50.0	49.4	49.5	49.5	51.8	53.2	52.7
16			62.2	64.3	56.0	57.0	57.6	57.8	59.6	61.3	61.4
21	53.6	58.6	60.1	62.4	50.8	50.8	51.3	52.3	57.7	55.0	55.4
22	52.2	54.7	54.5	56.2	49.2	48.6	48.8	49.3	53.2	52.2	52.3
23	53.0	55.8	55.9	57.2	50.0	49.5	49.6	50.0	52.7	52.8	57.3
24	53.0	55.4	55.9	57.2	50.3	50.0	49.9	50.1	53.4	53.2	53.1
25	51.7	56.1	59.1	61.0	49.7	48.0	50.5	52.0	52.0	53.1	52.6
26	51.7	54.6	53.8	55.0	48.6	47.7	48.1	48.8	51.7	51.7	51.4
27	51.7	54.6	54.2	55.6	48.6	49.1	47.8	48.6	51.3	51.3	50.9
28	53.1	55.6	55.1	57.2	49.7	49.0	49.2	49.6	52.2	52.3	52.2
41	68.9	81.9	77.0	70.0	54.4	54.9	54.8	69.4	69.4	67.2	66.8
42	65.9	74.4	71.8	70.2	58.7	54.9	55.3	68.5	67.1	66.0	66.8
43	69.5	81.2	77.4	70.2	54.6	54.9	54.9	69.4	69.7	66.8	67.9
44	62.3	70.4	67.4	67.1	55.7	55.7	56.2	62.0	64.5	66.8	64.5
45	62.7	72.3	67.7	68.2	56.2	56.7	57.0	63.3	65.8	64.5	65.9
46	63.7	69.2	74.6	74.4	61.0	62.6	64.0	67.1	70.2	66.4	71.3
47	67.9	70.3	75.6	77.2	71.3	70.8	71.9	72.7	71.7	71.6	71.7
51			53.1	49.6	43.5	43.6	45.0	48.8		49.4	48.7
52			53.1	48.4	46.8	43.8	47.0	57.3		52.7	50.6

Thermocouple Number	Run 7b-8a	Run 8b	Run 9a	Run 9b-10a	Run 10b-11a	Run 11b	Run 12a	Run 12b-13a	Run 13b	Run 14a	Run 14b
1	52.1	51.9	51.3	51.8	52.7	52.7	51.3	50.6	50.5	47.1	49.0
2	54.8	54.7	53.3	54.5	55.8	55.9	51.8	51.7	51.8	47.4	49.2
3	51.5	53.7	52.2	53.2	54.2	54.6	51.8	51.7	51.5	46.8	49.0
4	51.8	51.4	52.2	53.2			50.9	50.8	50.7	46.4	48.3
5	52.2	51.8	51.7	52.2	52.8	52.8	51.0	50.8	50.7	46.6	48.3
6	52.7	52.7	51.3	52.2	52.8	53.2	51.4	51.4	50.9	46.6	48.2
7	52.7	52.7	51.4	51.9	52.8	53.1	51.5	51.3	51.4	46.6	48.2
8	52.8	52.7	51.3	51.9	52.8	53.2	51.4	51.4	51.5	46.4	48.0
9	52.8	52.9	51.4	51.8	53.1	53.3	51.5	51.7	51.8	46.2	48.0
10	53.2	52.9	51.3	51.8	53.2	53.3	51.8	51.8	51.8	46.7	48.2
11	54.3	54.2	52.1	52.8	54.4	54.6	53.0	52.8	53.2	47.5	49.7
12	55.0	54.9	52.8	53.9	55.2	55.4	52.7	52.8	53.1	47.5	49.6
13	54.1	54.2	52.0	53.1	54.4	54.7	52.2	52.3	52.5	46.9	49.0
14	53.1	52.8	51.5	52.3	53.6	53.7	51.8	52.2	52.5	46.4	48.7
15	53.1	52.9	51.4	52.3	53.1	53.3	51.8	52.2	51.9	46.7	48.2
16	62.3	62.3	56.0	59.6	61.5	61.4	62.0	62.7	63.6	54.9	57.9
21	56.2	56.1	53.2	55.0	61.0	56.7	54.5	55.5	55.7	49.9	52.2
22	53.1	52.8	51.1	51.9	53.3	53.6	51.3	51.4	56.4	46.4	48.7
23	52.8	52.5	51.9	53.1	53.7	54.0	51.4	51.8	51.7	47.2	48.8
24	53.2	53.1	52.1	52.6	53.7	53.8	51.1	51.0	51.4	46.9	48.8
25	53.0	52.8	51.8	52.7	53.5	54.0	52.3	50.9	52.8	49.4	50.9
26	51.4	51.0	50.9	51.4	51.7	51.7	49.7	49.7	54.0	46.2	47.6
27	51.0	50.9	50.9	51.5	51.7	51.7	49.9	49.6	49.4	45.8	47.2
28	52.2	51.9	51.7	52.2	52.6	52.8	50.6	50.6	50.5	46.5	48.1
41	65.3	63.5	70.0	70.7	68.2	64.9	73.9	74.3	70.3	65.0	68.2
42	65.0	63.2	64.9	69.3	66.4	64.4	67.2	73.1	69.8	61.4	68.8
43	65.1	63.2	70.1	71.1	73.5	65.0	73.5	73.1	70.3	65.4	68.8
44	62.2	61.2	61.5	64.3	63.7	62.0	66.4	66.8	65.7	57.9	61.6
45	65.3	64.2	61.4	64.3	65.3	64.9	69.8	70.8	65.8	59.6	63.6
46	69.5	70.3	68.5	70.0	71.2	69.3	73.1	72.7	71.3	66.2	68.6
47	72.2	72.1	69.4	71.3	72.7	72.2	74.2	74.7	75.3	79.0	74.8
51	47.6	48.7	50.0	50.4	48.2	47.6	43.5	44.1	48.9	47.2	47.4
52	48.6	47.6	53.3	53.7	49.5	47.6	58.7	44.5	43.0	48.7	50.4

Thermocouple Number	Run 15a	Run 15b	Run 16a	Run 16b	Run 17a	Run 17b	Run 18a	Run 18b-19a	Run 19b-20a	Run 20b	Run 21a
1	48.1	47.8	48.2	48.2	49.0	48.7	42.5	42.5	42.4	41.6	47.3
2	49.7	49.5	49.0	49.0	50.1	49.6	42.6	42.8	42.8	42.0	47.3
3	49.4	49.0	48.7	48.6	49.1	49.2	43.0	42.9	42.8	42.3	47.3
4	48.5	48.2	47.7	47.7	48.2	48.4	41.8	42.3	42.0	42.3	46.7
5	48.5	47.8	47.8	47.7	48.2	48.2	42.6	42.4	42.2	41.3	47.1
6	49.0	48.6	48.1	48.0	48.6	48.6	42.6	42.6	42.5	41.4	46.6
7	49.0	48.8	48.1	48.1	48.6	48.6	42.9	42.7	42.7	42.3	46.6
8	49.1	49.0	48.3	48.1	48.7	48.7	43.1	42.8	43.0	42.6	46.4
9	49.1	49.0	48.2	48.2	48.8	49.0	43.1	42.8	43.1	42.7	46.2
10	49.4	49.3	48.5	48.2	48.8	49.0	43.1	42.9	43.1	42.7	46.5
11	50.6	50.3	50.0	49.6	50.0	50.0	43.6	43.5	44.0	43.6	47.9
12	50.4	50.3	49.9	49.6	50.0	50.1	43.2	43.4	43.6	43.2	47.2
13	50.0	50.0	49.2	49.1	49.6	49.6	43.2	43.4	43.6	43.2	46.8
14	50.0	49.2	49.0	48.7	49.4	49.5	42.6	42.8	43.2	42.8	46.4
15	49.4	49.2	48.3	48.2	48.7	49.0	43.1	43.0	43.1	42.8	46.5
16	60.0	60.7	57.0	56.4	57.1	57.3	45.0	50.9	51.4	51.0	52.3
21	51.8	51.4	50.6	51.4	52.3	52.3	43.2	44.0	45.0	44.2	48.9
22	49.6	49.4	48.1	48.3	49.1	49.2	42.2	42.5	42.6	42.2	46.4
23	49.0	48.7	48.6	48.6	49.1	49.2	42.2	42.6	42.4	41.6	46.9
24	49.2	49.0	48.7	48.7	49.1	49.2	43.0	43.1	42.8	42.1	48.2
25	52.4	52.3	50.2	50.4	51.0	51.2	43.4	43.6	43.4	42.8	49.5
26	47.6	47.1	47.2	47.0	47.6	47.6	42.1	42.4	41.8	41.0	47.2
27	47.4	47.1	47.2	47.0	47.6	47.6	41.6	42.0	41.6	40.8	46.4
28	48.4	47.8	47.8	48.1	47.5	47.6	42.2	42.6	42.2	41.4	47.1
41	67.8	65.4	63.2	62.8	62.1	62.6	51.8	52.8	51.4	48.7	67.6
42	66.3	65.4	61.4	62.6	55.4	61.9	51.0	47.4	47.7	45.2	63.2
43	67.4	65.4	63.2	62.8	61.2	63.1	51.8	51.6	49.1	45.5	66.3
44	62.2	61.6	58.4	58.5	58.3	59.0	49.3	50.2	49.0	46.4	58.2
45	65.4	64.8	60.2	60.3	60.0	61.0	50.4	51.3	50.3	47.7	60.7
46	70.3	70.0	62.8	62.7	63.2	63.0	54.6	58.2	56.0	57.5	64.0
47	73.8	74.2	81.0	71.7	71.2	72.4	67.2	70.3	72.2	70.4	71.6
51	46.9	45.9	45.3	45.9	45.8	46.3	41.5	42.0	40.0	37.9	48.2
52	51.4	46.2	48.2	46.4	47.8	46.8	43.4	42.2	40.6	37.7	53.4

Thermocouple Number	Run 21b-22a	Run 22b-23a	Run 23b-24a	Run 24b-25a	Run 25b	Run 26a	Run 26b-27a	Run 27b-28a	Run 28b-29a	Run 29b
1	48.0	49.1	49.5	49.9	49.6	40.8	39.9	40.0	39.4	38.9
2	48.2	49.6	50.0	50.6	50.2	41.6	41.6	41.2	40.5	39.9
3	48.1	49.3	50.0	50.4	50.1	41.8	41.6	41.2	40.8	40.3
4	47.4	49.0	49.6	49.9	49.3	40.6	40.4	40.3	39.6	39.0
5	47.6	48.9	49.2	49.7	49.6	41.2	40.9	40.4	40.2	39.4
6	47.3	48.7	49.2	49.8	49.6	41.6	41.1	40.8	40.4	39.9
7	47.3	48.7	49.4	50.0	50.0	41.6	41.2	40.9	40.4	39.9
8	47.2	48.7	49.3	50.0	50.0	41.6	41.2	41.0	40.4	39.9
9	46.9	48.4	49.1	50.0	50.0	41.8	41.4	41.0	40.8	40.0
10	47.3	49.1	49.7	50.2	50.2	41.8	41.2	41.0	40.8	40.4
11	48.9	50.2	50.8	51.4	51.4	41.8	41.2	40.8	40.3	40.0
12	48.2	49.9	50.4	51.1	51.2	42.0	42.3	41.6	41.0	40.8
13	47.8	49.5	50.3	50.8	50.8	42.2	42.6	41.6	41.0	40.8
14	47.6	49.2	50.0	50.4	50.3	41.3	41.0	40.8	40.2	39.8
15	47.2	49.2	49.6	54.6	50.3	41.8	41.4	41.2	40.4	40.0
16	55.0	56.8	48.8	58.2	57.6	45.5	45.7	45.4	45.0	44.6
21	50.3	52.7	49.1	54.0	53.6	42.6	42.4	42.3	41.8	40.9
22	47.2	49.1	49.8	50.3	50.1	40.9	40.6	40.4	39.8	39.1
23	47.8	49.2	50.0	50.3	49.9	41.5	41.2	40.3	40.3	39.9
24	48.6	49.9	50.0	50.3	49.9	42.3	41.8	41.4	41.0	40.4
25	49.6	50.8	51.8	51.8	51.4	41.7	41.4	41.2	40.4	39.8
26	47.2	48.2	48.9	48.9	48.7	40.9	40.4	40.0	39.4	38.9
27	46.6	47.8	48.5	48.7	48.2	38.4	40.3	40.0	39.1	38.6
28	47.6	48.3	49.1	49.5	49.2	41.4	40.9	40.6	40.1	39.5
41	68.2	69.5	68.3	64.9	62.2	47.8	48.3	46.4	48.4	45.8
42	69.0	69.4	67.9	61.3	60.2	46.2	42.5	40.8	40.8	37.2
43	69.5	68.0	67.8	64.0	59.6	43.9	43.1	40.8	39.3	36.2
44	59.6	61.8	61.4	60.1	58.4	45.8	45.4	44.8	43.5	42.2
45	62.7	64.3	64.5	63.1	60.9	46.2	46.4	45.6	44.7	43.6
46	66.3	68.1	67.7	61.7	66.0	54.2	46.0	53.2	52.8	48.8
47	70.0	70.6	70.8	70.8	73.5	76.5	76.6	79.7	76.3	75.3
51	47.2	47.6	49.1	46.6	45.4	34.9	34.3	32.6	32.9	32.0
52	48.6	49.0	49.5	47.6	46.3	39.4	40.9	40.5	33.3	32.0